Lawrence Berkeley Laboratory
UNIVERSITY OF CALIFORNIA

Physics, Computer Science & Mathematics Division

AN ANALYSIS OF FLAME PROPAGATION

James A. Sethian
(Ph.D. thesis)

May 1982

Prepared for the U.S. Department of Energy under Contract DE-AC03-76SF00098

DISCLAIMER

LBL-14125

AN ANALYSIS OF FLAME PROPAGATION[1]

James A. Sethian

Department of Mathematics
and
Lawrence Berkeley Laboratory
University of California
Berkeley, California 94720

Ph.D. Dissertation

May 1982

[1]Supported in part by the Director, Office of Basic Energy Sciences, Engineering, Mathematical, and Geosciences Division of the U.S. Department of Energy under Contract DE-AC03-76SF00098.

An Analysis of Flame Propagation

James A. Sethian

Abstract

We develop a mathematical theory of flame propagation and analyze the stability of a flame front. We consider a premixed, combustible fluid and model the front between the burnt and unburnt regions as an infinitely thin curve propagating in a direction normal to itself at a constant speed. We assume that the specific volume of a fluid particle increases by a fixed amount when it burns.

Our results show a deep analogy between the equations of flame propagation and hyperbolic systems of conservation laws. We introduce the notion of ignition curves and an entropy condition which enable us to solve the equations of flame propagation in the absence of fluid motion. We prove that any initial front asymptotically approaches a circle as it burns, and that if two fronts start close to each other, they remain so. As the front moves, it may form cusps, which are the result of colliding ignition curves and form in the same way that shocks develop in the solution of hyperbolic systems. These cusps absorb sections of the flame front, destroying information about the initial shape of the front: once a cusp forms, it is impossible to retrieve the initial data by solving the equations of motion backwards in time. We use our theory to discuss the difficulties involved in a numerical approximation to the equations of flame propagation. Finally, we analyze a numerical technique, developed by Chorin, that does not rely on a discrete parameterization of the initial front, and use it to illustrate the results of our theorems.

Acknowledgements

I would like to thank my thesis advisor, Alexandre Chorin, for the generous encouragement and guidance he gave me during my years at Berkeley. I benefited greatly from his mathematical intuition and insight. It was a privilege to work with him.

I would also like to thank Ole Hald for his unbounded enthusiasm. Our countless discussions were invaluable to me.

I would like to thank Antoni Oppenheim for serving as the outside reader, and Carl Quong for making available to me the facilities of the Computer Science and Mathematics Group at the Lawrence Berkeley Laboratory. I am honored to have been a Danforth Fellow while in graduate school. The financial support and encouragement of the Danforth Foundation gave me the opportunity and freedom to pursue my research. Finally, I would like to thank Catherine Willis for her patience and help in editing this work.

CONTENTS

Introduction

One of the main goals of a theory of combustion is to predict the shape of a flame as it burns. In this work, we develop a mathematical theory of flame propagation to analyze the stability and smoothness of a flame front. We then present a numerical technique to model the motion of a burning front, and use this technique to illustrate the results of our theorems.

In the past few decades, a considerable amount of attention has been focussed on flame stability. The pioneering work in this field is the analysis of a plane flame front by L. Landau in 1944 [10]. By ignoring all but hydrodynamic effects, Landau was able to show that such a front is unstable with respect to small perturbations. Since then, there have been numerous investigations of flame stability for a variety of combustion models, see Markstein, [11], Zeldovich, [17], Zeldovich, [18] and Istratov and Librovich [8]. A comprehensive, though now outdated, account may be found in Markstein [12]. A review of current work may be found in Sivashinsky [15].

A standard technique employed in stability investigations is linear perturbation analysis. As Markstein points out, such a technique has its drawbacks. For example, the results are valid only in the limit as the amplitude of the perturbations goes to zero. There may be steady-state amplitudes in regions of linear instability. Furthermore, there are phenomena that are so fundamentally non-linear that they do not submit to a linearized analysis.

In this work, we proceed in a different manner. We solve, analytically and geometrically, the equations of a particular model of flame propagation. Our results show a deep analogy between the solutions of the equations describing the propagation of a flame front and the solutions of hyperbolic systems of conservation laws. We show that, as the flame front moves, cusps form and then disappear, and prove that, in our particular model of flame propagation,

flame fronts are stable.

In Chapter One we consider an incompressible, viscous, premixed, combustible fluid. A "premixed, combustible fluid" is a fuel that exists in one of two states, burnt and unburnt. The flame front is idealized as an infinitely thin curve separating the burnt and the unburnt regions. We assume that the flame propagates into the unburnt fluid in a direction normal to itself at a uniform speed. We further assume that the specific volume of each fluid particle increases by a fixed amount as it changes from unburnt to burnt. Thus, there is a velocity field induced by the propagation of the flame.

With these assumptions, our problem becomes one of following a flame propagating in a direction normal to itself while interacting with a moving fluid. A somewhat related problem concerning the motion of a surface whose velocity equals its mean curvature at any point was analyzed with some interesting results by Brakke [1].

In Chapter Two, we suppress the effects of the velocity field produced by volume expansion. We introduce the idea of ignition curves, which enable us to solve the equations of flame propagation. These ignition curves are seen to play a role in our equations analogous to that of characteristics in the solutions of hyperbolic equations. Continuing the analogy with conservation laws, we develop an entropy condition for flame propagation. With these tools, we prove the following:

1) If two initial fronts start close together, they remain close together. In this sense, flame fronts are stable. Furthermore, any initial front asymptotically approaches a circle as it burns.

2) As the front moves, it forms cusps, which are the result of colliding ignition curves, and develop in the same way that shocks form when characteristics collide. These cusps "swallow up" sections of the flame front as they move, destroying information about the initial shape of the flame front. Once a cusp forms, it is impossible to retrieve the original flame shape by solving the equations of motion backwards in time.

In Chapter Three, we use our theory of flame propagation to show that numerical methods that attempt to solve the equations of motion by finite difference techniques face serious obstacles. In particular, numerical techniques that rely on marker particles placed along the front will have great difficulty following the front. In Chapter Four, we present a numerical method for following flame fronts, developed by Chorin [2], that does not rely on a discrete parameterization of the flame front. We show that the reason for the great success of this method is clear when viewed from within the framework of our theory of flame propagation. Finally, we use the numerical technique to illustrate the results of our theorems.

Chapter One

Formulation of the Model

In this chapter, we present our model of turbulent combustion. We give a physical description, followed by a mathematical formulation.

We consider two-dimensional, viscous flow inside a given region. On solid walls, we require that the normal and tangential velocities are zero. We make the following assumptions:

1) The fluid is a mixture of fuel and air, in which each fluid particle can exist in one of two states, burnt and unburnt. When the temperature of an unburnt particle becomes sufficiently high, it undergoes an instantaneous change in volume due to heating and becomes burnt. The ratio of the density of an unburnt particle to that of a burnt particle depends on the mixture under study and is a prescribed constant. Thus, we regard the interface between the burnt and the unburnt regions as an infinitely thin flame front, acting as a source of specific volume.

2) The front propagates at a fixed speed in a direction normal to itself into the unburnt fluid. The lower the ignition temperature of the fuel, the faster the flame propagates.

3) Compressibility effects can be ignored and sound waves travel infinitely fast. This balances pressure forces.

In our model, the fluid motion affects the position of the flame front, and the exothermic expansion along the front influences the fluid velocity. As an illustration of this process, consider a fluid flowing down a channel. Suppose we ignite this fluid near the inlet, i.e., raise the temperature beyond the ignition point. The flame will propagate as the surrounding particles are ignited.

The resulting change in volume of these particles pushes the nearby fluid, and this exothermic velocity field, added to the underlying fluid flow, carries the flame front down the channel.

In this model, we ignore variations in the flame propagation speed due to molecular diffusion and chemical kinetics, and disregard three-dimensional effects such as vorticity stretching.

We now develop a mathematical formulation of this model. Let $\vec{u}$ be the velocity of the fluid at a point (x,y), i.e., $\vec{u}=(u(x,y),v(x,y))$. Let $\gamma(s,t)$ parameterize by s the position of the flame front at time t; given s, $\gamma(s,t)$ yields the coordinates (X_F,Y_F) of a fluid particle that changes from unburnt to burnt at time t. Thus

$$\gamma(s,t)=(X_F(s,t),Y_F(s,t)) \tag{1.1}$$

Let R be the Reynolds number, and let k be the prescribed speed at which the flame burns.

The fluid motion on either side of the flame front must satisfy the momentum equation for viscous flow, namely

$$\frac{D\vec{u}}{Dt}=\frac{1}{R}\nabla^2\vec{u}-\frac{\nabla\vec{P}}{\rho} \tag{1.2}$$

where $\frac{D}{Dt}$ is the total derivative, $\vec{P}=\vec{P}(x,y)$ is the pressure, $\rho=\rho(x,y)$ is the density, ∇ is the gradient and ∇^2 is the two-dimensional Laplacian. We restrict ρ to two possible values; ρ_u in the unburnt fluid and ρ_b in the burnt fluid. The boundary conditions for viscous flow are

$$\vec{u} = (u(x,y),v(x,y)) = 0 \tag{1.3}$$

on solid walls.

Since the flow is incompressible on both sides of the flame front,

$$\nabla \cdot \vec{u}(x,y)=0 \tag{1.4}$$

in the burnt and the unburnt regions. However, along the front, where the fluid undergoes a volume expansion as it burns, the divergence is necessarily non-zero; each expanding particle pushes the surrounding fluid, and thus in any small domain along the flame front, the flow in cannot equal the flow out. By using the conservation of mass, we will derive an expression for the effect of this volume expansion on the fluid velocity.

Across the moving front, mass coming in from one side equals the mass leaving on the other side, that is, (ρu_n) must be continuous across the front, where ρ is the density and u_n is the velocity component normal to the front. Suppose the flame is moving from left to right. The fluid on the left is burnt and has a lower density (due to expansion) than the unburnt fluid on the right. (See Figure (1.1))

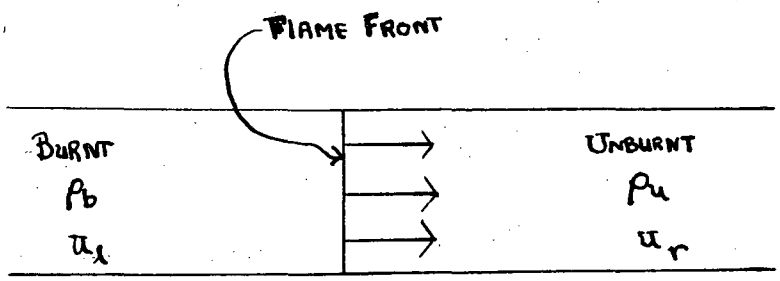

Figure 1.1

If we imagine a coordinate system moving with the front, then the conservation of mass requires that

$$\rho_u \bar{u}_r = \rho_b \bar{u}_l \tag{1.5}$$

where $\bar{u}_r$ and $\bar{u}_l$ are the velocities of the fluid normal to the front on the unburnt and burnt sides, respectively. Here, an overbar denotes velocities relative to the moving front. Let u_r and u_l be the velocities on the right and left respectively, and let S be the velocity of the front, all taken in a fixed frame. From conservation of mass, we have that

$$\rho_u(u_r - S) = \rho_b(u_l - S) \tag{1.6}$$

Thus,

$$\rho_u(u_r - u_l) = (\rho_u - \rho_b)(S - u_l) \tag{1.7}$$

Adding $(\frac{u_l - u_r}{2})(\rho_u - \rho_b)$ to both sides and solving for $(u_r - u_l)$, we find

$$(u_r - u_l) = 2\left\{\frac{\rho_u - \rho_b}{\rho_u + \rho_b}\right\}\left\{S - (\frac{u_l + u_r}{2})\right\} \tag{1.8}$$

Recall that k is the prescribed speed of propagation. This speed, plus the average of the velocity on the left and the right, equals the observed speed of the front as seen from the fixed frame:

$$S = k + (\frac{u_l + u_r}{2}) \tag{1.9}$$

Substitution yields

$$(u_r - u_l) = 2\left\{\frac{\rho_u - \rho_b}{\rho_u + \rho_b}\right\}(k) \tag{1.10}$$

Hence, across the flame there is a jump in the normal velocity of magnitude

$$2\left\{\frac{\rho_u - \rho_b}{\rho_u + \rho_b}\right\}(k) \tag{1.11}$$

We now consider the motion of the flame front. As seen from the fixed reference frame, the front is both carried by the flow and advanced normal to

itself by the burning process. For the moment, we assume that the front $\gamma(s,t)$ is a regular, closed, smooth curve. Then, at a point (X_F, Y_F) on the front, the normal vector of unit length is

$$\left\{ \frac{\frac{\partial Y_F}{\partial s}}{\left\{ \left(\frac{\partial Y_F}{\partial s}\right)^2 + \left(\frac{\partial X_F}{\partial s}\right)^2 \right\}^{1/2}}, - \frac{\frac{\partial X_F}{\partial s}}{\left\{ \left(\frac{\partial Y_F}{\partial s}\right)^2 + \left(\frac{\partial X_F}{\partial s}\right)^2 \right\}^{1/2}} \right\} \tag{1.12}$$

The requirement that the front move normal to itself at speed k, as well as ride with the fluid flow means that we have the system of partial differential equations

$$\frac{\partial X_F}{\partial t} = k \left\{ \frac{\frac{\partial Y_F}{\partial s}}{\left\{ \left(\frac{\partial Y_F}{\partial s}\right)^2 + \left(\frac{\partial X_F}{\partial s}\right)^2 \right\}^{1/2}} \right\} + u(X_F, Y_F) \tag{1.13}$$

$$\frac{\partial Y_F}{\partial t} = -k \left\{ \frac{\frac{\partial Y_F}{\partial s}}{\left\{ \left(\frac{\partial Y_F}{\partial s}\right)^2 + \left(\frac{\partial X_F}{\partial s}\right)^2 \right\}^{1/2}} \right\} + v(X_F, Y_F) \tag{1.14}$$

In Chapter Two, we will show that the front may lose its smoothness as it moves. This will require us to amend our equations for the motion of the flame.

We summarize the equations of our model. On both sides of the flame,

$$\frac{D\vec{u}}{Dt} = \frac{1}{R}\nabla^2\vec{u} - \frac{\nabla\vec{P}}{\rho} \tag{1.15}$$

$$\nabla \cdot \vec{u} = 0 \tag{1.16}$$

where $\rho=\rho_u$ in the unburnt region and $\rho=\rho_b$ in the burnt region. On solid walls

$$\vec{u} = (u, v) = 0 \tag{1.17}$$

Across the front, there is a jump in the normal velocity of magnitude

$$2\left\{\frac{\rho_u-\rho_b}{\rho_u+\rho_b}\right\}(k) \tag{1.18}$$

If we parameterize the flame front by s at time t, then the trajectory of each point $(X_F(s,t),Y_F(s,t))$ of the front must satisfy

$$\frac{\partial X_F}{\partial t}=k\left\{\frac{\frac{\partial Y_F}{\partial s}}{\left\{\left(\frac{\partial Y_F}{\partial s}\right)^2+\left(\frac{\partial X_F}{\partial s}\right)^2\right\}^{1/2}}\right\}+u(X_F,Y_F) \tag{1.19}$$

$$\frac{\partial Y_F}{\partial t}=-k\left\{\frac{\frac{\partial X_F}{\partial s}}{\left\{\left(\frac{\partial Y_F}{\partial s}\right)^2+\left(\frac{\partial X_F}{\partial s}\right)^2\right\}^{1/2}}\right\}+v(X_F,Y_F) \tag{1.20}$$

where R,k,ρ_u,ρ_b are all prescribed constants.

In this chapter, we have developed our combustion equations as a time-dependent free boundary value problem. In the next chapter, we analyze the stability of the flame front.

Chapter Two

The Evolution of Flame Fronts

In this chapter, we study the motion of a flame propagating in a premixed, combustible fluid with no boundaries. We ignore the effects of the velocity field produced by volume expansion along the front by assuming that the densities of the burnt and unburnt fluids are the same. In addition, we ignore pre-existing vorticity. Thus, we consider a simplified version of our original equations (1.15)-(1.20).

Let D be an unbounded domain filled with a premixed, combustible fluid, and let γ be a simple closed curve lying in D. Suppose that all the particles inside γ are burnt and all the particles outside are unburnt. We ignite the particles along γ. The position of the front changes as the surrounding unburnt fuel is ignited. We prove that flame front asymptotically approaches a circle as t goes to infinity. In particular, we show that, as the fluid burns, cusps may develop in the front. These cusps form in the same way that shocks form in the solutions of hyperbolic equations. We develop an entropy condition, similar to the one employed in gas dynamics, that allows us to continue the solution beyond the time when cusps first appear. When a cusp forms, information about the initial shape of the flame is lost.

2.1. Equations of Motion

We begin by considering the equations of motion for the flame front. Let $\gamma(s)$ be a simple closed curve in D, parameterized by s; for each $s \in [0,S]$, $\gamma(s)$ yields a point $(x(s),y(s))$ in D with $\gamma(0)=\gamma(S)$. Suppose the particles inside γ are burnt and those outside are unburnt. We shall always assume that γ is

parameterized so that the burned region is on the left as we travel along the curve in the direction of increasing s. At $t=0$ we ignite the particles along γ. As the surrounding unburnt fuel is ignited, the boundary between the burnt and the unburnt particles changes. Let $\gamma(s,t)=(x(s,t),y(s,t))$ be the position of the front at time t and let α and β be the coordinate functions of γ at $t=0$; that is, $\gamma(s,0)=(\alpha(s),\beta(s))$. For the moment, we assume that α and β are both twice differentiable, and that $\alpha_s^2+\beta_s^2\neq 0$ everywhere.

The flame front propagates in a direction normal to itself with constant speed k. At a point $(x(s,t),y(s,t))$ on the front, the tangent vector is (x_s,y_s) and the velocity vector is (x_t,y_t). Thus,

$$(x_t,y_t)\cdot(x_s,y_s)=0 \tag{2.1}$$

$$x_t^2+y_t^2=k^2 \tag{2.2}$$

$$x(s,0)=\alpha(s) \qquad y(s,0)=\beta(s) \tag{2.3}$$

$$0\leq s\leq S$$

Equation (2.1) is simply

$$x_t x_s+y_t y_s=0 \tag{2.4}$$

Differentiation of (2.2) with respect to s yields

$$x_t x_{ts}+y_t y_{ts}=0 \tag{2.5}$$

and with respect to t yields

$$x_{tt} x_t+y_{tt} y_t=0 \tag{2.6}$$

We show that $x_{tt}=y_{tt}=0$. Differentiating (2.4) with respect to t, and using (2.5), we find that

$$0=\frac{\partial(x_t x_s+y_t y_s)}{\partial t}=x_t x_{st}+x_{tt} x_s+y_t y_{st}+y_{tt} y_s \tag{2.7}$$

$$=x_{tt} x_s+y_{tt} y_s$$

Together with (2.6), this implies that either $x_{tt}=y_{tt}=0$ or $x_s y_t=x_t y_s$. Suppose $x_s y_t=x_t y_s$. Together with (2.4), this implies that $x_t^2+y_t^2=0$, which violates

(2.2), or that $x_s^2+y_s^2=0$. Since $\alpha_s^2+\beta_s^2\neq 0$, there exists some $t_1>0$ such that for $0\leq t<t_1$, $x_s^2+y_s^2\neq 0$. Let t_1 be the smallest time such that $x_s^2+y_s^2\neq 0$. Then, for $0\leq t<t_1$,

$$x_{tt}=0 \tag{2.8}$$

$$y_{tt}=0 \tag{2.9}$$

Integrating (2.8) and (2.9) with respect to s and using the initial conditions, we get

$$x(s,t) = f(s)t + \alpha(s) \tag{2.10}$$

$$y(s,t) = g(s)t + \beta(s) \tag{2.11}$$

where f and g are unknown functions of s. Substitution of (2.10) and (2.11) into (2.2), (2.4) and (2.5) yields

$$f^2+g^2 = k^2 \tag{2.12}$$

$$ff_s+gg_s = 0 \tag{2.13}$$

$$f(f_st+\alpha_s)+g(g_st+\beta_s) = 0 \tag{2.14}$$

Substitution of (2.13) into (2.14) yields

$$f\alpha_s+g\beta_s = 0 \tag{2.15}$$

Substitution of (2.12) into (2.15) yields

$$f(s) = k\,\frac{\beta_s}{(\alpha_s^2+\beta_s^2)^{1/2}} \tag{2.16}$$

$$g(s) = -k\,\frac{\alpha_s}{(\alpha_s^2+\beta_s^2)^{1/2}} \tag{2.17}$$

Thus, the position of the front at time t is given by

$$x(s,t) = k\,\frac{\beta_s}{(\alpha_s^2+\beta_s^2)^{1/2}}t + \alpha(s) \tag{2.18}$$

$$y(s,t) = -k\,\frac{\alpha_s}{(\alpha_s^2+\beta_s^2)^{1/2}}t + \beta(s) \tag{2.19}$$

Remark. We can extend the solution beyond the time when $x_s^2+y_s^2=0$ if we consider only real analytic solutions. Then, since $x_{tt}=y_{tt}=0$ for $t<t_1$ and the solutions are real analytic, we have $x_{tt}=y_{tt}=0$ for all $t\geq 0$, and the solutions (2.18)-(2.19) hold. Furthermore, this shows the solution is unique in the space of analytic solutions.

Example 2.1 As an example, consider the parabola $y=x^2$. Suppose that the particles above the parabola are burnt and those particles below are unburnt. At $t=0$, we ignite the particles along the curve $y=x^2$. We wish to determine the position of front as it moves in a direction normal to itself with speed k. Although this is not a closed curve, (2.18) and (2.19) still determine the motion of the parabola, since (2.1), (2.2) and (2.3) express only the local behavior of a point on the curve. Let $\alpha(s)=s$ and $\beta(s)=s^2$. Then

$$x(s,t) = k\,\frac{2s}{(4s^2+1)^{1/2}}t + s \tag{2.20}$$

$$y(s,t) = -k\,\frac{1}{(4s^2+1)^{1/2}}t + s^2 \tag{2.21}$$

See Figure (2.1).

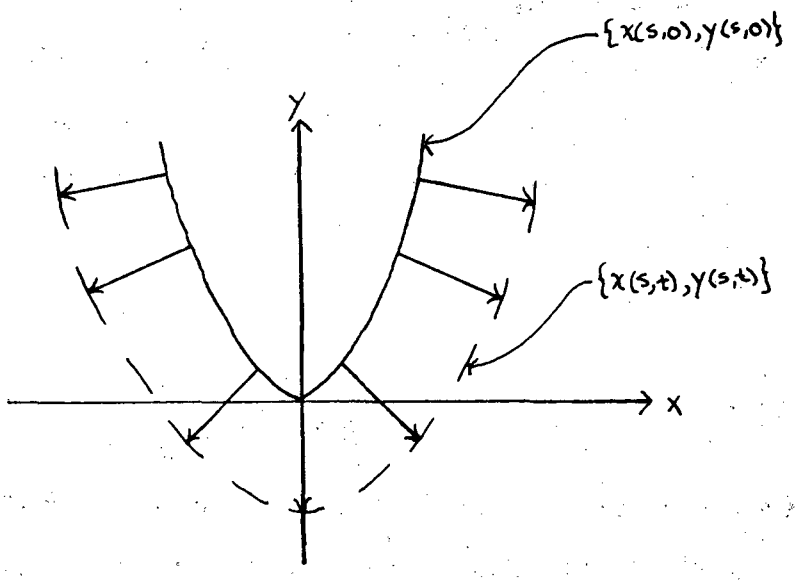

Figure 2.1

This completes the example.

The following example shows that we cannot simultaneously require that s parameterize the curve by arc length for all time and demand that each section of the curve move in a direction normal to itself with constant speed.

Example 2.2 Let $\gamma(s)=(\alpha(s),\beta(s))=(\cos(s),\sin(s))$, $s \in [0,2\pi]$, thus $\alpha_s^2+\beta_s^2=1$. Using (2.18) and (2.19), we have, with $k=1$,

$$x(s,t) = (t+1)\cos(s) \qquad y(s,t) = (t+1)\sin(s) \qquad (2.22)$$

$$s\in[0,2\pi]$$

Given t, $(x(s,t),y(s,t))$ maps the interval $[0,2\pi]$ onto a circle of radius $(t+1)$, centered at the origin. In Figure (2.2), we show the position of the front for

several values of t.

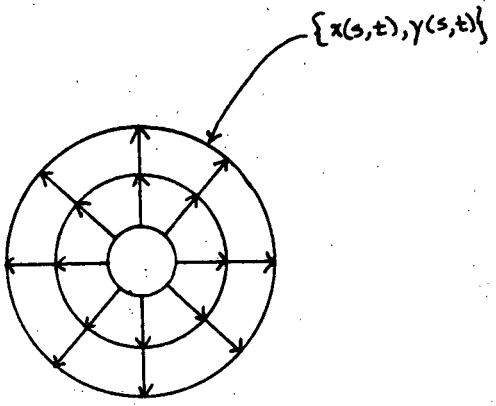

Figure 2.2

Note that $x_s^2+y_s^2 = (t+1)$, and thus, for $t>0$, the curve is not parameterized by arc length. This is because there must be some "stretching" in the image of the parameter s if we are to require that for each t, $s=0$ and $s=2\pi$ are sent to the same point, regardless of the length of the flame.

If we define

$$x^*(s,t) = (t+1)\cos\left(\frac{s}{(t+1)}\right) \tag{2.23}$$

$$y^*(s,t) = (t+1)\sin\left(\frac{s}{(t+1)}\right) \tag{2.24}$$

then $(x^*(s,t),y^*(s,t))$ maps the interval $[0,2\pi(t+1)]$ onto a circle of radius $(t+1)$ centered at the origin, with $\alpha_s^2+\beta_s^2=1$. However, this does not satisfy the differential equation (2.1). The motion of this front is depicted in Figure (2.3).

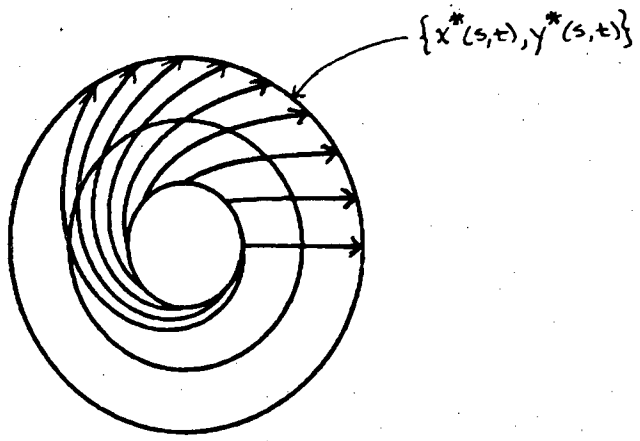

Figure 2.3

This completes the example.

Let $\vartheta(s)$ equal the angle between the directed tangent to the front at the point $(x(s,t),y(s,t))$ and the positive x axis. In our first lemma, we show that $\partial_s(\vartheta(s,t))$ is independent of t.

Lemma 1. Let $(x(s,t),y(s,t))$ be given by (2.18) and (2.19), where $\alpha_s^2+\beta_s^2\neq 0$. Then

1) For each s, the curve $(x(s,t),y(s,t)),t\in[0,\infty)$ is a straight line with slope equal to $\frac{-\alpha_s}{\beta_s}$.

2) If $\vartheta=\tan^{-1}(\frac{y_s}{x_s})$, then

$$\frac{\partial(\tan^{-1}(\vartheta))}{\partial s} = \frac{\beta_{ss}\alpha_s-\alpha_{ss}\beta_s}{(\alpha_s^2+\beta_s^2)}$$

Hence, both quantities are independent of t.

Proof. Differentiation of (2.18) and (2.19) with respect to t yields

$$x_t = k\ \beta_s(\alpha_s^2+\beta_s^2)^{-1/2} \tag{2.25}$$

$$y_t = -k\ \alpha_s(\alpha_s^2+\beta_s^2)^{-1/2} \tag{2.26}$$

Pick a point $(x(s_1,0),y(s_1,0))$ on the initial curve. The trajectory of the curve $(x(s_1,t),y(s_1,t))$, $t\in[0,\infty)$ must always be normal to the front, and have speed equal to k. Using (2.25) and (2.26), we have

$$\frac{y_t}{x_t} = \frac{-k\,\alpha_s(\alpha_s^2+\beta_s^2)^{-1/2}}{k\ \beta_s(\alpha_s^2+\beta_s^2)^{-1/2}} = \frac{-\alpha_s}{\beta_s} \tag{2.27}$$

Thus, the trajectory is a straight line with slope $\frac{-\alpha_s(s_1)}{\beta_s(s_1)}$.

Using (2.1), we have

$$\frac{y_s}{x_s} = \frac{-x_t}{y_t} = \frac{\beta_s}{\alpha_s} \tag{2.28}$$

Hence,

$$\frac{\partial\vartheta(s,t)}{\partial s} = \frac{\partial\tan^{-1}(\frac{y_s}{x_s})}{\partial s} = \frac{\partial\tan^{-1}(\frac{\beta_s}{\alpha_s})}{\partial s} \tag{2.29}$$

$$= \frac{(\beta_{ss}\alpha_s-\alpha_{ss}\beta_s)}{(\alpha_s^2+\beta_s^2)}$$

Thus, the change in ϑ as a function of s does not depend on t. This completes the proof.

2.2. Evolution of A Convex, Smooth Flame Front

Our objective is to show that the shape of the burnt region becomes circular as the front moves normal to itself into the unburnt fluid. Without loss of generality, we assume that the flame moves with unit speed.

Remark. Throughout this chapter, we assume that all curves have finite arc length.

Definition. We say that a curve $\gamma(s)$ is convex if, as we go along the curve in the direction of increasing parameters, the angle the directed tangent (α_s,β_s) makes with the positive x axis is non-decreasing, when measured in a counterclockwise direction. In other words, $\partial_s \tan^{-1}(\frac{\beta_s}{\alpha_s}) = (\beta_{ss}\alpha_s - \alpha_{ss}\beta_s)(\alpha_s^2+\beta_s^2)^{-1} \geq 0$ for $s\in[0,S]$.

Definition. We say that γ is a simple, closed, regular, parameterized, positively oriented plane curve of class C^2 if $\gamma(s)=(\alpha(s),\beta(s))$ is a map of the closed interval $I=[0,S]$ into R^2 such that

1) α and β are both C^2 functions of s.
2) $\gamma'(s)\neq 0$ for $s\in I$.
3) $\gamma(s)$ and its first two derivatives agree at 0 and at S; $\gamma(0)=\gamma(S)$, $\gamma'(0)=\gamma'(S)$, $\gamma''(0)=\gamma''(S)$.
4) If $t_1,t_2\in[0,S]$, $t_1\neq t_2$, then $\gamma(t_1)\neq\gamma(t_2)$.
5) If we go along the curve in the direction of increasing parameters, the interior of the curve remains to the left.

Theorem 1. Let γ be a simple, closed, regular, positively oriented, convex plane curve of class C^2. Suppose $(\beta_{ss}\alpha_s - \alpha_{ss}\beta_s)>0$. The particles inside γ are

burnt, those outside are unburnt, and at $t=0$, we ignite the particles along γ. Then the propagating front is always convex. Furthermore, let

$$(\bar{x}(s,t),\bar{y}(s,t)) = \frac{1}{L(t)}((x(s,t),y(s,t))$$

where $(x(s,t),y(s,t))$ is the solution (2.18)-(2.19) and $L(t)$ is the length of the front at time t. Then, as $t\to\infty$, the shape of the burned front becomes circular. That is, given ε, there exists t_0 such that for all $t>t_0$,

1) $(\bar{x}(s,t),\bar{y}(s,t))$ is outside a circle of radius $(\frac{1}{2\pi}-\varepsilon)$ and inside a circle of radius $(\frac{1}{2\pi}+\varepsilon)$.

2) $\left|\frac{1}{2\pi}-K(\bar{x},\bar{y})\right|<\varepsilon$, where $K(\bar{x},\bar{y})$ is the curvature of $(\bar{x}(s,t),\bar{y}(s,t))$.

Remark. The convexity of the initial curve is contained within the assumption that $(\beta_{ss}\alpha_s-\alpha_{ss}\beta_s)>0$. However, the strict inequality limits us to convex curves that are nowhere straight.

Proof. The proof will consist of three parts. First, we show that the front is always convex. Second, we show that as the front burns, its length increases. Finally, we show that the shape of the burnt region must become circular as $t\to\infty$.

Using (2.18) and (2.19), we have, for $k=1$,

$$x(s,t) = \frac{\beta_s}{(\alpha_s^2+\beta_s^2)^{1/2}}t + \alpha(s) \tag{2.30}$$

$$y(s,t) = -\frac{\alpha_s}{(\alpha_s^2+\beta_s^2)^{1/2}}t + \beta(s) \tag{2.31}$$

Since $\gamma'(s)\neq 0$ everywhere, we are assured that $(\alpha_s^2+\beta_s^2)$ can never vanish. From Lemma 1, we have

$$\delta_s(\tan^{-1}(\frac{y_s}{x_s})) = (\beta_{ss}\alpha_s - \alpha_{ss}\beta_s)(\alpha_s^2+\beta_s^2)^{-1} \tag{2.32}$$

Since $(\beta_{ss}\alpha_s - \alpha_{ss}\beta_s)>0$, this implies that the front is always convex. We now prove that as the front burns, its length increases. First, we show that $(x_s^2+y_s^2)>(\alpha_s^2+\beta_s^2)$. Differentiation of (2.30) and (2.31) with respect to s yields

$$x_s = \left\{\beta_{ss}(\alpha_s^2+\beta_s^2)^{-1/2} - \beta_s(\alpha_s\alpha_{ss}+\beta_s\beta_{ss})(\alpha_s^2+\beta_s^2)^{-3/2}\right\}t + \alpha_s \tag{2.33}$$

$$y_s = \left\{-\alpha_{ss}(\alpha_s^2+\beta_s^2)^{-1/2} + \alpha_s(\alpha_s\alpha_{ss}+\beta_s\beta_{ss})(\alpha_s^2+\beta_s^2)^{-3/2}\right\}t + \beta_s \tag{2.34}$$

Hence,

$$\begin{aligned} x_s^2+y_s^2 = {} & \beta_{ss}^2(\alpha_s^2+\beta_s^2)^{-1}t^2 + \beta_s^2(\alpha_s\alpha_{ss}+\beta_s\beta_{ss})^2(\alpha_s^2+\beta_s^2)^{-3}t^2 + \alpha_s^2 \\ & -2\beta_{ss}(\alpha_s^2+\beta_s^2)^{-1/2}\beta_s(\alpha_s\alpha_{ss}+\beta_s\beta_{ss})(\alpha_s^2+\beta_s^2)^{-3/2}t^2 \\ & + 2\alpha_s\beta_{ss}(\alpha_s^2+\beta_s^2)^{-1/2}t - 2\beta_s(\alpha_s\alpha_{ss}+\beta_s\beta_{ss})(\alpha_s^2+\beta_s^2)^{-3/2}t + \alpha_s \\ & + \alpha_{ss}^2(\alpha_s^2+\beta_s^2)^{-1}t^2 + \alpha_s^2(\alpha_s\alpha_{ss}+\beta_s\beta_{ss})^2(\alpha_s^2+\beta_s^2)^{-3}t^2 + \beta_s^2 \\ & -2\alpha_{ss}(\alpha_s^2+\beta_s^2)^{-1/2}\alpha_s(\alpha_s\alpha_{ss}+\beta_s\beta_{ss})(\alpha_s^2+\beta_s^2)^{-3/2}t^2 \\ & -2\beta_s\alpha_{ss}(\alpha_s^2+\beta_s^2)^{-1/2}t + 2\alpha_s(\alpha_s\alpha_{ss}+\beta_s\beta_{ss})(\alpha_s^2+\beta_s^2)^{-3/2}t + \beta_s \end{aligned} \tag{2.35}$$

Writing as a quadratic in t, we have

$$\begin{aligned} x_s^2+y_s^2 = {} & (\alpha_s^2+\beta_s^2) + \left\{(\beta_{ss}\alpha_s - \alpha_{ss}\beta_s)(\alpha_s^2+\beta_s^2)^{-1/2}\right\}t \\ & + \left\{(\beta_{ss}^2+\alpha_{ss}^2)(\alpha_s^2+\beta_s^2)^{-1} - (\alpha_s\alpha_{ss}+\beta_s\beta_{ss})^2(\alpha_s^2+\beta_s^2)^{-2}\right\}t^2 \\ = {} & (\alpha_s^2+\beta_s^2) + \left\{2(\beta_{ss}\alpha_s - \alpha_{ss}\beta_s)(\alpha_s^2+\beta_s^2)^{-1/2}\right\}t + \left\{(\alpha_s^2+\beta_s^2)^{-2}(\beta_{ss}\alpha_s - \alpha_{ss}\beta_s)^2\right\}t^2 \\ = {} & (\alpha_s^2+\beta_s^2)\left\{1 + 2(\beta_{ss}\alpha_s - \alpha_{ss}\beta_s)(\alpha_s^2+\beta_s^2)^{-3/2}t + (\beta_{ss}\alpha_s - \alpha_{ss}\beta_s)^2(\alpha_s^2+\beta_s^2)^{-3}t^2\right\} \\ = {} & (\alpha_s^2+\beta_s^2)\left\{1 + (\beta_{ss}\alpha_s - \alpha_{ss}\beta_s)(\alpha_s^2+\beta_s^2)^{-3/2}t\right\}^2 \end{aligned} \tag{2.36}$$

Since $(\beta_{ss}\alpha_s - \alpha_{ss}\beta_s)>0$, $(x_s^2+y_s^2)>(\alpha_s^2+\beta_s^2)$ for $t>0$. To show that the total length of the front increases as it burns, we show that any section of the initial

curve must increase in length as it moves. Choose $s_1, s_2 \in [0,S]$, $s_1 \neq s_2$. The length of the initial curve from s_1 to s_2 is

$$\int_{s_1}^{s_2} (\alpha_s^2+\beta_s^2)^{1/2} ds \tag{2.37}$$

At any time t, the length of the front from s_1 to s_2 is

$$\int_{s_1}^{s_2} (x_s^2+y_s^2)^{1/2} ds \tag{2.38}$$

Since $(x_s^2+y_s^2) > (\alpha_s^2+\beta_s^2)$ for $t>0$, the section must lengthen as it moves.

We want to show that the shape of the burnt region approaches a circle as $t \to \infty$. Let

$$\vartheta(s,t) = \tan^{-1}\left(\frac{y_s}{x_s}\right) \tag{2.39}$$

$\vartheta(s,t)$ is the angle the directed tangent to the front at $(x(s,t),y(s,t))$ makes with the positive x axis, measured in the counterclockwise direction. Let

$$l(s,t) = \frac{\int_0^s (x_\xi^2+y_\xi^2)^{1/2} d\xi}{\int_0^S (x_s^2+y_s^2)^{1/2} ds} \tag{2.40}$$

At any time t, $l(s,t)$ is the length of the front from 0 to s, divided by the total length of the front. Thus $l(0,t)=0$ and $l(S,t)=1$. Since $(x_s^2+y_s^2) \geq (\alpha_s^2+\beta_s^2)>0$, the denominator in (2.40) cannot vanish. We now prove that, as we go along the front in the direction of increasing s, the change in ϑ with respect to l approaches the constant 2π as $t \to \infty$. Differentiation of (2.40) with respect to s yields

$$\frac{\partial l(s,t)}{\partial s} = \frac{(x_s^2+y_s^2)^{1/2}}{\int_0^S (x_s^2+y_s^2)^{1/2} ds} \tag{2.41}$$

Using (2.29) and (2.36), we have

$$\frac{\partial \vartheta(s,t)}{\partial l} = \frac{\partial \tan^{-1}\left(\frac{y_s}{x_s}\right)}{\partial l} \tag{2.42}$$

$$= \frac{\partial \tan^{-1}\left(\frac{y_s}{x_s}\right)}{\partial s}\,\frac{\partial s}{\partial l}$$

$$= \left\{\frac{(\beta_{ss}\alpha_s - \alpha_{ss}\beta_s)}{(\alpha_s^2+\beta_s^2)}\right\}\left\{\frac{\int_0^S (\alpha_s^2+\beta_s^2)^{1/2}\left\{1 + (\beta_{ss}\alpha_s - \alpha_{ss}\beta_s)(\alpha_s^2+\beta_s^2)^{-3/2}t\right\}ds}{(\alpha_s^2+\beta_s^2)^{1/2}\left\{1 + (\beta_{ss}\alpha_s - \alpha_{ss}\beta_s)(\alpha_s^2+\beta_s^2)^{-3/2}t\right\}}\right\}$$

Evaluating the limit of (2.42) as $t \to \infty$, we have

$$\lim_{t\to\infty}\frac{\partial \vartheta(s,t)}{\partial l} = \left\{\frac{(\beta_{ss}\alpha_s - \alpha_{ss}\beta_s)}{(\alpha_s^2+\beta_s^2)}\right\}\left\{\frac{\int_0^S (\alpha_s^2+\beta_s^2)^{-1}(\beta_{ss}\alpha_s - \alpha_{ss}\beta_s)ds}{(\alpha_s^2+\beta_s^2)^{-1}(\beta_{ss}\alpha_s - \alpha_{ss}\beta_s)}\right\} \tag{2.43}$$

$$= \int_0^S (\alpha_s^2+\beta_s^2)^{-1}(\beta_{ss}\alpha_s - \alpha_{ss}\beta_s)ds$$

$$= \int_0^S \frac{\partial \tan^{-1}\left(\frac{\beta_s}{\alpha_s}\right)}{\partial s}ds$$

Since the curve is simple and closed, the tangent vector must go through a rotation of 2π as we go along the curve from beginning to end. Hence,

$$\lim_{t\to\infty}\frac{\partial \vartheta(s,t)}{\partial t} = 2\pi \tag{2.44}$$

We can now complete the proof. Two curves have the same shape if there exists a rescaling, a translation and a rigid body rotation that carries the first onto the second. Define $L(t)$ to be the length of the front $(x(s,t),y(s,t))$ at time t,

$$L(t) = \int_0^S (\alpha_s^2+\beta_s^2)^{1/2}ds \tag{2.45}$$

and define a rescaled version $\bar{\gamma}(s,t)$ of the front:

$$\bar{\gamma}(s,t) \equiv (\bar{x}(s,t),\bar{y}(s,t)) \equiv \left\{ \frac{x(s,t)}{L(t)}, \frac{y(s,t)}{L(t)} \right\} \tag{2.46}$$

For any t, $\bar{\gamma}(s,t)$ has length one, since

$$\int_0^S (\bar{x}_s^2+\bar{y}_s^2)^{1/2} ds = \int_0^S \left\{ \frac{x_s^2}{L^2} + \frac{y_s^2}{L^2} \right\}^{1/2} ds \tag{2.47}$$

$$= \frac{1}{L}\int_0^S (x_s^2+y_s^2)^{1/2} ds$$

$$= \frac{1}{L}(L) = 1$$

Under this scaling, the expression $\frac{\partial \vartheta}{\partial l}$ is invariant, as can be seen by checking that

$$\frac{\partial \tan^{-1}\left(\frac{\bar{y}_s}{\bar{x}_s}\right)}{\partial l} = \frac{\partial \tan^{-1}\left(\frac{y_s/L}{x_s/L}\right)}{\partial l} \tag{2.48}$$

$$= \frac{\partial \tan^{-1}\left(\frac{y_s}{x_s}\right)}{\partial l}$$

Here, we have used the fact that $l(\bar{x}(s,t),\bar{y}(s,t)) = l(x(s,t),y(s,t))$. Since $\bar{\gamma}(s,t)$ has total length one, then l is the same as arc length, as may been seen from (2.40):

$$l(\bar{x},\bar{y}) = \frac{\int_0^s (\bar{x}_\xi^2+\bar{y}_\xi^2)^{1/2} d\xi}{\int_0^S (\bar{x}_s^2+\bar{y}_s^2)^{1/2} ds} = \int_0^s (\bar{x}_\xi^2+\bar{y}_\xi^2)^{1/2} d\xi \tag{2.49}$$

Thus, $\frac{\partial \tan^{-1}\left(\frac{\bar{y}_s}{\bar{x}_s}\right)}{\partial l}$ is the change in the angle between the directed tangent and the positive x axis with respect to arc length.

Choose ε. We now show that we can put a circle of radius $\left(\frac{1}{2\pi} - \varepsilon\right)$ inside $\bar{\gamma}(s,t)$ for t greater than some t_0. From (2.44), we know that there exists a t_0 such that, for $t > t_0$,

$$\frac{\partial \tan^{-1}\left(\frac{y_s}{x_s}\right)}{\partial l} < 2\pi\left(\frac{1}{1-2\pi\varepsilon}\right) \tag{2.50}$$

Since (2.48) is invariant under the rescaling, we have

$$\frac{\partial \tan^{-1}\left(\frac{\bar{y}_s}{\bar{x}_s}\right)}{\partial l} < 2\pi\left(\frac{1}{1-2\pi\varepsilon}\right) \tag{2.51}$$

We translate $\bar{\gamma}(s,t_o)$ so that $\bar{\gamma}(0,t_o)=(\frac{1}{2\pi},0)$ and rotate so that the tangent to $\bar{\gamma}(s,t_o)$ at $\bar{\gamma}(0,t_o)$ points straight up.

Let C^1 be the circle of radius $(\frac{1}{2\pi}-\varepsilon)$ centered at $(\varepsilon,0)$. We parameterize C_1 by arc length and let

$$C_1(s) \equiv (u(s),v(s)) \tag{2.52}$$

$$\equiv \left\{\left(\frac{1}{2\pi}-\varepsilon\right)\cos\left\{\frac{s}{\left(\frac{1}{2\pi}-\varepsilon\right)}\right\}+\varepsilon\,,\left(\frac{1}{2\pi}-\varepsilon\right)\sin\left\{\frac{s}{\left(\frac{1}{2\pi}-\varepsilon\right)}\right\}\right\}$$

$$0 \le s \le \left(\frac{1}{2\pi}-\varepsilon\right)$$

Clearly, $C_1(0) = (\frac{1}{2\pi},0)$ and the tangent to C_1 points straight up at $s=0$. Thus, C_1 and $\bar{\gamma}$ are tangent at $s=0$ and are both positively oriented. Furthermore, since $u_s^2+v_s^2=1$, we have that

$$\frac{\partial \tan^{-1}\left(\frac{v_s}{u_s}\right)}{\partial s} = \frac{v_{ss}u_s - u_s v_{ss}}{u_s^2+v_s^2} \tag{2.53}$$

$$= v_{ss}u_s - u_{ss}v_s$$

$$= \left\{\frac{1}{\left(\frac{1}{2\pi}-\varepsilon\right)}\right\}\sin^2\left\{\frac{s}{\left\{\frac{1}{\left(\frac{1}{2\pi}-\varepsilon\right)}\right\}}\right\}+\left\{\frac{1}{\left(\frac{1}{2\pi}-\varepsilon\right)}\right\}\cos^2\left\{\frac{s}{\left\{\frac{1}{\left(\frac{1}{2\pi}-\varepsilon\right)}\right\}}\right\}$$

$$= \left\{ \frac{1}{\frac{1}{2\pi} - \varepsilon} \right\} = 2\pi \left[\frac{1}{1-2\pi\varepsilon} \right]$$

$$> \frac{\partial \tan^{-1}(\frac{\bar{y}_s}{\bar{x}_s})}{\partial l}$$

Thus, for all $t > t_0$, the change in the angle the directed tangent makes with the positive x axis is greater for C_1 than it is for $\bar{\gamma}(s)$; C_1 "curves in" faster than $\bar{\gamma}(s)$, and thus they cannot cross. Therefore, for $t > t_0$, $\bar{\gamma}$ is outside C_1. (See Figure (2.4))

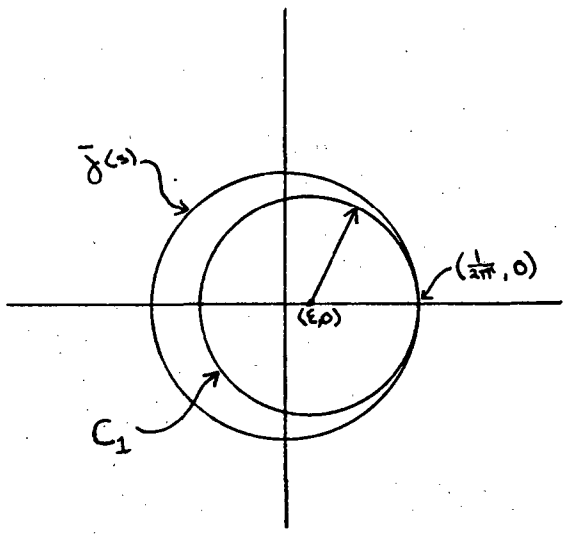

Figure 2.4

A similar argument shows that there is a circle C_2 of radius $(\frac{1}{2\pi} + \varepsilon)$ lying outside $\bar{\gamma}$. Curvature is defined as the change in the angle between the directed tangent and the positive x axis with respect to arc length. Thus, the curvature of the inner circle is greater than that of $\bar{\gamma}$, and the curvature of the outer circle is less than that of $\bar{\gamma}$. As $\varepsilon \to 0$, the inner circle and outer circles come together, trapping the scaled front, and the curvature of $\bar{\gamma}(s)$ approaches $\frac{1}{2\pi}$.

This completes the proof.

We would like to extend Theorem 1 to include convex curves with straight line segments. However, the curvature of the rescaled version of such a curve cannot approach a constant, since the straight line segments always have zero curvature. Thus, we are content to prove that the scaled front can be trapped between two arbitrarily close circles.

Theorem 2. Let γ be a simple, closed, regular, parameterized, positively oriented, convex plane curve of class C^2. Then

1) The propagating front is always convex.

2) Given ε, there exists a t_o such that for all $t>t_o$, the interior of $(\bar{x}(s,t),\bar{y}(s,t))$ contains a circle of radius $(\frac{1}{2\pi}-\varepsilon)$, and $(\bar{x}(s,t),\bar{y}(s,t))$ lies inside a circle of radius $(\frac{1}{2\pi}+\varepsilon)$.

Proof. By Lemma 1, $\partial_s(\tan^{-1}(\frac{y_s}{x_s})) = (\beta_{ss}\alpha_s-\alpha_{ss}\beta_s)(\alpha_s^2+\beta_s^2)^{-1}$. By assumption, this is non-negative, hence the front is convex.

We now show that

$$\lim_{t\to\infty}\left\{\bar{x}^2(s,t)+\bar{y}^2(s,t)\right\}^{1/2} = \frac{1}{2\pi} \tag{2.54}$$

Using (2.36) and (2.43), we have

$$L(t) = \int_0^S (x_s^2+y_s^2)^{1/2} ds \tag{2.55}$$

$$= \int_0^S (\alpha_s^2+\beta_s^2)^{1/2} \left\{ 1+(\beta_{ss}\alpha_s - \alpha_{ss}\beta_s)(\alpha_s^2+\beta_s^2)^{-3/2} t \right\} ds$$

$$= \int_0^S (\alpha_s^2+\beta_s^2)^{1/2} ds + t \int_0^S \frac{(\beta_{ss}\alpha_s - \alpha_{ss}\beta_s)}{(\alpha_s^2+\beta_s^2)} ds$$

$$= \int_0^S (\alpha_s^2+\beta_s^2)^{1/2} ds + t \int_0^S \partial_s (\tan^{-1}(\frac{\beta_s}{\alpha_s})) ds$$

$$= L(0)+2\pi t$$

Thus, using (2.18), (2.19) and (2.46),

$$\bar{x}^2+\bar{y}^2 = \left[\frac{x}{L(t)}\right]^2 + \left[\frac{y}{L(t)}\right]^2 = \frac{1}{L(t)}\left[x^2+y^2\right] \tag{2.56}$$

$$= \frac{1}{(L(0)+2\pi t)^2}\left[t^2 + 2(\alpha\beta_s - \beta\alpha_s)(\alpha_s^2+\beta_s^2)^{-1/2} t + (\alpha_s^2+\beta_s^2)\right]$$

Evaluation of the limit as $t \to \infty$ yields

$$\lim_{t\to\infty} (\bar{x}^2 + \bar{y}^2) = \frac{1}{(2\pi)^2} \tag{2.57}$$

Therefore, given ε, we can find a t_o such that for $t > t_o$, the distance from any point on the scaled front $(\bar{x},\bar{y})$ to the origin is greater than $(\frac{1}{2\pi} - \varepsilon)$ and less than $(\frac{1}{2\pi} + \varepsilon)$. Hence, we can inscribe inside the front a circle of radius $(\frac{1}{2\pi} - \varepsilon)$ and one outside of radius $(\frac{1}{2\pi} + \varepsilon)$.

All that remains is to show that the interior of $(\bar{x},\bar{y})$ contains the smaller circle. We do this by proving that

$$\lim_{t\to\infty} \partial_s (\tan^{-1}(\frac{y}{x})) > 0 \tag{2.58}$$

This will mean that the original front and the rescaled front contain the origin. We have that

$$\partial_s(\tan^{-1}(\frac{y}{x})) = \frac{xy_s - yx_s}{(x_s^2+y_s^2)^{1/2}} \tag{2.59}$$

{N.B. By (2.36), $(x_s^2+y_s^2) \geq (\alpha_s^2+\beta_s^2) > 0$, thus the denominator cannot vanish.} Using (2.18) and (2.19), we have that

$$xy_s - yx_s = (\beta_{ss}\alpha_s - \alpha_{ss}\beta_s)(\alpha_s^2+\beta_s^2)^{-1}\, t^2 \tag{2.60}$$

$$+ \left[(\alpha_s^2+\beta_s^2)^{1/2} + (\alpha\beta_s - \beta\alpha_s)(\beta_{ss}\alpha_s - \alpha_{ss}\beta_s)(\alpha_s^2+\beta_s^2)^{-3/2} \right] t$$

$$+ \alpha\beta_s - \alpha\beta_s$$

If $(\beta_{ss}\alpha_s - \alpha_{ss}\beta_s) > 0$, then the coefficient of t^2 is positive. If $(\beta_{ss}\alpha_s - \alpha_{ss}\beta_s) = 0$, then the coefficient of t^2 is zero and the coefficient of t is positive. Thus, $\lim_{t\to\infty} (xy_s - yx_s) > 0$ and hence $\lim_{t\to\infty} \partial_s(\tan^{-1}(\frac{x}{y})) > 0$. This completes the proof.

Remark. We present here an alternate proof when $(\beta_{ss}\alpha_s - \alpha_{ss}\beta_s) > 0$. Let $A(t)$ be the area inside the scaled front at time t. If A is bounded by a positively oriented, simple, closed curve $\omega(s) = (\alpha(s), \beta(s))$, where $s \in [a,b]$ is an arbitrary parameter and $\omega(a) = \omega(b)$, then

$$A = \frac{1}{2}\int_a^b (\alpha\beta' - \beta\alpha')dt \tag{2.61}$$

(See Do Carmo [4]). Thus, the area of the scaled front at time t is

$$A(t) = \frac{1}{2}\int_0^S \frac{(xy_s - yx_s)}{L^2(t)} ds \tag{2.62}$$

Recall that

$$L(t) = L(0) + 2\pi t \tag{2.63}$$

Thus,

$$A(t) = \frac{1}{2}\left\{ \frac{1}{(L(0) + 2\pi t)^2} \right\} \int_0^S (xy_s - yx_s) ds \tag{2.64}$$

Using (2.60), evaluation of the limit as $t \to \infty$ yields

$$\lim_{t\to\infty} A(t) = \frac{1}{2}\frac{1}{4\pi^2}\int_0^S \frac{(\beta_{ss}\alpha_s - \alpha_{ss}\beta_s)}{(\alpha_s^2+\beta_s^2)}ds \tag{2.65}$$

$$= \frac{1}{2}\frac{1}{4\pi^2}\int_0^S \frac{\partial \tan^{-1}(\frac{\beta_s}{\alpha_s})}{\partial s}ds$$

$$= \frac{1}{2}\frac{1}{4\pi^2}2\pi$$

$$= \frac{1}{4\pi}$$

Thus, as $t \to 0$, the area enclosed by the scaled-down front $\bar{\gamma}(s)$ approaches $\frac{1}{4\pi}$.

We state without proof the Isoperimetric Inequality: Let C be a simple , closed, plane curve with length 1, and let A be the area of the region bounded by C. Then $(1 - 4\pi A) \geq 0$, and equality holds if and only if C is a circle. (See Do Carmo [4]). We have shown that

$$\lim_{t\to\infty} (1 - 4\pi A(t)) = (1 - 4\pi(\frac{1}{4\pi})) = 0 \tag{2.66}$$

Thus, since the curve is convex, the front approaches a circle.

We have studied the propagation of a smooth, convex flame front. The trajectory of each point $s_1 \in [0,S]$ on the front (that is, the curve $(x(s_1,t), y(s_1,t))$, $t \in [0,\infty)$) always points in a direction normal to the front, and has a constant speed k. (See Figure (2.5)).

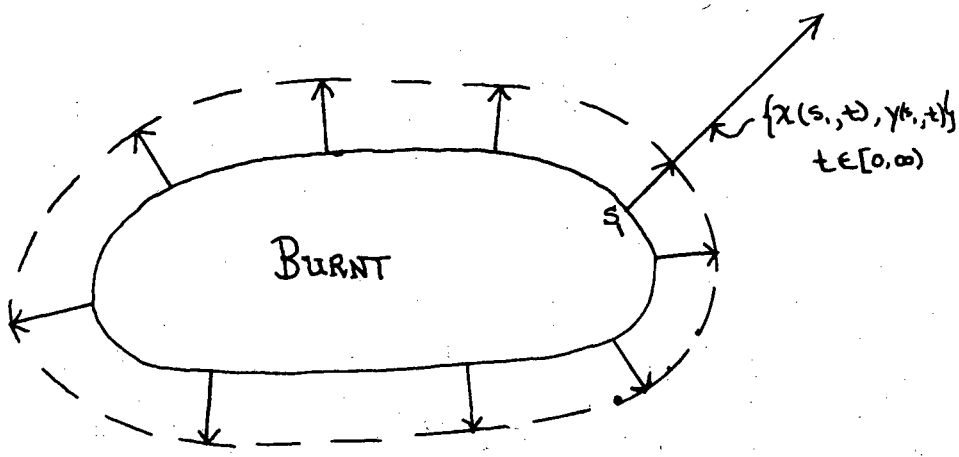

Figure 2.5

We may view these trajectories as objects akin to characteristics; they are curves along which the temperature required for ignition is transported. Our equations

$$x(s,t) = k\,\frac{\beta_s}{(\alpha_s^2+\beta_s^2)^{1/2}}t + \alpha(s) \tag{2.67}$$

$$y(s,t) = -k\,\frac{\alpha_s}{(\alpha_s^2+\beta_s^2)^{1/2}}t + \beta(s) \tag{2.68}$$

describe a family of ignition curves; given $s_1 \in [0,S]$, $(x(s_1,t),y(s_1,t))$, $t \in [0,\infty)$ is the ignition curve starting from $(\alpha(s_1),\beta(s_1))$ with speed k. Since we require that the flame always burn in a direction normal to itself, by definition the ignition curves must be normal to the front at all times. In addition, in Lemma 1 we showed that the ignition curves are straight lines with slope $\frac{-\alpha_s}{\beta_s}$ if the flame propagates at a constant speed.

We mention in passing that there are other models of flame propagation in which the ignition curves are not straight lines. For example, Markstein [11]

proposed that the flame speed be taken as a function of the curvature at any point. The flatter the curve, the faster the flame burns. In this case, the ignition curves are normal to the front but are not straight lines. (See Figure (2.6)).

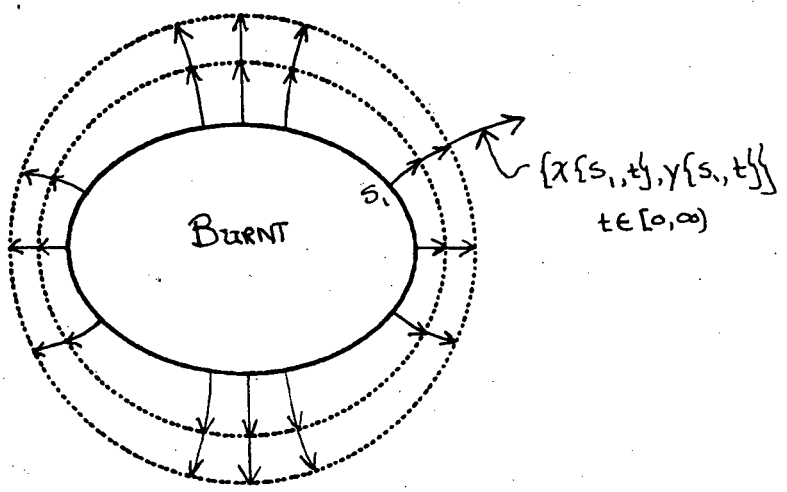

Figure 2.6

Returning to our model of a flame propagating at a uniform, constant speed, in our next lemma we prove that the ignition curves leaving the initial front fan out over all of the unburnt fluid. That is, given any point in the unburnt fluid, there is one and only one ignition curve passing through that point.

Lemma 2. Let $\gamma(s)=(\alpha(s),\beta(s))$ be a simple, closed, regular, convex, parameterized, positively oriented, plane curve of class C^2. Assume that the particles inside γ are burnt, and those outside are unburnt. At $t=0$, ignite the particles on the curve γ, and assume that the flame propagates in a direction normal to itself with constant speed. Suppose (x_1,y_1) is a point that lies outside γ. Then there is one and only one ignition curve leaving γ and passing through (x_1,y_1).

Proof. We need only check that the mapping $(x(s,t),y(s,t))$ given in (2.67) and (2.68) is invertible. Then, given (x_1,y_1), there will be a unique s_1 and t_1 such that $(x(s_1,t_1),y(s_1,t_1)) = (x_1,y_1)$, and the unique ignition curve will be the one leaving $\gamma(s_1)$ with slope $\dfrac{-\alpha_s(s_1)}{\beta_s(s_1)}$. Without loss of generality, let $k=1$. The Jacobian of (2.28) and (2.29) is

$$\begin{vmatrix} x_s & x_t \\ y_s & y_t \end{vmatrix} = x_s y_t - y_s x_t \tag{2.69}$$

$$= \left\{\left\{\beta_{ss}(\alpha_s^2+\beta_s^2)^{-1/2} - \beta_s(\alpha_s\alpha_{ss}+\beta_s\beta_{ss})(\alpha_s^2+\beta_s^2)^{-3/2}\right\}t + \alpha_s\right\}\left\{-\alpha_s(\alpha_s^2+\beta_s^2)^{-1/2}\right\}$$

$$-\left\{\left\{-\alpha_{ss}(\alpha_s^2+\beta_s^2)^{-1/2} + \alpha_s(\alpha_s\alpha_{ss}+\beta_s\beta_{ss})(\alpha_s^2+\beta_s^2)^{-3/2}\right\}t + \beta_s\right\}\left\{\beta_s(\alpha_s^2+\beta_s^2)^{-1/2}\right\}$$

$$= -\left\{\frac{(\beta_{ss}\alpha_s - \alpha_{ss}\beta_s)}{(\alpha_s^2+\beta_s^2)}t + (\alpha_s^2+\beta_s^2)^{1/2}\right\}$$

For a convex curve,

$$(\beta_{ss}\alpha_s - \alpha_{ss}\beta_s) > 0 \tag{2.70}$$

therefore

$$\begin{vmatrix} x_s & x_t \\ y_s & y_t \end{vmatrix} \neq 0 \tag{2.71}$$

Thus, the mapping is invertible and there exists a unique s_1 and t_1 such that $(x(s_1,t_1),y(s_1,t_1)) = (x_1,y_1)$. This completes the proof.

Given any point in the unburnt fluid, its ignition curve provides the location of the "fuse" that ignites that point. The temperature required for ignition is passed with speed k along the ignition curve to that point.

2.3. Evolution of Convex, Piecewise Smooth Flame Fronts

What happens if the initial curve is not of class C^2? For example, consider a convex curve with an outward pointing cusp, as shown in Figure (2.7)

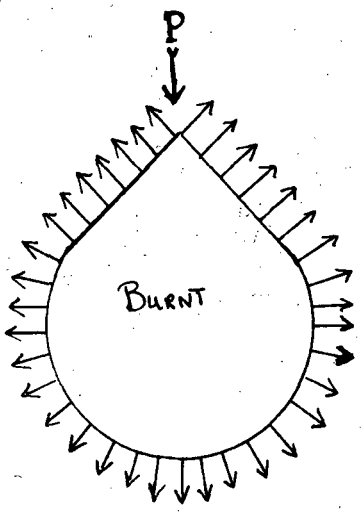

Figure 2.7

Suppose that the curve is twice differentiable everywhere except at the point P. At P, the normal is not defined, and thus the direction of motion is unspecified. We do not know how to draw the ignition curves in the triangular region above P. A similar question occurs in the study of the motion of a gas behind a piston. If the piston is withdrawn at a supersonic speed, the characteristics fan out, leaving an open area. In that area, we construct a rarefaction wave to bridge the solution. For the outward pointing cusp, how shall we fill in the ignition curves above P to provide a physically correct solution?

Consider a domain D in which all the particles are unburnt, and suppose that at $t=0$ we ignite the particle located at a point $(x,y) \in D$. The surrounding unburnt particles will become ignited as the high ignition temperature is passed on, and these newly burnt particles will ignite their surrounding unburnt neighbors. For $t>0$, the flame front will be a circle, centered at (x,y).

with radius kt. (See Figure (2.8)).

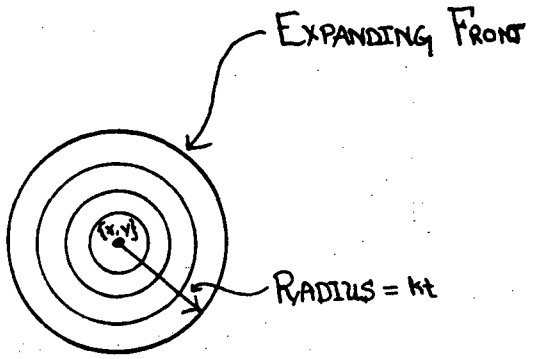

Figure 2.8

The ignition curves spread radially out from (x,y), and the front moves in a direction normal to itself with speed k.

With this in mind, we return to the outward pointing cusp and extend ignition curves radially from the point P into the unburnt fluid at the same speed as elsewhere on the front. (See Figure (2.9))

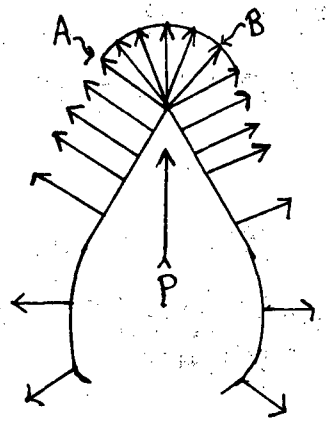

Figure 2.9

This will provide the bridge between ignition curves $\overline{PA}$ and $\overline{PC}$, and will give us a way to move the front so that, for $t>0$, there will be a well-defined and continuously turning normal vector.

We now make these ideas more precise.

Definition. Let $\gamma(s)=(\alpha(s),\beta(s))$, $s\in[0,S]$, $\gamma(0)=\gamma(S)$ be a closed, parameterized, positively oriented, plane curve. Suppose that

1) γ is a piecewise C^2 function of s. That is, a) γ is a continuous function of s and b) there exists a finite number of points $0=s_0<s_1<\ldots\ldots<s_n=S$ such that on every closed interval $[s_i,s_{i+1}]$, $0\le i\le n-1$, γ is twice differentiable.

2) $\gamma(0)=\gamma(S)$, $\gamma'(0)=\gamma'(S)$, $\gamma''(0)=\gamma''(S)$.

3) Wherever the curve is twice differentiable, $(\alpha_s^2+\beta_s^2)\neq 0$.

4) γ is convex; that is a) at all points where the curve is twice differentiable, $\partial_s(\tan^{-1}(\frac{\beta_s}{\alpha_s}))\geq 0$, and b) if s_i is a point where γ is not

twice differentiable, $\lim_{s \to s_i^-} \left\{\tan^{-1}\left(\frac{\beta_s}{\alpha_s}\right)\right\} \leq \lim_{s \to s_i^+} \left\{\tan^{-1}\left(\frac{\beta_s}{\alpha_s}\right)\right\}$. In other words, the angle the directed tangent makes with the positive x axis is a non-decreasing function of s, wherever it is defined and measured in the counterclockwise direction.

Then we shall refer to any curve satisfying the above as a convex, piecewise C^2 and piecewise regular curve, where it is understood that the curve is also closed, parameterized, and positively oriented.

We can now describe the propagation of a convex, piecewise C^2 and piecewise regular initial front. At any point $(\alpha(s),\beta(s))$ where the curve is twice differentiable, the normal is well-defined, and we may use (2.67)-(2.68) to determine the path of the ignition curve starting at $(\alpha(s),\beta(s))$. From any point $s_i \in (0,S)$ where the curve is not twice differentiable, we extend a group of ignition curves, one for each angle between $\lim_{s \to s_i^-} (\tan^{-1}(\frac{-\alpha_s}{\beta_s}))$ and $\lim_{s \to s_i^+} (\tan^{-1}(\frac{-\alpha_s}{\beta_s}))$, inclusive. (Note that the slope of the ignition curve is the negative reciprocal of the slope of the tangent, and that if $a<b$, then $-1/a < -1/b$). These ignition curves fan out radially from $(\alpha(s_i),\beta(s_i))$, carrying the high ignition temperature and bridging the solution between the ignition curve on the right with slope $\lim_{s \to s_i^-} (\tan^{-1}(\frac{-\alpha_s}{\beta_s}))$ and the one on the left with slope $\lim_{s \to s_i^+} (\tan^{-1}(\frac{-\alpha_s}{\beta_s}))$.

Example 2.3 We give an example of the propagation of a convex, piecewise C^2 and piecewise regular flame front. Let $\gamma(s)=(\alpha(s),\beta(s))$, $s\in[0,3\pi/2+2]$, where

$$\alpha(s)=\begin{cases}\cos(s-\pi/2) & 0\le s<\pi/2\\ 1 & \pi/2\le s<\pi/2+1\\ -s+(\pi/2+2) & \pi/2+1\le s<\pi/2+2\\ \cos(s-2) & \pi/2+2\le s\le 3\pi/2+2\end{cases} \tag{2.72}$$

$$\beta(s)=\begin{cases}\sin(s-\pi/2) & 0\le s<\pi/2\\ s-\pi/2 & \pi/2\le s<\pi/2+1\\ 1 & \pi/2+1\le s<\pi/2+2\\ \sin(s-2) & \pi/2+2\le s\le 3\pi/2+2\end{cases} \tag{2.73}$$

A check shows that α and β are both C^2 functions of s everywhere except at $s=\pi/2$, $\pi/2+1$, and at $\pi/2+2$. Furthermore, γ is closed, convex, and positively oriented. Thus, γ is a convex, piecewise C^2 and piecewise regular curve. The trace of γ is shown in Figure (2.10).

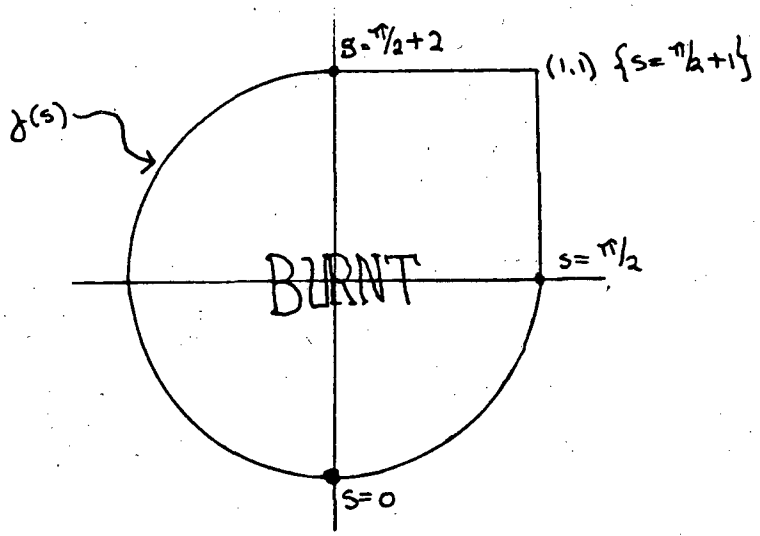

Figure 2.10

Assume that the particles inside γ are burnt, and those outside are unburnt. At $t=0$, we ignite the particles along γ.

Except at $s=\pi/2+1$, α and β are C^1 functions of s, with $(\alpha_s^2+\beta_s^2)=1$. Thus, given $s_1\in[0,3\pi/2+2]$, $s_1\neq\pi/2+1$, the normal at $(\alpha(s),\beta(s))$ exists and we can use (2.67) and (2.68) to determine the path of the ignition curve emanating from $(\alpha(s_1),\beta(s_1))$. In Figure (2.11), we show those ignition curves.

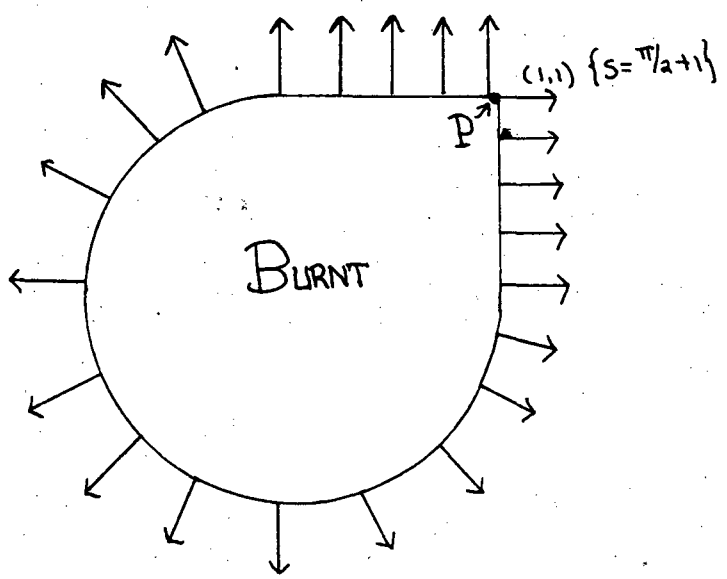

Figure 2.11

$$x(s,t)=\left\{\begin{array}{cc} k\cos(s-\pi/2)t+\cos(s-\pi/2) & 0\le s<\pi/2 \\ kt+1 & \pi/2\le s<\pi/2+1 \\ -s+(\pi/2+2) & \pi/2+1\le s<\pi/2+2 \\ k\cos(s-2)t+\cos(s-2) & \pi/2+2\le s\le 3\pi/2+2 \end{array}\right\} \quad (2.74)$$

$$y(s,t)=\left\{\begin{array}{cc} -k\sin(s-\pi/2)t+\sin(s-\pi/2) & 0\le s<\pi/2 \\ s-\pi/2 & \pi/2\le s<\pi/2+1 \\ -kt+1 & \pi/2+1\le s<\pi/2+2 \\ k\sin(s-2)t+\sin(s-2) & \pi/2+2\le s\le 3\pi/2+2 \end{array}\right\} \quad (2.75)$$

This gives the position of the front at time t for $s\in[0,3\pi/2+2]$, $s\neq\pi/2+1$.

At point P, we wish to extend ignition curves into the unburnt fluid, as shown in Figure (2.12).

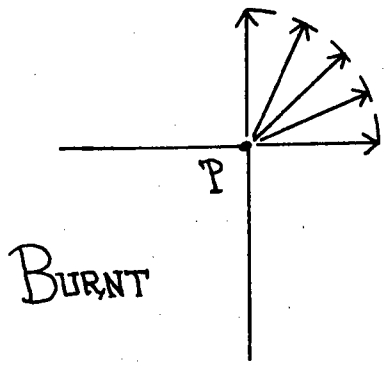

Figure 2.12

Unfortunately, such a construction poses a minor difficulty. We need to be able to distinguish one ignition curve from another, but we have only the value $s=\pi/2+1$ at our disposal. (Elsewhere on the front, there is a one-to-one correspondence between values of $s\in[0,3\pi/2+2]$ and ignition curves). We choose to reparameterize the initial curve γ in such a way that there are "enough" values of s at P to facilitate a full set of ignition curves. Let $\gamma_1=(\alpha_1(s),\beta_1(s))$, $s\in[0,3\pi/2+3]$, where

$$\alpha_1(s)=\left\{\begin{array}{cc}\cos(s-\pi/2) & 0\le s<\pi/2\\ 1 & \pi/2\le s<\pi/2+1\\ 1 & \pi/2+1\le s\le\pi/2+2\\ -s+(\pi/2+3) & \pi/2+2<s<\pi/2+3\\ \cos(s-3) & \pi/2+3\le s\le 3\pi/2+3\end{array}\right\} \qquad (2.76)$$

$$\beta_1(s) = \begin{cases} \sin(s-\pi/2) & 0 \le s < \pi/2 \\ (s-\pi/2) & \pi/2 \le s < \pi/2+1 \\ 1 & \pi/2+1 \le s \le \pi/2+2 \\ 1 & \pi/2+2 < s < \pi/2+3 \\ \sin(s-3) & \pi/2+3 \le s \le 3\pi/2+3 \end{cases} \tag{2.77}$$

Note that the trace of γ_1 is the same as that of γ, but that for all $s \in [\pi/2+1, \pi/2+2]$, $(\alpha_1(s), \beta_1(s)) = (1,1)$. This will provide us with "enough" values of s at P to give one to each radial ignition curve. (From now on, we omit the subscript 1). Also, α and β are C^1 functions of s with $\alpha_s^2 + \beta_s^2 = 1$ for s not in $[\pi/2+1, \pi/2+2]$. Let

$$x(s,t) = k(\cos(\frac{\pi}{2}(s-\pi/2+1)))t+1 \tag{2.78}$$

$$y(s,t) = k(\sin(\frac{\pi}{2}(s-\pi/2+1)))t+1 \tag{2.79}$$

for $t \ge 0$, $\pi/2+1 \le s \le \pi/2+2$. This corresponds to a family of ignition curves leaving P; given $s \in [\pi/2+1, \pi/2+2]$, we have $(x(s,0), y(s,0)) = (1,1)$, $x_t^2 + y_t^2 = k^2$, and $\frac{y_t}{x_t} = \tan(\frac{\pi}{2}(s-(\pi/2+1)))$. (See Figure (2.13)).

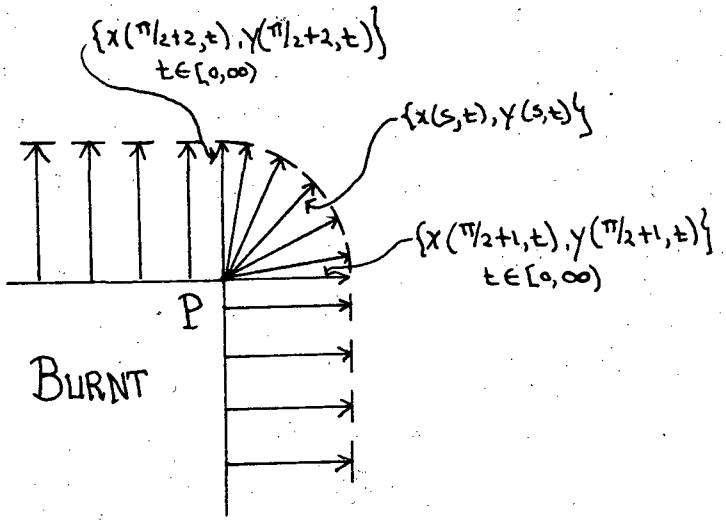

Figure 2.13

We need only check that ignition curves leaving P match up with the ignition curves given in (2.78) and (2.79). Using (2.76),(2.77),(2.78) and (2.79), we have

$$\lim_{(s\to(\pi/2+1))^-}(x(s,t),y(s,t)) = (kt+1,1) = \lim_{(s\to(\pi/2+1))^+}(x(s,t),y(s,t))$$

$$\lim_{(s\to(\pi/2+2))^-}(x(s,t),y(s,t)) = (1,kt+1) = \lim_{(s\to(\pi/2+2))^+}(x(s,t),y(s,t))$$

Thus we have extended ignition curves from every point on the initial front. The full set of ignition curves are

$$x(s,t) = \begin{cases} k\cos(s-\pi/2)t+\cos(s-\pi/2) & 0\le s<\pi/2 \\ kt+1 & \pi/2\le s<\pi/2+1 \\ k(\cos((\pi/2)(s-\pi/2+1)))t+1 & \pi/2+1\le s\le\pi/2+2 \\ -s+(\pi/2+3) & \pi/2+2<s<\pi/2+3 \\ k\cos(s-3)t+\cos(s-3) & \pi/2+3\le s\le 3\pi/2+3 \end{cases} \quad (2.80)$$

$$y(s,t) = \begin{cases} k\sin(s-\pi/2)t+\sin(s-\pi/2) & 0\le s<\pi/2 \\ s-\pi/2 & \pi/2\le s<\pi/2+1 \\ k(\sin((\pi/2)(s-\pi/2+1)))t+1)+1 & \pi/2+1\le s\le\pi/2+2 \\ kt+1 & \pi/2+2<s<\pi/2+3 \\ k\sin(s-3)t+\sin(s-3) & \pi/2+3\le s\le 3\pi/2+3 \end{cases} \quad (2.81)$$

This gives the position of the front for $t\ge 0$ and $s\in[0,3\pi/2+3]$. This completes the example.

Our technique for deciding how to move a curve in a direction normal to itself when the normal is not defined has been based on physical arguments. We developed a smooth transition from the ignition curve defined from the right at a corner to the ignition curve defined from the left by means of a set of ignition curves fanning out from the point in question. In our next theorem, we show that such a construction is a natural extension of our earlier results.

Theorem 3. Let γ be a convex, piecewise C^2 and piecewise regular curve. Suppose that the particles inside γ are burnt, and those outside are unburnt. At

$t=0$, we ignite the particles along γ.

1) There exists a sequence $\gamma_\varepsilon(s)=(\alpha_\varepsilon(s),\beta_\varepsilon(s))$, $s\in[0,S^\varepsilon]$, $\gamma_\varepsilon(0)=\gamma_\varepsilon(S^\varepsilon)$ of simple, closed, regular, convex, parameterized, positively oriented plane curves of class C^1 such that

$$\lim_{\varepsilon\to 0}\gamma_\varepsilon(s)=\gamma(s) \tag{2.82}$$

for $s\in[0,S^\varepsilon]$.

2) For each γ_ε, suppose that the particles inside γ_ε are burnt and those outside are unburnt. At $t=0$ we ignite the particles along γ_ε. Assume that the flame front γ_ε propagates in a direction normal to itself with speed k, and let its position at any time t be given by $(x_\varepsilon(s,t),y_\varepsilon(s,t))$, $s\in[0,S^\varepsilon]$. Suppose we allow the front initially at $\gamma(s)$ to move in a direction normal to itself with speed k, wherever the normal is defined. Then, at those points where the normal is not defined, we can construct ignition curves in such a way that

$$\lim_{\varepsilon\to 0} tr(x_\varepsilon(s,t),y_\varepsilon(s,t))= tr(x(s,t),y(s,t)) \tag{2.83}$$

where $(x(s,t),y(s,t))$ is the position of the front at time t. Here, $tr(x(s,t),y(s,t))$ is the trace of the curve $(x(s,t),y(s,t))$, $s\in[0,S]$, and $tr(x_\varepsilon(s,t),y_\varepsilon(s,t))$ is the trace of the approximating curve γ_ε.

3) For $t>0$, $(x(s,t),y(s,t))$ is a curve of class C^0. Furthermore, the normal to $(x(s,t),y(s,t))$ exists everywhere and is a continuous function of s.

Proof. We begin by parameterizing $\gamma(s)$ by arc length; this can be done since γ is piecewise C^2. Thus, we assume that $\alpha_s^2+\beta_s^2=1$ wherever the derivative is defined.

We now construct a sequence of curves γ_ε of class C^1 that tend to γ as ε tends to zero. Let s_1 be a point where $\gamma(s)$ is not differentiable with respect to

s. Let $\alpha_s^-(s_1) = \lim_{s \to s_1^-} \alpha_s$, $\alpha_s^+(s_1) = \lim_{s \to s_1^+} \alpha_s$, $\beta_s^-(s_1) = \lim_{s \to s_1^-} \beta_s$, and $\beta_s^+(s_1) = \lim_{s \to s_1^+} \beta_s$; these limits must exist since the curve is piecewise C^2. Since the curve is parameterized by arc length, $\alpha_s^+(s_1) \neq \alpha_s^-(s_1)$ if and only if $\beta_s^+(s_1) \neq \beta_s^-(s_1)$. We shall assume here, for the sake of space, that $\alpha_s^+(s_1)$, $\alpha_s^-(s_1)$, $\beta_s^+(s_1)$, and $\beta_s^-(s_1)$ are all non-zero; the formulation of γ_ε is only slightly different when one or more of them is negative.

We claim that $\frac{\beta_s^+(s_1)}{\alpha_s^+(s_1)} \neq \frac{\beta_s^-(s_1)}{\alpha_s^-(s_1)}$. We prove this indirectly. Suppose they were equal. Since the curve is parameterized by arc length, either $\alpha_s^+(s_1)=\alpha_s^-(s_1)$ and $\beta_s^+(s_1)=\beta_s^-(s_1)$, or $\alpha_s^+(s_1)=-\alpha_s^+(s_1)$ and $\beta_s^+(s_1)=-\beta_s^+(s_1)$. The former cannot be true since it implies that γ is differentiable at s_1. The latter cannot be true since it implies that the curve is not positively oriented.

Since γ is piecewise C^2, there exists some δ such that for $s \in [s_1-\delta, s_1) \cup (s_1, s_1+\delta]$, α_s and β_s are non-zero. Furthermore, $\frac{\beta_s(s)}{\alpha_s(s)} \neq \frac{\beta_s(s_1+(s_1-s))}{\alpha_s(s_1+(s_1-s))}$ for $s_1-\delta \leq s \leq s_1$, since γ is convex and $\frac{\beta_s^+(s_1)}{\alpha_s^+(s_1)} \neq \frac{\beta_s^-(s_1)}{\alpha_s^-(s_1)}$.

Choose ε such that $0<\varepsilon<\delta$. Draw the line tangent to γ at $(\alpha(s_1+\varepsilon), \beta(s_1+\varepsilon))$ in the direction $(-\alpha_s(s_1+\varepsilon), -\beta_s(s_1+\varepsilon))$. Draw the line tangent to γ at $(\alpha(s_1-\varepsilon), \beta(s_1-\varepsilon))$ in the direction $(\alpha_s(s_1-\varepsilon), \beta_s(s_1-\varepsilon))$. They must intersect at some point P, since their slopes are not equal. Assume, without loss of generality, that $(\alpha_s(s_1-\varepsilon), \beta_s(s_1-\varepsilon))$ is closer than $(\alpha_s(s_1+\varepsilon), \beta_s(s_1+\varepsilon))$ to the point P, (see Figure (2.14)) and consider the curve $\gamma_\varepsilon(s)=(\alpha_\varepsilon(s), \beta_\varepsilon(s))$ defined by

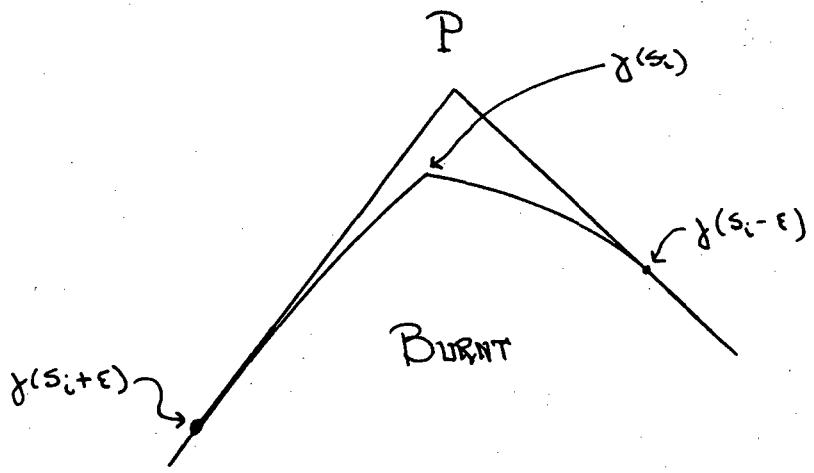

Figure 2.14

(2.84)

$$\alpha_\varepsilon(s)=\begin{cases} \alpha(s) & s\le Z_1 \\ R\left[\cos\left(\dfrac{s-s_1+\varepsilon}{R}-\sin^{-1}(\alpha_s(s_1-\varepsilon))\right)-\beta_s(s_1-\varepsilon)\right]+\alpha(s_1-\varepsilon) & Z_1<s\le Z_2 \\ \dfrac{\alpha(s_1+\varepsilon)-\bar{\alpha}}{L_{BQ}}(s-(\bar{R}-s_1-\varepsilon))+\bar{\alpha} & Z_2<s<Z_3 \\ \alpha(s-\bar{R}-L_{BQ}+2\varepsilon) & Z_3\le s\le Z_4 \end{cases}$$

and

(2.85)

$$\beta_\varepsilon(s)=\begin{cases} \beta(s) & s\le Z_1 \\ R\left[\sin\left(\dfrac{s-s_1+\varepsilon}{R}-\sin^{-1}(\alpha_s(s_1-\varepsilon))\right)+\alpha_s(s_1-\varepsilon)\right]+\beta(s_1-\varepsilon) & Z_1<s\le Z_2 \\ \dfrac{\beta(s_1+\varepsilon)-\bar{\beta}}{L_{BQ}}(s-(\bar{R}-s_1+\varepsilon))+\bar{\beta} & Z_2<s<Z_3 \\ \beta(s-\bar{R}-L_{BQ}+2\varepsilon) & Z_3\le s\le Z_4 \end{cases}$$

$$Z_1 = s_1 - \varepsilon$$

$$Z_2 = \bar{R} + s_1 - \varepsilon$$

$$Z_3 = \bar{R} + s_1 - \varepsilon + L_{BQ}$$

$$Z_4 = \bar{R} + L_{BQ} + S - 2\varepsilon$$

where

$$R = \frac{R_1}{\frac{\beta_s(s_1+\varepsilon)}{\alpha_s(s_1+\varepsilon)} - \frac{\beta_s(s_1-\varepsilon)}{\alpha_s(s_1-e\,1)}} \left[\frac{\beta_s(s_1+\varepsilon)}{\alpha_s(s_1+\varepsilon)} (\alpha(s_1+\varepsilon) - \alpha(s_1-\varepsilon)) + \beta(s_1-\varepsilon) - \beta(s_1+\varepsilon) \right]$$

$$R_1 = \frac{1}{\alpha_s(s_1-\varepsilon)} \left[\frac{1+\alpha_s(s_1-\varepsilon)\alpha_s(s_1+\varepsilon)+\beta_s(s_1-\varepsilon)\beta_s(s_1+\varepsilon)}{(1-(\alpha_s(s_1-\varepsilon)\alpha_s(s_1+\varepsilon)+\beta_s(s_1-\varepsilon)\beta_s(s_1+\varepsilon))^2)^{1/2}} \right]$$

$$\bar{R} = R \left[\sin^{-1}(\alpha_s(s_1-\varepsilon)) + \cos^{-1}(\beta_s(s_1+\varepsilon)) \right]$$

$$\bar{\alpha} = R \left[\beta_s(s_1+\varepsilon) - \beta_s(s_1-\varepsilon) \right] + \alpha(s_1-\varepsilon)$$

$$\bar{\beta} = R \left[-\alpha_s(s_1+\varepsilon) + \alpha_s(s_1-\varepsilon) \right] + \beta(s_1-\varepsilon)$$

$$L_{BQ} = ((\bar{\alpha} - \alpha(s_1+\varepsilon))^2 + (\bar{\beta} - \beta(s_1+\varepsilon))^2)^{1/2}$$

For $s \le s_1 - \varepsilon$, γ_ε is the same as γ. For $s_1 - \varepsilon < s \le \bar{R} + s_1 - \varepsilon$, the trace of γ_ε is the arc of the circle, parameterized by arc length, tangent to the line $\vec{AP}$ at the point $\gamma(s_1-\varepsilon)$ and tangent to the line $\vec{PB}$ at the point Q. For $\bar{R} + s_1 - \varepsilon < s < \bar{R} + s_1 - \varepsilon + L_{BQ}$, the trace of γ_ε is just the straight line, again parameterized by arc length , connecting Q to the point $\gamma(s_1+\varepsilon)$; here L_{BQ} is just distance from Q to B. For $\bar{R} + s_1 - \varepsilon + L_{BQ} \le s < \bar{R} + L_{BQ} + S - 2\varepsilon$, the trace of γ_ε is the same as the trace of $\gamma(s)$ from $s_1+\varepsilon$ to S. (See Figure (2.15))

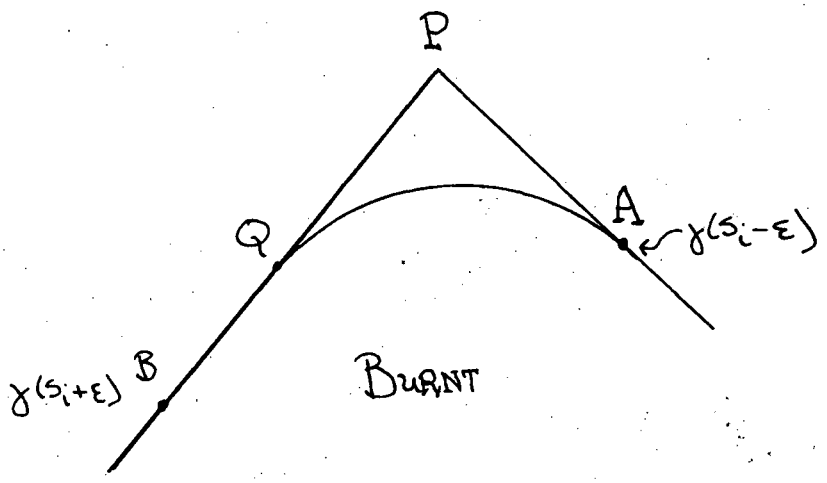

Figure 2.15

We need to check two things; first, that $\lim_{\varepsilon\to 0}\gamma_\varepsilon(s)=\gamma(s)$ and second, that $\gamma_\varepsilon(s)$ is a curve of class C^1.

Since γ is parameterized by arc length, $\lim_{\varepsilon\to 0}(\alpha(s_1-\varepsilon),\beta(s_1-\varepsilon))=\lim_{\varepsilon\to 0}(\alpha(s_1+\varepsilon),\beta(s_1+\varepsilon))=(\alpha(s_1),\beta(s_1))$. Hence, as $\varepsilon\to 0$, R vanishes and $\bar{\alpha}=\alpha(s_1)$ and $\bar{\beta}=\beta(s_1)$. By construction, L_{BQ} vanishes, thus $\lim_{\varepsilon\to 0}\gamma_\varepsilon=\gamma$, $s\in[0,S]$.

We now check that γ_ε is a curve of class C^1 for $s_1-\delta<s<s_1+\delta$. We only check at the points $s=s_1-\varepsilon$, $\bar{R}+s_1-\varepsilon$ and $\bar{R}+s_1-\varepsilon+L_{BQ}$, since the curve is infinitely differentiable everywhere else. We note that $\sin(\cos^{-1}(\alpha_s))=-\beta_s$, $\sin(\cos^{-1}(\beta_s))=-\alpha_s$, $\cos(\sin^{-1}(\alpha_s))=-\beta_s$ and $\cos(\sin^{-1}(\beta_s))=-\alpha_s$.

We first check α_ε and α_ε' at $s=s_1-\varepsilon$.

$$\lim_{s\to(s_1-\varepsilon)^-}\alpha_\varepsilon=\alpha(s_1-\varepsilon) \tag{2.86}$$

$$\lim_{s\to(s_1-\varepsilon)^+}\alpha_\varepsilon = R(\beta_s(s_1-\varepsilon)-\beta_s(s_1-\varepsilon))+\alpha(s_1-\varepsilon) = \alpha(s_1-\varepsilon)$$

$$\lim_{s\to(s_1-\varepsilon)^-}\alpha_\varepsilon' = \alpha_s(s_1-\varepsilon)$$

$$\lim_{s\to(s_1-\varepsilon)^+}\alpha_\varepsilon' = -\sin(-\sin^{-1}(\alpha_s(s_1-\varepsilon))) = \alpha_s(s_1-\varepsilon)$$

Thus, α_ε and its derivative match at $s=s_1-\varepsilon$. We now check β_ε and β_ε' at the same point.

$$\lim_{s\to(s_1-\varepsilon)^-}\beta_\varepsilon = \beta(s_1-\varepsilon) \tag{2.87}$$

$$\lim_{s\to(s_1-\varepsilon)^+}\beta_\varepsilon = R(\sin(-\sin^{-1}(\alpha(s_1-\varepsilon)))+\alpha(s_1-\varepsilon))+\beta(s_1-\varepsilon)$$

$$= \beta(s_1-\varepsilon)$$

$$\lim_{s\to(s_1-\varepsilon)^-}\beta_s' = \beta_s(s_1-\varepsilon)$$

$$\lim_{s\to(s_1-\varepsilon)^+}\beta_s' = \cos(-\sin^{-1}(\alpha_s(s_1-\varepsilon)))+\alpha_s(s_1-\varepsilon)+\beta_s(s_1-\varepsilon)$$

$$= \beta_s(s_1-\varepsilon)$$

Thus, γ_ε is differentiable at $s=s_1-\varepsilon$. We check α_ε at $s=\bar{R}+s_1-\varepsilon$.

$$\lim_{s\to(\bar{R}+s_1-\varepsilon)^-}\alpha_\varepsilon = R\Big[\cos(\sin^{-1}(\alpha_s(s_1-\varepsilon))+\cos^{-1}(\beta_s(s_1+\varepsilon))-\sin^{-1}(\alpha_s(s_1-\varepsilon)))$$

$$-\beta_s(s_1-\varepsilon)\Big] + \alpha(s_1-\varepsilon) \tag{2.88}$$

$$R\Big[\beta_s(s_1+\varepsilon)-\beta_s(s_1-\varepsilon)\Big] + \alpha(s_1-\varepsilon) = \bar{\alpha}$$

$$\lim_{s\to(\bar{R}+s_1-\varepsilon)^+}\alpha_\varepsilon = \bar{\alpha}$$

Checking α_ε', we have

$$\lim_{s\to(\bar{R}+s_1-\varepsilon)^-}\alpha_\varepsilon' = -\sin(\sin^{-1}(\alpha_s(s_1-\varepsilon))+\cos^{-1}(\beta_s(s_1+\varepsilon))-\sin^{-1}(\alpha_s(s_1-\varepsilon)))$$

$$= -\sin(\cos^{-1}(\beta_s(s_1+\varepsilon))) = \alpha_s(s_1+\varepsilon) \tag{2.89}$$

$$\lim_{s\to(\bar{R}+s_1-\varepsilon)^+}\alpha_\varepsilon' = \frac{\alpha(s_1+\varepsilon)-\bar{\alpha}}{L_{BQ}}$$

$$= \frac{\alpha(s_1+\varepsilon)-\bar{\alpha}}{((\bar{\alpha}-\alpha(s_1+\varepsilon))^2+(\bar{\beta}-\beta(s_1+\varepsilon))^2)^{1/2}}$$

$$= \frac{1}{\left\{1+\dfrac{\beta(s_1+\varepsilon)+R\left[\alpha_s(s_1+\varepsilon)-\alpha_s(s_1-\varepsilon)\right]-\beta(s_1-\varepsilon)}{\alpha(s_1+\varepsilon)-R\left[\beta_s(s_1+\varepsilon)-\beta_s(s_1-\varepsilon)\right]-\alpha(s_1-\varepsilon)}\right\}}$$

$$= \alpha_s(s_1+\varepsilon)$$

Thus, α_ε and its derivatives match at $s=\bar{R}+s_1-\varepsilon$. We check β_ε and β_ε' at the same point.

$$\lim_{s\to(\bar{R}+s_1-\varepsilon)^-}\beta_\varepsilon = R\Big[\sin(\sin^{-1}(\alpha_s(s_1-\varepsilon))+\cos^{-1}(\beta_s(s_1+\varepsilon))-\sin^{-1}(\alpha_s(s_1+\varepsilon)))$$

$$+\alpha_s(s_1-\varepsilon)\Big]+\beta(s_1-\varepsilon) \qquad (2.90)$$

$$= R\Big[-\alpha_s(s_1+\varepsilon)+\alpha_s(s_1-\varepsilon)\Big]+\beta(s_1-\varepsilon)=\bar{\beta}$$

$$\lim_{s\to(\bar{R}+s_1-\varepsilon)^+}\beta_\varepsilon = \bar{\beta}$$

Checking β_ε', we have

$$\lim_{s\to(\bar{R}+s_1-\varepsilon)^-}\beta_\varepsilon' = \cos(\sin^{-1}(\alpha_s(s_1-\varepsilon))+\cos^{-1}(\beta_s(s_1+\varepsilon))-\sin^{-1}(\alpha_s(s_1-\varepsilon)))$$

$$= \beta_s(s_1+\varepsilon) \qquad (2.91)$$

$$\lim_{s\to(\bar{R}+s_1-\varepsilon)^+}\beta_\varepsilon' = \frac{\beta(s_1+\varepsilon)-\bar{\beta}}{L_{BQ}}$$

$$= \frac{\beta(s_1+\varepsilon)-\bar{\beta}}{((\bar{\alpha}-\alpha(s_1+\varepsilon))^2+(\bar{\beta}-\beta(s_1+\varepsilon))^2)^{1/2}}$$

$$= \frac{1}{\left\{1+\left\{\dfrac{\alpha(s_1+\varepsilon)-R\left[\beta_s(s_1+\varepsilon)-\beta_s(s_1-\varepsilon)\right]-\alpha(s_1-\varepsilon)}{\beta(s_1+\varepsilon)+R\left[\alpha_s(s_1+\varepsilon)-\alpha_s(s_1-\varepsilon)\right]}\right\}^2\right\}^{1/2}}$$

$$= \frac{1}{\left\{1+\left\{\dfrac{1}{\dfrac{1}{\alpha_s^2(s_1+\varepsilon)}-1}\right\}\right\}^{1/2}}$$

$$= \frac{1}{(1+\frac{\alpha_s^2(s_1+\varepsilon)}{1-\alpha_s^2(s_1+\varepsilon)})^{1/2}}$$

$$= \frac{1}{(1+\frac{\alpha_s^2(s_1+\varepsilon)}{\beta_s^2(s_1+\varepsilon)})^{1/2}}$$

$$= \frac{\beta_s(s_1+\varepsilon)}{(\beta_s^2(s_1+\varepsilon)+\alpha_s^2(s_1+\varepsilon))^{1/2}}$$

$$= \beta_s(s_1+\varepsilon)$$

Thus, γ_ε is differentiable at $s=\bar{R}+s_1-\varepsilon$. Next, we check the point $s=\bar{R}+s_1-\varepsilon+L_{BQ}$. For α_ε, we have

$$\lim_{s\to(\bar{R}+s_1-\varepsilon+L_{BQ})^-} \alpha_\varepsilon = \alpha(s_1+\varepsilon) \qquad (2.92)$$

$$\lim_{s\to(\bar{R}+s_1-\varepsilon+L_{BQ})^+} \alpha_\varepsilon = \alpha(s_1+\varepsilon)$$

For α_ε', we have previously shown that the section of γ_ε between $\bar{R}+s_1-\varepsilon$ and $\bar{R}+s_1-\varepsilon+L_{BQ}$ has slope $\alpha_\varepsilon(s_1+\varepsilon)$, thus α_ε' matches. For β_ε, we have

$$\lim_{s\to(\bar{R}+s_1-\varepsilon+L_{BQ})^-} \beta_\varepsilon = \beta(s_1+\varepsilon) \qquad (2.93)$$

$$\lim_{s\to(\bar{R}+s_1-\varepsilon+L_{BQ})^+} \beta_\varepsilon = \beta(s_1+\varepsilon)$$

Similarly, we have shown that $\beta_\varepsilon' = \beta_s(s_1+\varepsilon)$ for the line, thus β_ε' matches at $s=\bar{R}+s_1-\varepsilon+L_{BQ}$. Finally, $\alpha_\varepsilon(\bar{R}+L_{BQ}+S-2\varepsilon)=\alpha(S)=\alpha(0)$ and $\beta_\varepsilon(\bar{R}+L_{BQ}+S-2\varepsilon)=\beta(S)=\beta(0)$. Thus, $\gamma_\varepsilon(s)$ is a curve of class C^1 for $s\in(s_1-\delta,s_1+\delta)$, and $\gamma_\varepsilon(s)\to\gamma(s)$ as $\varepsilon\to 0$. We repeat this process at each of the points s_j where γ is not differentiable, until we produce a curve γ_ε of class C^1 that tends to γ as $\varepsilon\to 0$. This completes the first part of the proof.

We now construct ignition curves for $\gamma(s)$ at a point s_1 where γ is not differentiable. Our goal is to show that if we allow the family of curves γ_ε to burn for a time t_1, then as $\varepsilon\to 0$, they will tend towards the solution $(x(s,t_1),y(s,t_1))$, where $(x(s,t_1),y(s,t_1))$ is the position of γ after it has burned

for a time t_1.

We first reparametrize $\gamma(s)$ so that there are "enough" values of s at $\gamma(s_1)$. (We followed this procedure in the previous example.) Let $\bar{\gamma}(s)=(\bar{\alpha}(s),\bar{\beta}(s))$, $s\in[0,S]$, where

$$\bar{\alpha}(s) = \begin{Bmatrix} \alpha(s) & s<s_1 \\ \alpha(s_1) & s_1\le s\le s_1+1 \\ \alpha(s-1) & s_1+1<s\le S+1 \end{Bmatrix} \tag{2.94}$$

$$\bar{\beta}(s) = \begin{Bmatrix} \beta(s) & s<s_1 \\ \beta(s_1) & s_1\le s\le s_1+1 \\ \beta(s-1) & s_1+1<s\le S+1 \end{Bmatrix} \tag{2.95}$$

γ and $\bar{\gamma}$ have the same trace with $\bar{\gamma}(s)=\gamma(s)$ for $s\le s_1$ and $\bar{\gamma}(s+1)=\gamma(s)$ for $s>s_1$. From now on, we omit the overbar.

We extend ignition curves from $\gamma(s)$ at the point $\gamma(s_1)$. Let $\omega_r = \lim_{s\to s_1^-} \tan^{-1}(\frac{-\alpha_s}{\beta_s})$ and $\omega_l = \lim_{s\to s_1^+} \tan^{-1}(\frac{-\alpha_s}{\beta_s})$; both these limits exist since the curve is piecewise C^1. We construct ignition curves

$$x(s,t) = k\cos((\omega_l-\omega_r)(s-s_1)+\omega_r+\pi)t + \alpha(s_1) \tag{2.96}$$

$$y(s,t) = k\sin((\omega_l-\omega_r)(s-s_1)+\omega_r+\pi)t + \beta(s_1) \tag{2.97}$$

for $t\ge 0$, $s_1\le s\le s_1+1$. Thus, using (2.93)-(2.94) to provide ignition curves for $s<s_1$ and $s_1+1<s$, we have the full set of ignition curves

$$x(s,t) = \begin{Bmatrix} k\beta_s(s)t + \alpha(s) & s<s_1 \\ k\cos((\omega_l-\omega_s)(s-s_1)+\omega_r+\pi)t + \alpha(s_1) & s_1\le s\le s_1+1 \\ k\beta_s(s-1)t + \alpha(s-1) & s_1+1<s\le S+1 \end{Bmatrix} \tag{2.98}$$

$$y(s,t) = \begin{Bmatrix} -k\alpha_s(s)t + \beta(s) & s<s_1 \\ k\sin((\omega_l-\omega_r)(s-s_1)+\omega_r+\pi)t + \beta(s_1) & s_1\le s\le s_1+1 \\ -k\alpha_s(s-1)t + \beta(s-1) & s_1+1<s\le S+1 \end{Bmatrix} \tag{2.99}$$

This gives the position of the front at time t.

We now check that, for $t>0$, the normal to $(x(s,t),y(s,t))$ is a continuous function of s. We need only check at $s=s_1$ and $s=s_1+1$, since both x and y are differentiable everywhere else. We first check for continuity at $s=s_1$:

$$\lim_{s\to s_1^-}(x(s,t),y(s,t)) = (k\beta_s(s_1)t+\alpha(s_1),-k\alpha_s(s_1)t+\beta(s_1)) \qquad (2.100)$$

$$\lim_{s\to s_1^+}(x(s,t),y(s,t)) = (k\beta_s(s_1)t+\alpha(s_1),-k\alpha_s(s_1)t+\beta(s_1)$$

We now check the normal (y_t/x_t) at $s=s_1$.

$$\lim_{s\to s_1^-}(y_t/x_t) = -\alpha_s(s_1)/\beta_s(s_1) = \tan(\omega_r) \qquad (2.101)$$

$$\lim_{s\to s_1^+}(y_t/x_t) = \tan(\omega_r+\pi) = \tan(\omega_r) \qquad (2.102)$$

Checking continuity at $s=s_1+1$, we have

$$\lim_{s\to(s_1+1)^-}(x(s,t),y(s,t))=(k\beta_s(s_1+1)t+\alpha(s_1+1),-k\alpha_s(s_1+1)t+\beta(s_1)) \qquad (2.102)$$

$$\lim_{s\to(s_1+1)^-}(x(s,t),y(s,t))=(k\beta_s(s_1+1)t+\alpha(s_1+1),-k\alpha_s(s_1+1)t+\beta(s_1))$$

Finally, we check the normal (y_t/x_t) at $s=s_1+1$

$$\lim_{s\to(s_1+1)^-}(y_t/x_t) = \tan(\omega_l+\pi) = \tan(\omega_l) \qquad (2.103)$$

$$\lim_{s\to(s_1+1)^+}(y_t/x_t) = -\frac{\alpha_s(s_1+1)}{\beta_s(s_1+1)} = \tan(\omega_l)$$

Thus, the third claim of the theorem is verified.

Let $(x_\varepsilon(s,t),y_\varepsilon(s,t))$ be the ignition curves of the initial curve $\gamma_\varepsilon=(\alpha_\varepsilon(s),\beta_\varepsilon(s))$. All that remains is to show that $\lim_{\varepsilon\to 0} tr(x_\varepsilon(s,t),y_\varepsilon(s,t))=tr(x(s,t),y(s,t))$. Since γ_ε is a curve of class C^1, we may use (2.67) and (2.68) to find its ignition curves. We have

$$x_\varepsilon(s,t) = k\,\frac{\beta_{\varepsilon_s}}{(\alpha_{\varepsilon_s}^2+\beta_{\varepsilon_s}^2)^{1/2}}t + \alpha_\varepsilon(s) \qquad (2.104)$$

$$y_\varepsilon(s,t) = -k\,\frac{\alpha_{\varepsilon_s}}{(\alpha_{\varepsilon_s}^2+\beta_{\varepsilon_s}^2)^{1/2}}t + \beta_\varepsilon(s) \tag{2.105}$$

where α_ε and β_ε are defined in (2.84) and (2.85). Since $\alpha_{\varepsilon_s}^2+\beta_{\varepsilon_s}^2=1$, we have

$$x_\varepsilon(s,t) = k\,\beta_{\varepsilon_s}t + \alpha_\varepsilon(s) \tag{2.106}$$

$$y_\varepsilon(s,t) = -k\,\alpha_{\varepsilon_s}t + \beta_\varepsilon(s) \tag{2.107}$$

We now check that $\lim_{\varepsilon\to 0} tr(x_\varepsilon(s,t),y_\varepsilon(s,t))=tr(x(s,t),y(s,t))$ for $t\geq 0$. We check this in four sections; for $s\leq s_1-\varepsilon$, for $s_1-\varepsilon<s<\bar{R}+s_1-\varepsilon$, for $\bar{R}+s_1-\varepsilon\leq s<\bar{R}+s_1-\varepsilon+L_{BQ}$, and for $\bar{R}+s_1-\varepsilon+L_{BQ}\leq s\leq\bar{R}+L_{BQ}+S-2\varepsilon$. At first glance, it would seem that the section of $(x_\varepsilon,y_\varepsilon)$ for $s_1-\varepsilon<s\leq\bar{R}+s_1-\varepsilon$ must disappear as $\varepsilon\to 0$, since $\bar{R}\to 0$ as $\varepsilon\to 0$. However, the length of the front $(x_\varepsilon(s,t),y_\varepsilon(s,t))$ between those two points is a function of ε. thus we must be extremely careful in our analysis.

Our technique will be to reparameterize sections of the curve by arc length and then make comparisons. Note that $\lim_{\varepsilon\to 0}\bar{R}=0$, $\lim_{\varepsilon\to 0}L_{BQ}=0$, $\lim_{s\to s_1^-}(-\alpha_s)=\sin(\omega_r)$, and $\lim_{s\to s_1^+}(\beta_s)=\cos(\omega_l)$.

1) $s<s_1-\varepsilon$. For $s<s_1-\varepsilon$, $\alpha_\varepsilon(s)=\alpha(s)$ and $\beta_\varepsilon(s)=\beta(s)$ for all $\varepsilon\geq 0$. Thus, $tr(x_\varepsilon,y_\varepsilon) = tr(x,y)$ for $s<s_1-\varepsilon$.

2) $s_1-\varepsilon\leq s\leq\bar{R}+s_1-\varepsilon$. For any fixed $t_1\geq 0$, we show that, as $\varepsilon\to 0$, the trace of the curve $(x_\varepsilon,y_\varepsilon)$ for $s_1-\varepsilon\leq s\leq\bar{R}+s_1-\varepsilon$ approaches the trace of the curve (x,y) for $s_1\leq s\leq s_1+1$. Let

$$\bar{x}(s^*,t_1) = kt_1\cos\left(\frac{s^*}{kt_1}+\omega_r+\pi\right)+\alpha(s_1)$$

$$\bar{y}(s^*,t_1) = kt_1\sin\left(\frac{s^*}{kt_1}+\omega_r+\pi\right)+\beta(s_1)$$

$$0 \le s^* \le (\omega_l - \omega_r)\, kt_1 \qquad (2.108\text{-}2.109)$$

This is a parameterization by arc length of the section of $(x(s,t_1),y(s,t_1))$ between s_1 and s_1+1. Let

$$\bar{x}_\varepsilon(s^*,t_1) = \left\{ kt_1+R \right\}\cos\left\{ \frac{s^*}{kt_1+R} - \sin^{-1}(\alpha_s(s_1-\varepsilon)) \right\} - R\beta_s(s_1-\varepsilon)+\alpha(s_1-\varepsilon)$$

$$\bar{y}_\varepsilon(s^*,t_1) = \left\{ kt_1+R \right\}\sin\left\{ \frac{s^*}{kt_1+R} - \sin^{-1}(\alpha_s(s_1-\varepsilon)) \right\} R\alpha_s(s_1-\varepsilon)+\beta(s_1-\varepsilon)$$

$$0 \le s \le (kt_1+R)\,(\sin^{-1}(\alpha_s(s_1-\varepsilon))+\cos^{-1}(\beta_s(s_1+\varepsilon))) \qquad (2.110\text{-}2.111)$$

This is a parameterization by arc length of the section of $(x_\varepsilon(s,t_1),y_\varepsilon(s,t_1))$ for $s_1-\varepsilon \le s \le \bar{R}+s_1-\varepsilon$. Evaluation of the limit shows that

$$\lim_{\varepsilon\to 0} \bar{x}_\varepsilon(s^*,t_1) = kt_1\cos\left(\frac{s^*}{kt_1}+\omega_r+\pi\right)+\alpha(s_1) \qquad (2.112)$$

$$= \bar{x}(s^*,t_1) \qquad (2.113)$$

$$\lim_{\varepsilon\to 0} \bar{y}_\varepsilon(s^*,t_1) = kt_1\sin\left(\frac{s^*}{kt_1}+\omega_r+\pi\right)+\beta(s_1)$$

$$= \bar{y}(s^*,t_1)$$

Hence, they have the same trace in that range.

3) $\bar{R}+s_1-\varepsilon < s < \bar{R}+s_1-\varepsilon+L_{BQ}$. This section of $(x_\varepsilon,y_\varepsilon)$ is just the straight line segment of length L_{BQ}. As $\varepsilon\to 0$, $L_{BQ}\to 0$, and this section vanishes.

4) $\bar{R}+s_1-\varepsilon+L_{BQ} \le s \le \bar{R}+L_{BQ}+S-2\varepsilon$. We have that

$$\gamma_\varepsilon(s) = \gamma(s-\bar{R}+\varepsilon-L_{BQ}-1)$$

Evaluation of the limit yields

$$\lim_{\varepsilon\to 0} \gamma_\varepsilon(s) = \gamma(s-1)$$

Thus, as $\varepsilon\to 0$, the trace of $(x_\varepsilon,y_\varepsilon)$ approaches the trace of (x,y). This completes the proof.

Remark. We have constructed a specific set of C^1 curves γ_ε that tend to a piecewise C^1 curve γ and showed that, for $t \geq 0$, $(x_\varepsilon, y_\varepsilon) \to (x, y)$, where the ignition curves at the point of discontinuity are constructed in our special way. This is not the optimal result. Ideally, we should be able to show that our construction is unique; that is, any set of smooth initial data tending towards γ burns into a set of curves that tend towards our constructed solution. The main stumbling block in such an approach is that it is hard to determine if two curves have the same trace when they are not parameterized by the same object. In the specific case we chose, the approximation elements were straight lines and curves, both of which can easily be parameterized by arc length. This made our comparison straightforward. Unfortunately, it is not a simple matter to provide an actual parameterization by arc length of an arbitrary curve.

The arguments in Theorem 2 showing that any convex flame front burns into a circle require that the initial curve be of class C^2. In Theorem 3, we constructed ignition curves for initial curves that were only piecewise C^2. Now that we are able to follow the propagation of a piecewise C^2 flame front in a direction normal to itself, we wish to extend Theorem 2.

Theorem 4. Let γ be a convex, piecewise C^2, and piecewise regular curve. Suppose that the particles inside γ are burnt, and those outside are unburnt. At $t = 0$, the particles along γ are ignited. Assume that the flame moves along the

ignition curves constructed in Theorem 2. Then, as $t \to \infty$, the shape of the burned region becomes circular.

Proof. We assume, for the moment, that given ε, there exists a simple, closed, regular, parameterized, positively oriented, convex, plane curve $\gamma_1(s)=(\alpha_1(s),\beta_1(s))$, $s \in [0,S_1]$, $\gamma_1(0)=\gamma_1(S_1)$, of class C^2 that lies inside γ a distance less than ε. That is, given $s_1 \in [0,S_1]$, $\min_{s \in [0,S]} |\gamma(s)-\gamma_1(s_1)| < \varepsilon$, given $s_1 \in [0,S]$, $\min_{s \in [0,S_1]} |\gamma_1(s)-\gamma(s\,1)| < \varepsilon$, and every point on γ_1 is in the closure of the interior of γ. With this assumption (to be proved later), we now show that the original curve γ can be trapped between two curves that can be made arbitrarily close, both of which burn into circular regions. This will complete the proof.

Since γ_1 is a closed, convex curve of class C^2, we may use (2.67) and (2.68) to move it in a direction normal to itself with constant speed k. Let $\gamma_1(s,t)$ be the position of the front at time t, that is, $\gamma_1(s,0)=\gamma_1(s)$. Then, by Theorem 2, as $t \to \infty$, $\gamma_1(s,t)$ approaches a circle. Define another curve $\gamma_2(s)=(\alpha_2(s),\beta_2(s))$, $s \in [0,S_1]$ such that $\gamma_2(s)=\gamma_1(s,2\varepsilon/k)$; thus $\gamma_2(s)$ is the position of the propagating front γ_1 at time $t=2\varepsilon/k$. Let $\gamma_2(s,t)$ be the position of the front γ_2 at time t, that is, $\gamma_2(s,0)=\gamma_2$. Since $\gamma_2(s,t)=\gamma_1(s,t+2\varepsilon/k)$, $\gamma_2(s,t)$ also burns into a circle.

We claim that, for all t, $\gamma_1(s,t)$ and $\gamma_2(s,t)$ are exactly a distance 2ε from each other. We prove that, given $s_1 \in [0,S_1]$, $|\gamma_2(s_1,t)-\gamma_1(s,t)| = 2\varepsilon$. Let $\gamma_1(s,t) \equiv (x_1(s,t),y_1(s,t))$ and $\gamma_2(s,t) \equiv (x_2(s,t),y_2(s,t))$. Then, using (2.18) and (2.19), we have

$$x_1(s,t) = k\,\frac{\beta_{1_s}}{(\alpha_{1_s}^2+\beta_{1_s}^2)^{1/2}}t + \alpha_1(s) \tag{2.114}$$

$$y_1(s,t) = -k\,\frac{\alpha_{1_s}}{(\alpha_{1_s}^2+\beta_{1_s}^2)^{1/2}}t + \beta_1(s) \tag{2.115}$$

By definition, $\alpha_2 \equiv x_2(s,0) \equiv x_1(s,2\varepsilon/k)$, and $\beta_2(s) \equiv y_2(s,0) \equiv y_1(s,2\varepsilon/k)$. Hence,

$$x_2(s,t) = k\,\frac{y_{1_s}(s,2\varepsilon/k)}{((x_{1_s}(s,2\varepsilon/k))^2+(\beta_{1_s}(s,2\varepsilon/k))^2)^{1/2}}t + x_1(s,2\varepsilon/k) \tag{2.116}$$

$$= k\,\frac{\left\{-\alpha_{1_{ss}}(\alpha_{1_s}^2+\beta_{1_s}^2)^{-1/2}+\alpha_{1_s}(\alpha_{1_s}\alpha_{1_{ss}}+\beta_{1_s}\beta_{1_{ss}})(\alpha_{1_s}^2+\beta_{1_s}^2)^{-3/2}\right\}(2\varepsilon) + \beta_{1_s}}{(\alpha_{1_s}^2+\beta_{1_s}^2)^{-1/2}\left\{1 + (\beta_{1_{ss}}\alpha_{1_s}-\alpha_{1_{ss}}\beta_{1_s})(\alpha_{1_s}^2+\beta_{1_s}^2)^{-3/2}(2\varepsilon)\right\}}t$$

$$+ \frac{\beta_{1_s}}{(\alpha_{1_s}^2+\beta_{1_s}^2)^{1/2}}(2\varepsilon)+\alpha_1$$

$$= k\,\frac{\left\{-\alpha_{1_{ss}}(\alpha_{1_s}^2+\beta_{1_s}^2)+\alpha_{1_s}(\alpha_{1_s}\alpha_{1_{ss}}+\beta_{1_s}\beta_{1_{ss}})\right\}(\alpha_{1_s}^2+\beta_{1_s}^2)^{-3/2}(2\varepsilon)+\beta_{1_s}}{(\alpha_{1_s}^2+\beta_{1_s}^2)^{-1/2}\left\{1+(\beta_{1_{ss}}\alpha_{1_s}-\alpha_{1_{ss}}\beta_{1_s})(\alpha_{1_s}^2+\beta_{1_s}^2)^{-3/2}(2\varepsilon)\right\}}t$$

$$+ \frac{\beta_{1_s}}{(\alpha_{1_s}^2+\beta_{1_s}^2)^{1/2}}(2\varepsilon) + \alpha_1$$

$$= k\,\frac{\beta_{1_s}\left\{(\beta_{1_{ss}}\alpha_{1_s}-\alpha_{1_{ss}}\beta_{1_s})(\alpha_{1_s}^2+\beta_{1_s}^2)^{-3/2}(2\varepsilon)+1\right\}}{(\alpha_{1_s}^2+\beta_{1_s}^2)^{-1/2}\left\{1 + (\beta_{1_{ss}}\alpha_{1_s}-\alpha_{1_{ss}}\beta_{1_s})(\alpha_{1_s}^2+\beta_{1_s}^2)^{-3/2}(2\varepsilon)\right\}}t + \frac{\beta_{1_s}}{(\alpha_{1_s}^2+\beta_{1_s}^2)^{1/2}}(2\varepsilon)+\alpha_1$$

$$= k\,\frac{\beta_{1_s}}{(\alpha_{1_s}^2+\beta_{1_s}^2)^{1/2}}t + \frac{\beta_{1_s}}{(\alpha_{1_s}^2+\beta_{1_s}^2)^{1/2}}(2\varepsilon) + \alpha_1$$

Here, we have used (2.37)-(2.42). Similarly,

$$y_2(s,t) = -k\,\frac{x_{1_s}(s,2\varepsilon/k)}{((x_{1_s}(s,2\varepsilon/k))^2+(y_{1_s}(s,2\varepsilon/k))^2)^{1/2}}t + y_{1_s}(s,2\varepsilon/k) \tag{2.117}$$

$$= -k \frac{\left\{\beta_{1_{ss}}(\alpha_{1_s}^2+\beta_{1_s}^2)^{-1/2}-\beta_{1_s}(\alpha_{1_s}\alpha_{1_{ss}}+\beta_{1_s}\beta_{1_{ss}})(\alpha_{1_s}^2+\beta_{1_s}^2)^{-3/2}\right\}(2\varepsilon)+\alpha_{1_s}}{(\alpha_{1_s}^2+\beta_{1_s}^2)\left\{1+(\beta_{1_{ss}}\alpha_{1_s}-\alpha_{1_{ss}}\beta_{1_s})(\alpha_{1_s}^2+\beta_{1_s}^2)^{-3/2}(2\varepsilon)\right\}} t$$

$$+ \frac{-\alpha_{1_s}}{(\alpha_{1_s}^2+\beta_{1_s}^2)^{1/2}}(2\varepsilon)+\beta_1$$

$$= -k \frac{\left\{\beta_{1_{ss}}(\alpha_{1_s}^2+\beta_{1_s}^2)-\beta_{1_s}(\alpha_{1_s}\alpha_{1_{ss}}+\beta_{1_s}\beta_{1_{ss}})\right\}(\alpha_{1_s}^2+\beta_{1_s}^2)^{-3/2}(2\varepsilon)+\alpha_{1_s}}{(\alpha_{1_s}^2+\beta_{1_s}^2)^{1/2}\left\{1+(\beta_{1_{ss}}\alpha_{1_s}-\alpha_{1_{ss}}\beta_{1_s})(\alpha_{1_s}^2+\beta_{1_s}^2)^{-3/2}(2\varepsilon)\right\}} t$$

$$+ \frac{-\alpha_{1_s}}{(\alpha_{1_s}^2+\beta_{1_s}^2)^{1/2}}(2\varepsilon)+\beta_1$$

$$= -k \frac{\alpha_{1_s}\left\{(\alpha_{1_s}\alpha_{1_{ss}}+\beta_{1_s}\beta_{1_{ss}})(\alpha_{1_s}^2+\beta_{1_s}^2)^{-3/2}(2\varepsilon)+1\right\}}{(\alpha_{1_s}^2+\beta_{1_s}^2)^{1/2}\left\{1+(\beta_{1_{ss}}\alpha_{1_s}-\alpha_{1_{ss}}\beta_{1_s})(\alpha_{1_s}^2+\beta_{1_s}^2)^{-3/2}(2\varepsilon)\right\}} t + \frac{-\alpha_{1_s}}{(\alpha_{1_s}^2+\beta_{1_s}^2)^{1/2}}(2\varepsilon)+\beta_1$$

$$= -k \frac{\alpha_{1_s}}{(\alpha_{1_s}^2+\beta_{1_s}^2)^{1/2}} t + \frac{-\alpha_{1_s}}{(\alpha_{1_s}^2+\beta_{1_s}^2)^{1/2}}(2\varepsilon)+\beta_1$$

Therefore, given $s_1 \in [0, S_1]$,

$$\left\{\gamma_2(s_1,t)-\gamma_1(s_1,t)\right\} = \left|\left\{x_2(s_1,t)-x_1(s_1,t)\right\}^2+\left\{y_2(s_1,t)-y_1(s_1,t)\right\}^2\right|^{1/2} \quad (2.118)$$

$$= \left\{\left\{\frac{\beta_{1_s}}{(\alpha_{1_s}^2+\beta_{1_s}^2)}(2\varepsilon)\right\}^2+\left\{\frac{-\alpha_{1_s}}{(\alpha_{1_s}^2+\beta_{1_s}^2)}(2\varepsilon)\right\}^2\right\}^{1/2}$$

$$= (4\varepsilon^2)^{1/2} = 2\varepsilon$$

Thus, $\gamma_1(s,t)$ and $\gamma_2(s,t)$ are a distance 2ε from each other and therefore cannot cross.

We now prove that $\gamma_2(s,0)$ lies outside the original curve γ a distance less than 2ε. Suppose part of γ_2 is inside the original curve γ. Then there exists an $\bar{s} \in [0, S_1]$ such that $\gamma_2(\bar{s},0)$ is inside γ. By Lemma 2, we can draw the ignition curve from $\gamma_2(\bar{s},0)$ to the curve γ_1. By Lemma 1, this curve is a straight line

normal to γ_1, thus the shortest distance from $\gamma_2(\bar{s},0)$ to the curve γ_1 is the length of that ignition curve: $|\gamma_2(\bar{s},0)-\gamma_1(\bar{s},0)|=2\varepsilon$. Continue this ignition curve ahead in time until it crosses the original curve γ; the point where the two intersect will be more than 2ε from γ_1, which violates the assumption that all points of γ are within ε of γ_1. Thus, γ_2 is outside γ. Since γ_1 and γ_2 are 2ε apart, then γ_2 lies outside γ a distance less than 2ε .

We now claim that, for all t, $\gamma(s,t)$ remains between $\gamma_1(s,t)$ and $\gamma_2(s,t)$. We prove this by contradiction. Suppose there exists some s_1 and t_1 such that $\gamma(s_1,t_1)$ is outside $\gamma_2(s,t_1)$. If we draw the ignition curve from $\gamma(s_1,t_1)$ to the curve $\gamma_2(s,0)$, its length must be greater than kt_1. Since $\gamma(s,0)$ is inside $\gamma_2(s,0)$, this implies that $\gamma(s_1,t_1)$ is further than kt_1 from $\gamma(s,0)$, which is impossible. Conversely, suppose there exists some s_1 and t_1 such that $\gamma(s_1,t_1)$ is inside $\gamma_1(s,t_1)$. If we draw the ignition curve from $\gamma(s_1,0)$ passing through $\gamma(s_1,t_1)$, it has length kt_1. Continue this ignition curve ahead in time until it hits γ_1 at some point P. (This must happen since we are supposing that $\gamma(s_1,t_1)$ lies inside $\gamma_1(s,t_1)$). The distance from P on $\gamma_1(s,t_1)$ must be greater than kt_1 from $\gamma(s,0)$. Since $\gamma_1(s,0)$ is inside $\gamma(s,0)$, then the distance from P to $\gamma_1(s,0)$ is greater than kt_1, which is impossible. Thus, γ is trapped between two curves γ_1 and γ_2 which, by Theorem 2, must burn into circles.

All that remains is to show that there exists a convex curve γ_1 of class C^2 lying inside γ a distance less than ε. We construct such a curve in two steps: first, we inscribe a convex polygon that lies inside γ a distance less than $\varepsilon/2$, and second, we smooth out the corners of the polygon so that the resulting curve is of class C^2 , retains its convexity, and lies a distance less than $\varepsilon/2$ inside the polygon, thus yielding the result.

We start at the point $\gamma(0)=(\alpha(0),\beta(0))$, and let s_1 be the largest value of s such that each point of the chord connecting $\gamma(0)$ to $\gamma(s_1)$ is within $\varepsilon/2$ of the section of the initial curve between $s=0$ and $s=s_1$; this can be done since the curvature of the initial curve is piecewise C^2. Furthermore, since γ is convex, no part of the chord can lie outside γ. From $\gamma(s_1)$, we can find the largest value of s, say s_2, such that each point of the chord connecting $\gamma(s_1)$ to $\gamma(s_2)$ is within $\varepsilon/2$ of the section of the initial curve between $s=s_1$ and $s=s_2$. (We are doing nothing more than buiding a discrete approximation to the length of the curve, which can be done for any curve that is piecewise C^1). We continue this process until we reach $s=S$. (See Figure (2.16)).

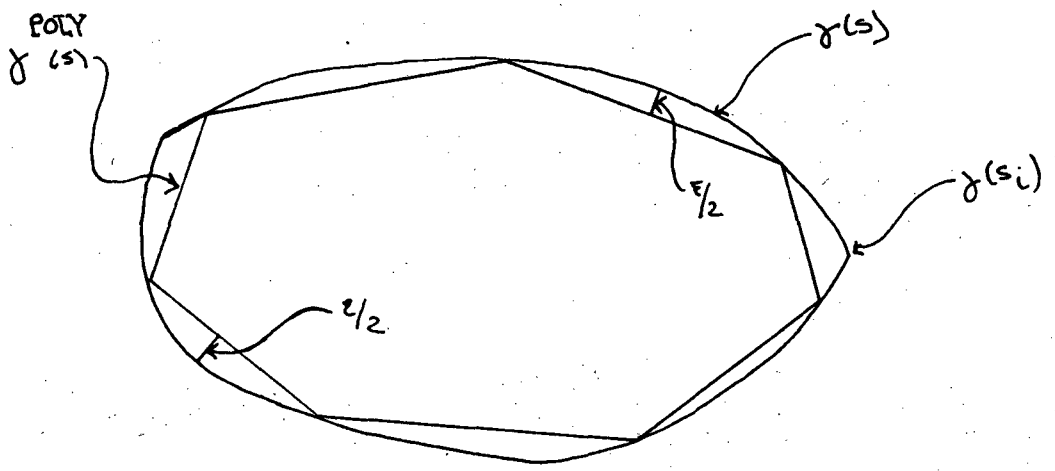

Figure 2.16

This produces a convex polygon lying a distance less than $\varepsilon/2$ inside γ. Our goal is to smooth out the corners of the polygon so that the resulting curve is convex, of class C^2, and lies a distance less than $\varepsilon/2$ inside the polygon. Let $\gamma^{POLY}(s)=(\alpha^{POLY}(s),\beta^{POLY}(s))$, $s\in[0,S^{POLY}]$ be a parameterization of the polygon by arc length.

We now exhibit a function that smooths corners. Consider the function $f(x)$ defined by

$$f(x) = \begin{cases} \frac{v}{u}x & x < u\varepsilon \\ \frac{v}{u}(2u\varepsilon - x) & x \geq u\varepsilon \end{cases} \tag{2.119}$$

where ε, u, and v are constants such that $\varepsilon>0$, $0<u<1$, $0<v<1$, and $u^2+v^2=1$. The graph of $f(x)$ is shown in Figure (2.17).

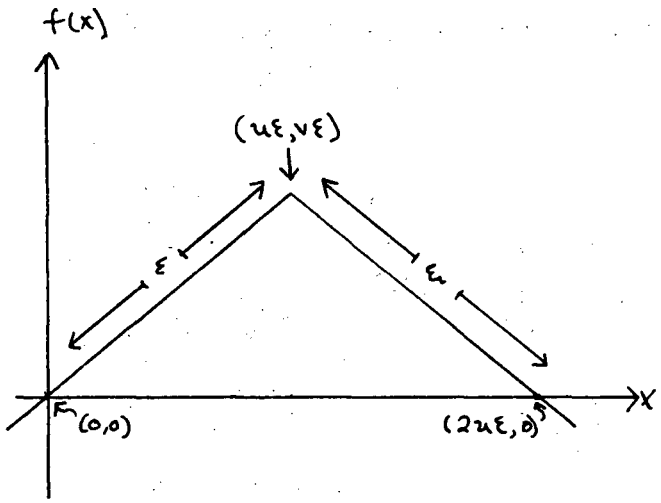

Figure 2.17

We will exhibit a convex curve of class C^2 that lies below $f(x)$ a distance less than ε.

We reparameterize the curve $(x, f(x)), -\infty<x<\infty$, by arc length as follows: $\bar{\gamma}(s)=(\bar{\alpha}(s),\bar{\beta}(s)), s\in(-\infty,\infty)$, where

$$\bar{\alpha}(s) = \begin{cases} u(2\varepsilon - s) & -\infty < s < \varepsilon \\ u(2\varepsilon - s) & \varepsilon \leq s < \infty \end{cases} \tag{2.120}$$

$$\bar{\beta}(s) = \begin{cases} vs & -\infty < s < \varepsilon \\ v(2\varepsilon - s) & \varepsilon \leq s < \infty \end{cases} \tag{2.121}$$

The trace of $\bar{\gamma}(s)$ is the same as the graph of $f(x)$, and $\bar{\alpha}_s^2+\bar{\beta}_s^2=1$ at points

where the derivative is defined. We define $\bar{\gamma}_\varepsilon(s)=(\bar{\alpha}_\varepsilon(s),\bar{\beta}_\varepsilon(s))$, $\in(-\infty,\infty)$as follows:

$$\bar{\alpha}_\varepsilon(s) = \left\{ u(2\varepsilon - s) \quad -\infty < s < \infty \right\} \tag{2.122}$$

$$\bar{\beta}_\varepsilon(s) = \begin{cases} vs & -\infty < s \le 0 \\ \frac{-v}{4\varepsilon^3}s^4 + vs & 0 < s \le \varepsilon \\ \frac{-v}{4\varepsilon^3}(2\varepsilon - s)^4 + v(2\varepsilon - s) & \varepsilon < s < 2\varepsilon \\ v(2\varepsilon - s) & 2\varepsilon \le s < \infty \end{cases} \tag{2.123}$$

(See Figure (2.18))

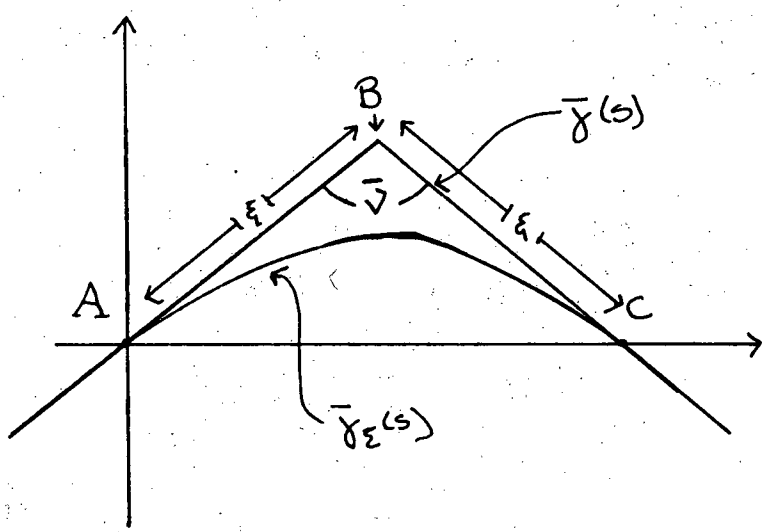

Figure 2.18

We claim that $\bar{\gamma}_\varepsilon(s)$ is a convex curve of class C^2 lying below $\bar{\gamma}(s)$ a distance less than ε.

1) We check that $\bar{\gamma}_\varepsilon(s)$ is of class C^2. We need only check $\bar{\beta}_\varepsilon(s)$ at the points $s=0$, $s=\varepsilon$, and $s=2\varepsilon$, since $\bar{\beta}_\varepsilon$ is infinitely differentiable everywhere else ($\bar{\alpha}_\varepsilon$ is infinitely differentiable). We have, for $\bar{\beta}_\varepsilon(s)$,

$$\lim_{s\to 0^-}(\upsilon s) = 0 = \lim_{s\to 0^+}\left(\frac{-\upsilon}{4\varepsilon^3}s^4 + \upsilon s\right) \tag{2.124}$$

$$\lim_{s\to \varepsilon^-}\left(\frac{-\upsilon}{4\varepsilon^3}s^4 + \upsilon s\right) = \frac{-\upsilon\varepsilon}{4} + \upsilon\varepsilon = \lim_{s\to \varepsilon^+}\left(\frac{-4}{4\varepsilon^3}(2\varepsilon - s)^4 + \upsilon(2\varepsilon - s)\right) \tag{2.125}$$

$$\lim_{s\to (2\varepsilon)^-}\left(\frac{-4}{4\varepsilon^3}(2\varepsilon - s)^4 + \upsilon(2\varepsilon - s)\right) = 0 = \lim_{s\to (2\varepsilon)^+}(\upsilon(2\varepsilon - s)) \tag{2.126}$$

Thus, $\bar{\beta}_\varepsilon$ is a continuous function of s. We now check the first derivative.

$$\lim_{s\to 0^-}(\upsilon) = \upsilon = \lim_{s\to 0^+}\left(\frac{-\upsilon}{\varepsilon^3}s^3 + \upsilon\right) \tag{2.127}$$

$$\lim_{s\to \varepsilon^-}\left(\frac{-\upsilon}{\varepsilon^3}s^3 + \upsilon\right) = 0 = \lim_{s\to \varepsilon^+}\left(\frac{\upsilon}{\varepsilon^3}(2\varepsilon - s)^3 - \upsilon\right) \tag{2.128}$$

$$\lim_{s\to (2\varepsilon)^-}\left(\frac{\upsilon}{\varepsilon^3}(2\varepsilon - s)^3 - \upsilon\right) = -\upsilon = \lim_{s\to (2\varepsilon)^+}(-\upsilon) \tag{2.129}$$

Thus, $\bar{\beta}_\varepsilon''$ is a continuous function of s. Finally, we check the second derivative:

$$\lim_{s\to 0^-}(0) = 0 = \lim_{s\to 0^+}\left(\frac{-3\upsilon}{\varepsilon^3}s^2\right) \tag{2.130}$$

$$\lim_{s\to \varepsilon^-}\left(\frac{-3\upsilon}{\varepsilon^3}s^2\right) = \frac{-3\upsilon}{\varepsilon} = \lim_{s\to \varepsilon^+}\left(\frac{-3\upsilon}{\varepsilon^3}(2\varepsilon - s)^2\right) \tag{2.131}$$

$$\lim_{s\to (2\varepsilon)^-}\left(\frac{-3\upsilon}{\varepsilon^3}(2\varepsilon - s)^2\right) = 0 = \lim_{s\to (2\varepsilon)^+}(0) \tag{2.132}$$

Thus, $\bar{\gamma}_\varepsilon(s)$ is a curve of class C^2.

2) We check that $\bar{\gamma}_\varepsilon$ lies below $\bar{\gamma}(s)$ a distance less than ε. For $s\le 0$ and $s\ge 2\varepsilon$, $\bar{\gamma}_\varepsilon(s)=\bar{\gamma}(s)$, thus we need only check for $0<s<2\varepsilon$. There are no values of s such that $\bar{\beta}_\varepsilon(s)=0$ in that interval, since υ and ε are both positive Since $\bar{\beta}_\varepsilon(\varepsilon)=3\upsilon\varepsilon/4>0$, $\bar{\beta}_\varepsilon(s)\ge 0$ for all $0<s<2\varepsilon$, thus $\bar{\gamma}_\varepsilon(s)$ is above the x axis in that interval. Since $\bar{\beta}_\varepsilon(s)<\upsilon s$ for $0<s<\varepsilon$, and $\bar{\beta}_\varepsilon(s)<\upsilon(2\varepsilon - s)$ for $\varepsilon<s<2\varepsilon$, $\bar{\gamma}_\varepsilon(s)$ is below $\bar{\gamma}$. All points in the triangle ABC lie a distance less than ε away from $\bar{\gamma}$, therefore $\bar{\gamma}_\varepsilon$ lies below $\bar{\gamma}$ a distance less than ε.

3) Since $\bar{\beta}_\varepsilon''(s)$ is negative for $0<s<2\varepsilon$, $\bar{\gamma}_\varepsilon(s)$ is convex.

We can now use the curve $\bar{\gamma}_\varepsilon(s)$ to smooth the corners of $\gamma^{POLY}(s)$. Let $\gamma^{POLY}(s_i)=(\alpha^{POLY}(s_i),\beta^{POLY}(s_i))$, $s_i\in[0,S^{POLY}]$ be the location of a corner of the polygon. (See Figure (2.19))

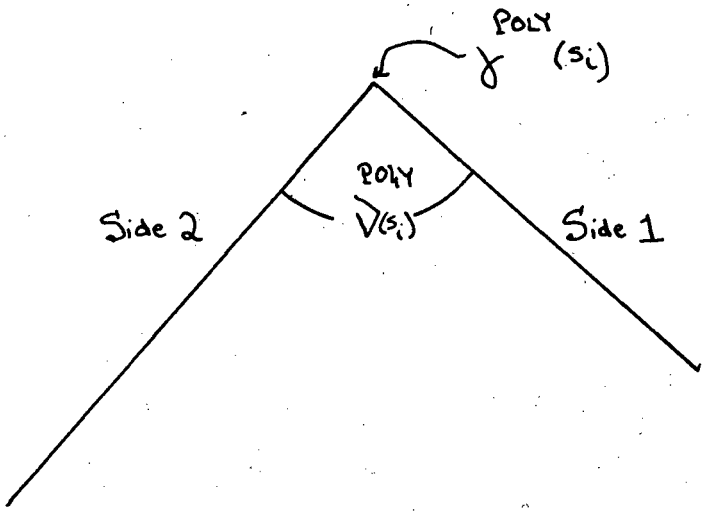

Figure 2.19

Since the polygon is parameterized by arc length, the directed unit vector tangent to side 1 is $\lim_{s\to s_i^-}(\alpha_s^{POLY}(s),\beta_s^{POLY}(s))$; and that tangent to side 2 is $\lim_{s\to s_i^+}(\alpha_s^{POLY}(s),\beta_s^{POLY}(s))$, both taken in the direction of increasing s. Let

$(\cos\vartheta_1,\sin\vartheta_1) = \lim_{s\to s_i^-}(\alpha_s^{POLY}(s),\beta_s^{POLY}(s))$ and

$(\cos\vartheta_2,\sin\vartheta_2) = \lim_{s\to s_i^+}(\alpha_s^{POLY}(s),\beta_s^{POLY}(s))$. Then,

$$\cos\vartheta^{POLY} = (-\cos\vartheta_2\,,\,-\sin\vartheta_2)\cdot(\cos\vartheta_1\,,\,\sin\vartheta_1) \tag{2.133}$$

$$= -\cos\vartheta_2\cos\vartheta_1 - \sin\vartheta_2\sin\vartheta_1$$

$$= -\cos(\vartheta_2-\vartheta_1)$$

We wish to graft $\bar{\gamma}_\varepsilon(s)$ onto the corner located at $\gamma^{POLY}(s_i)$. The first step is make $\bar{\vartheta}=\vartheta^{POLY}$ ($\bar{\vartheta}$ is defined in Figure (2.18)). If we define ω, $0\le\omega\le\pi/2$, such

that $(\cos\omega\ ,\ \sin\omega)=(u,v)$,($u$ and v were assumed to be between 0 and 1 in Figure (2.18)), then

$$\begin{aligned}\cos\bar{\vartheta} &= (-\cos\omega\ ,\ \sin\omega)\cdot(\cos\omega\ ,\ -\sin\omega) \\ &= -\cos^2\omega - \sin^2\omega \\ &= -\cos^2\omega\end{aligned} \tag{2.134}$$

If $\bar{\vartheta}=\vartheta^{POLY}$, then $\cos(2\omega)=\cos(\vartheta_1-\vartheta_1)$. Since $0<\vartheta^{POLY}<\pi$, $\left|\vartheta_2-\vartheta_1\right|<\pi$. If $\vartheta_2\geq\vartheta_1$, take $\omega=\frac{\vartheta_2-\vartheta_1}{2}$ and the requirement that $0<\omega<\pi/2$ is satisfied (if $\vartheta_1>\vartheta_2$, choose $\omega=\frac{\vartheta_1-\vartheta_2}{2}$). This implies

$$u = \cos\left(\frac{\vartheta_2-\vartheta_1}{2}\right) \qquad v = \sin\left(\frac{\vartheta_2-\vartheta_1}{2}\right) \tag{2.135}$$

Next, shrink the side $\overline{AB}$ in Figure (2.18) so that it has length $\varepsilon/2$. (It is possible that another corner of the polygon is located within $\varepsilon/2$ of $\gamma^{POLY}(s_i)$; if so, let the length of $\overline{AB}$ be one-quarter the distance along the curve to the closest corner.). Thus, we have

$$\bar{\alpha}_{\varepsilon/2}(s) = \cos\left(\frac{\vartheta_2-\vartheta_1}{2}\right)(\varepsilon-s) \qquad -\infty<s<\infty \tag{2.136}$$

$$\bar{\beta}_{\varepsilon/2}(s) = \begin{cases} \sin\left(\frac{\vartheta_2-\vartheta_1}{2}\right)s & -\infty<s\leq 0 \\ -\frac{\sin\left(\frac{\vartheta_2-\vartheta_1}{2}\right)}{4(\varepsilon/2)^3}s^4+\sin\left(\frac{\vartheta_2-\vartheta_1}{2}\right)s & 0<s\leq\varepsilon/2 \\ -\frac{\sin\left(\frac{\vartheta_2-\vartheta_1}{2}\right)}{4(\varepsilon/2)^3}(s-\varepsilon)^4+\sin\left(\frac{\vartheta_2-\vartheta_1}{2}\right)(\varepsilon-s) & \varepsilon/2<s\leq\varepsilon \\ \sin\left(\frac{\vartheta_2-\vartheta_1}{2}\right)(\varepsilon-s) & \varepsilon<s<\infty \end{cases} \tag{2.137}$$

This curve $\bar{\gamma}_{\varepsilon/2}=(\bar{\alpha}_{\varepsilon/2}(s),\bar{\beta}_{\varepsilon/2}(s))$ is convex, of class C^2, and stays within $\varepsilon/2$ of a corner with the same angle as ϑ^{POLY}. All that remains is to rotate and translate the curve until it fits on top of the corner located at $\gamma^{POLY}(s_i)$ (such a transformation preserves lengths, angles and differentiability, hence the

properties of $\bar{\gamma}_{\varepsilon/2}$ are not disturbed).

The angle the vector $\vec{BC}$ in Figure (2.18) makes with the positive x axis is $-\omega$. The angle the vector pointing away from the corner along side 1 in Figure (2.20) makes with the x axis is $\vartheta_1-\pi$. Thus, we rotate $\bar{\gamma}_{\varepsilon/2}$ through an angle of $(\vartheta_1-\pi)-(-\omega)=\frac{\vartheta_2-\vartheta_1}{2}-\pi$ in the counterclockwise direction about the point $B=(\varepsilon/2\cos(\frac{\vartheta_2-\vartheta_1}{2}),\ \varepsilon/2\sin(\frac{\vartheta_2-\vartheta_1}{2}))$. Finally, we translate the curve so that the point B is sent to $\gamma^{POLY}(s_i)$. (See Figure (2.20))

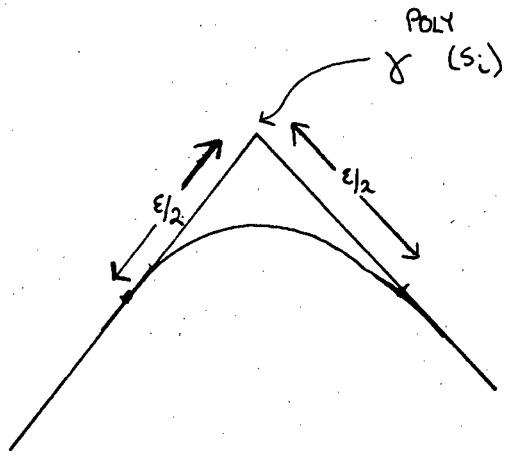

Figure 2.20

Any point (x,y) is sent to (x^*,y^*), where

$$\begin{bmatrix} x^* \\ y^* \end{bmatrix} = \begin{bmatrix} \cos(\frac{\vartheta_2+\vartheta_1}{2}-\pi) & -\sin(\frac{\vartheta_2+\vartheta_1}{2}-\pi) \\ \sin(\frac{\vartheta_2+\vartheta_1}{2}-\pi) & \cos(\frac{\vartheta_2+\vartheta_1}{2}-\pi) \end{bmatrix} \begin{bmatrix} x-\frac{\varepsilon}{2}\cos(\frac{\vartheta_2-\vartheta_1}{2}) \\ y-\frac{\varepsilon}{2}\sin(\frac{\vartheta_2-\vartheta_1}{2}) \end{bmatrix} + \begin{bmatrix} \alpha^{POLY}(s_i) \\ \beta^{POLY}(s_i) \end{bmatrix} \quad (2.38)$$

Thus,

$$x^* = \cos\left(\frac{\vartheta_2+\vartheta_1}{2}-\pi\right)\left(x-\frac{\varepsilon}{2}\cos\left(\frac{\vartheta_2-\vartheta_1}{2}\right)\right) - \sin\left(\frac{\vartheta_2+\vartheta_1}{2}\pi\right)\left(y-\frac{\varepsilon}{2}\sin\left(\frac{\vartheta_2-\vartheta_1}{2}\right)\right)$$

$$+\alpha^{POLY}(s_i) \tag{2.139}$$

$$= -x\cos\left(\frac{\vartheta_2+\vartheta_1}{2}\right)+\frac{\varepsilon}{2}\cos\left(\frac{\vartheta_2+\vartheta_1}{2}\right)\cos\left(\frac{\vartheta_2-\vartheta_1}{2}\right)+y\sin\left(\frac{\vartheta_2+\vartheta_1}{2}\right)$$

$$-\frac{\varepsilon}{2}\sin\left(\frac{\vartheta_2+\vartheta_1}{2}\right)\sin\left(\frac{\vartheta_2-\vartheta_1}{2}\right)+\alpha^{POLY}(s_i)$$

$$= -x\cos\left(\frac{\vartheta_2+\vartheta_1}{2}\right)+y\sin\left(\frac{\vartheta_2+\vartheta_1}{2}\right)+\frac{\varepsilon}{2}\cos(\vartheta_2)+\alpha^{POLY}(s_i)$$

$$y^* = \sin\left(\frac{\vartheta_2+\vartheta_1}{2}-\pi\right)\left(x-\frac{\varepsilon}{2}\cos\left(\frac{\vartheta_2-\vartheta_1}{2}\right)\right)+\cos\left(\frac{\vartheta_2+\vartheta_1}{2}-\pi\right)\left(y-\frac{\varepsilon}{2}\sin\left(\frac{\vartheta_2-\vartheta_1}{2}\right)\right)$$

$$+\beta^{POLY}(s_i) \tag{2.140}$$

$$= -x\sin\left(\frac{\vartheta_2+\vartheta_1}{2}\right)+\frac{\varepsilon}{2}\sin\left(\frac{\vartheta_2+\vartheta_1}{2}\right)\cos\left(\frac{\vartheta_2-\vartheta_1}{2}\right)-y\cos\left(\frac{\vartheta_2+\vartheta_1}{2}\right)$$

$$+\frac{\varepsilon}{2}\cos\left(\frac{\vartheta_2+\vartheta_1}{2}\right)\sin\left(\frac{\vartheta_2-\vartheta_1}{2}\right)+\beta^{POLY}(s_i)$$

$$= -x\sin\left(\frac{\vartheta_2+\vartheta_1}{2}\right)-y\cos\left(\frac{\vartheta_2+\vartheta_1}{2}\right)+\frac{\varepsilon}{2}\sin(\vartheta_2)+\beta^{POLY}(s_i)$$

Thus, we "glue" the section $\bar{\gamma}_{\varepsilon/2}(s)$ from $s=0$ to $s=\varepsilon$ into the corner located at $\gamma^{POLY}(s_i)$. Rotation and translation of $\bar{\gamma}_{\varepsilon/2}$ yield

For $-\infty<s\leq 0$:

$$\alpha^*_{\varepsilon/2} = (s-\varepsilon)\cos\left(\frac{\vartheta_2-\vartheta_1}{2}\right)\cos\left(\frac{\vartheta_2+\vartheta_1}{2}\right)+(s)\sin\left(\frac{\vartheta_2-\vartheta_1}{2}\right)\sin\left(\frac{\vartheta_2+\vartheta_1}{2}\right) \tag{2.141}$$

$$+\left(\frac{\varepsilon}{2}\right)\cos(\vartheta_2)+\alpha^{POLY}(s_1)$$

For $0<s\leq\frac{\varepsilon}{2}$:

$$\alpha^*_{\varepsilon/2} = (s-\varepsilon)\cos\left(\frac{\vartheta_2-\vartheta_1}{2}\right)\cos\left(\frac{\vartheta_2+\vartheta_1}{2}\right)+\left(\frac{-s^4}{4\frac{\varepsilon^3}{2}}+s\right)\sin\left(\frac{\vartheta_2-\vartheta_1}{2}\right)\sin\left(\frac{\vartheta_2+\vartheta_1}{2}\right)$$

$$+\left(\frac{\varepsilon}{2}\right)\cos(\vartheta_2)+\alpha^{POLY}(s_i)$$

For $\frac{\varepsilon}{2}<s\leq\varepsilon$:

$$\alpha^2_{\varepsilon/2} = (s-\varepsilon)\cos\left(\frac{\vartheta_2-\vartheta_1}{2}\right)\cos\left(\frac{\vartheta_2+\vartheta_1}{2}\right)+\left(\frac{-(\varepsilon-s)^4}{4\frac{\varepsilon^3}{2}}+(\varepsilon-s)\right)\sin\left(\frac{\vartheta_2-\vartheta_1}{2}\right)\sin\left(\frac{\vartheta_2+\vartheta_1}{2}\right)$$

$$= \left(\frac{\varepsilon}{2}\right)\cos(\vartheta_2)+\alpha^{POLY}(s_i)$$

For $\varepsilon<s<\infty$;

$$\alpha^{\bullet}_{\varepsilon/2} = (s-\varepsilon)\cos\left(\frac{\vartheta_2-\vartheta_1}{2}\right)\cos\left(\frac{\vartheta_2+\vartheta_1}{2}\right)+(\varepsilon-s)\sin\left(\frac{\vartheta_2-\vartheta_1}{2}\right)\sin\left(\frac{\vartheta_2+\vartheta_1}{2}\right)$$

$$+ \left(\frac{\varepsilon}{2}\right)\cos(\vartheta_2)+\alpha^{POLY}(s_i)$$

For $-\infty<s\leq 0$;

$$\beta^{\bullet}_{\varepsilon/2} = (s-\varepsilon\cos\left(\frac{\vartheta_2-\vartheta_1}{2}\right)\sin\left(\frac{\vartheta_2+\vartheta_1}{2}\right)-(s)\sin\left(\frac{\vartheta_2-\vartheta_1}{2}\right)\cos\left(\frac{\vartheta_2+\vartheta_1}{2}\right) \quad (2.142)$$

$$+ \left(\frac{\varepsilon}{2}\right)\sin(\vartheta_2)+\beta^{POLY}(s_i)$$

For $0<s<\frac{\varepsilon}{2}$;

$$\beta^{\bullet}_{\varepsilon/2} = (s-\varepsilon)\cos\left(\frac{\vartheta_2-\vartheta_1}{2}\right)\sin\left(\frac{\vartheta_2+\vartheta_1}{2}\right)-\left(\frac{-s^4}{4\frac{\varepsilon^3}{2}}+s\right)\sin\left(\frac{\vartheta_2-\vartheta_1}{2}\right)\cos\left(\frac{\vartheta_2+\vartheta_1}{2}\right)$$

$$+ \left(\frac{\varepsilon}{2}\right)\sin(\vartheta_2)+\beta^{POLY}(s_i)$$

For $\frac{\varepsilon}{2}<s<\varepsilon$;

$$\beta^{\bullet}_{\varepsilon/2} = (s-\varepsilon)\cos\left(\frac{\vartheta_2-\vartheta_1}{2}\right)\sin\left(\frac{\vartheta_2+\vartheta_1}{2}\right)-\left(\frac{-(\varepsilon-s)^4}{4\frac{\varepsilon^3}{2}}+(\varepsilon-s)\right)\sin\left(\frac{\vartheta_2-\vartheta_1}{2}\right)\cos\left(\frac{\vartheta_2+\vartheta_1}{2}\right)$$

$$+ \left(\frac{\varepsilon}{2}\right)\sin(\vartheta_2) + \beta^{POLY}(s_i)$$

For $\varepsilon<s<\infty$;

$$\beta^{\bullet}_{\varepsilon/2} = (s-\varepsilon)\cos\left(\frac{\vartheta_2-\vartheta_1}{2}\right)\sin\left(\frac{\vartheta_2+\vartheta_1}{2}\right)-(\varepsilon-s)\sin\left(\frac{\vartheta_2-\vartheta_1}{2}\right)\cos\left(\frac{\vartheta_2+\vartheta_1}{2}\right)$$

$$+ \left(\frac{\varepsilon}{2}\right)\sin(\vartheta_2) + \beta^{POLY}(s_i)$$

Thus, we define $\gamma_\varepsilon(s)=(\alpha_\varepsilon(s),\beta_\varepsilon(s))$, $s\in[0,S^{POLY}]$ as follows;

For $0\le s\le(s_1-\frac{\varepsilon}{2})$;

$$\alpha_\varepsilon(s) = \alpha^{POLY}(s_i) \tag{2.143}$$

For $(s_i-\frac{\varepsilon}{2})<s\le s_i$;

$$\alpha_\varepsilon(s) = \left\{(s-(s_i-\frac{\varepsilon}{2}))\right\}\cos(\frac{\vartheta_2-\vartheta_1}{2})\cos(\frac{\vartheta_2+\vartheta_1}{2}) +$$

$$\left\{\frac{-(s-(s_i-\frac{\varepsilon}{2}))^4}{4\frac{\varepsilon^3}{2}}+(s-(s_i-\frac{\varepsilon}{2}))\right\}\sin(\frac{\vartheta_2-\vartheta_1}{2})\sin(\frac{\vartheta_2+\vartheta_1}{2})$$

$$+\ (\frac{\varepsilon}{2})\cos(\vartheta_2)+\alpha^{POLY}(s_i)$$

For $s_i<s<(s_i+\frac{\varepsilon}{2})$;

$$\alpha_\varepsilon(s) = \left\{(s-(s_i-\frac{\varepsilon}{2}))\right\}\cos(\frac{\vartheta_2-\vartheta_1}{2})\cos(\frac{\vartheta_2+\vartheta_1}{2})+$$

$$\left\{\frac{-(\varepsilon-(s-(s_i-\frac{\varepsilon}{2})))^4}{4\frac{\varepsilon^3}{2}}+(\varepsilon-(s-(s_i-\frac{\varepsilon}{2})))\right\}\sin(\frac{\vartheta_2-\vartheta_1}{2})\sin(\frac{\vartheta_2+\vartheta_1}{2})$$

$$+\ (\frac{\varepsilon}{2})\cos(\vartheta_2)+\alpha^{POLY}(s_i)$$

For $s_i+\frac{\varepsilon}{2}\le s\le S^{POLY}$;

$$\alpha_\varepsilon(s) = \alpha^{POLY}(s_i)$$

For $0\le s\le(s_i-\frac{\varepsilon}{2})$;

$$\beta_\varepsilon(s) = \beta^{POLY}(s_i) \tag{2.144}$$

For $(s_i-\varepsilon/2)<s\le s_i$:

$$\beta_\varepsilon(s) = \left\{(s-(s_i-\varepsilon/2))-\varepsilon\right\}\cos\left(\frac{\vartheta_2-\vartheta_1}{2}\right)\sin\left(\frac{\vartheta_2+\vartheta_1}{2}\right)-$$

$$\left\{\frac{-(s-(s_i-\varepsilon/2))^4}{4\frac{\varepsilon}{2}^3}+(s-(s_i-\varepsilon/2))\right\}\sin\left(\frac{\vartheta_2-\vartheta_1}{2}\right)\cos\left(\frac{\vartheta_2+\vartheta_1}{2}\right)$$

$$+\frac{\varepsilon}{2}\sin(\vartheta_2)+\beta^{POLY}(s_i)$$

For $s_i<s<(s_i+\varepsilon/2)$:

$$\beta_\varepsilon(s) = \left\{(s-(s_i-\varepsilon/2))-\varepsilon\right\}\cos\left(\frac{\vartheta_2-\vartheta_1}{2}\right)\sin\left(\frac{\vartheta_2+\vartheta_1}{2}\right)-$$

$$\left\{\frac{-(\varepsilon-(s-(s_i-\varepsilon/2)))^4}{4\frac{\varepsilon}{2}^3}+(\varepsilon-(s-(s_i-\varepsilon/2)))\right\}\sin\left(\frac{\vartheta_2-\vartheta_1}{2}\right)\cos\left(\frac{\vartheta_2+\vartheta_1}{2}\right)$$

$$+\frac{\varepsilon}{2}\sin(\vartheta_2)+\beta^{POLY}(s_i)$$

For $(s_i+\varepsilon/2)\le s\le S_{POLY}$:

$$\beta_\varepsilon(s) = \beta^{POLY}(s_i)$$

Here, we have shifted the parameterization by $(s_i-\varepsilon/2)$ so that the two curves match up. By construction, $\gamma_\varepsilon(s)$, $s\in[0,S^{POLY}]$ is a convex curve, lying a distance less than $\frac{\varepsilon}{2}$ inside $\gamma^{POLY}(s)$, and thus a distance less than ε inside the original curve $\gamma(s)$. Furthermore, we claim that $\gamma_\varepsilon(s)$ is of class C^2 for $s_i-\frac{\varepsilon}{2}\le s\le s_i+\frac{\varepsilon}{2}$. We check that $\alpha_\varepsilon(s)$ and $\beta_\varepsilon(s)$ and their derivatives match up at $s=s_i-\frac{\varepsilon}{2}$ and $s=s_i+\frac{\varepsilon}{2}$. Using the definition of ϑ_1 and ϑ_2, we note that $\frac{\varepsilon}{2}\cos(\vartheta_2)+\alpha^{POLY}(s_i)=\alpha^{POLY}(s_i+\frac{\varepsilon}{2})$, $\frac{\varepsilon}{2}\sin(\vartheta_2)+\beta^{POLY}(s_i)=\beta^{POLY}(s_i+\frac{\varepsilon}{2})$, $-\frac{\varepsilon}{2}\cos(\vartheta_1)+\alpha^{POLY}(s_i)=\alpha^{POLY}(s_i-\frac{\varepsilon}{2})$, and $-\frac{\varepsilon}{2}\sin(\vartheta_1)+\beta^{POLY}(s_i)=\beta^{POLY}(s_i-\frac{\varepsilon}{2})$

We first check α_ε and its derivatives at $s=s_i+\frac{\varepsilon}{2}$. For α_ε at $s_i+\frac{\varepsilon}{2}$, we have

$$\lim_{s\to(s_i+\frac{\varepsilon}{2})^+}(\alpha_\varepsilon)=\alpha^{POLY}(s_i+\frac{\varepsilon}{2})=\frac{\varepsilon}{2}\cos(\vartheta_2)+\beta^{POLY}(s_i) \tag{2.145}$$

$$\lim_{s\to(s_i+\frac{\varepsilon}{2})^-}(\alpha_\varepsilon)=\frac{\varepsilon}{2}\cos(\vartheta_2)+\beta^{POLY}(s_i)$$

For α_ε', we have

$$\lim_{s\to(s_i+\frac{\varepsilon}{2})^+}(\alpha_\varepsilon')=\cos(\vartheta_2) \tag{2.146}$$

$$\lim_{s\to(s_i+\frac{\varepsilon}{2})^-}(\alpha_\varepsilon')=\lim_{s\to(s_i+\frac{\varepsilon}{2})^-}\cos(\frac{\vartheta_2-\vartheta_1}{2})\cos(\frac{\vartheta_2+\vartheta_1}{2})+$$

$$\left\{\frac{(\varepsilon-(s-(s_i-\varepsilon/2)))^3}{4\frac{\varepsilon}{2}^3}-1\right\}\sin(\frac{\vartheta_2-\vartheta_1}{2})\sin(\frac{\vartheta_2+\vartheta_1}{2})$$

$$=\cos(\frac{\vartheta_2-\vartheta_1}{2})\cos(\frac{\vartheta_2+\vartheta_1}{2})-\sin(\frac{\vartheta_2-\vartheta_1}{2})\sin(\frac{\vartheta_2+\vartheta_1}{2})=\cos(\vartheta_2)$$

For α_ε'', we have

$$\lim_{s\to(s_i+\frac{\varepsilon}{2})^+}(\alpha_\varepsilon'')=0 \tag{2.147}$$

$$\lim_{s\to(s_i+\frac{\varepsilon}{2})^-}(\alpha_\varepsilon'')=\lim_{s\to(s_i+\frac{\varepsilon}{2})^-}\left\{\frac{-3(\varepsilon-(s-(s_i-\varepsilon/2)))^2}{\varepsilon^3}\sin(\frac{\vartheta_2-\vartheta_1}{2})\sin(\frac{\vartheta_2+\vartheta_1}{2})\right\}=0$$

Thus, α_ε and its first two derivatives check at $s=s_i+\frac{\varepsilon}{2}$. We now check β_ε.

$$\lim_{s\to(s_i+\frac{\varepsilon}{2})^+}(\beta_\varepsilon)=\beta^{POLY}(s_i+\frac{\varepsilon}{2})=\frac{\varepsilon}{2}\sin(\vartheta_2)+\beta^{POLY}(s_i) \tag{2.148}$$

$$\lim_{s\to(s_i+\frac{\varepsilon}{2})^-}(\beta_\varepsilon)=\frac{\varepsilon}{2}\sin(\vartheta_2)+\beta^{POLY}(s_i)$$

For β_ε', we have

$$\lim_{s\to(s_i+\frac{\varepsilon}{2})^+}(\beta_\varepsilon')=\sin(\vartheta_2) \tag{2.149}$$

$$\lim_{s\to(s_i+\frac{\varepsilon}{2})^-}(\beta_\varepsilon') = \lim_{s\to(s_i+\frac{\varepsilon}{2})^-}\cos(\frac{\vartheta_2-\vartheta_1}{2})\sin(\frac{\vartheta_2+\vartheta_1}{2})-$$

$$\left\{\frac{(\varepsilon-(s-(s_i-\varepsilon/2)))^3}{4\frac{\varepsilon}{2}^3}1\right\}\sin(\frac{\vartheta_2-\vartheta_1}{2})\cos(\frac{\vartheta_2+\vartheta_1}{2})$$

$$=\cos(\frac{\vartheta_2-\vartheta_1}{2})\sin(\frac{\vartheta_2+\vartheta_1}{2})+\sin(\frac{\vartheta_2-\vartheta_1}{2})\cos(\frac{\vartheta_2+\vartheta_1}{2}) = \sin(\vartheta_2)$$

For β_ε'', we have

$$\lim_{s\to(s_i+\frac{\varepsilon}{2})^+}(\beta_\varepsilon'') = 0 \tag{2.150}$$

$$\lim_{s\to(s_i+\frac{\varepsilon}{2})^-}(\beta_\varepsilon'') = \lim_{s\to(s_i+\frac{\varepsilon}{2})^-}\frac{3(\varepsilon-(s-(s_i-\varepsilon/2)))^2}{\frac{\varepsilon}{2}^3}\sin(\frac{\vartheta_2-\vartheta_1}{2})\cos(\frac{\vartheta_2+\vartheta_1}{2}) = 0$$

Thus, β_ε and its first two derivatives agree at $s=s_i+\frac{\varepsilon}{2}$. We now check α_ε at $s=s_i-\frac{\varepsilon}{2}$.

$$\lim_{s\to(s_i-\frac{\varepsilon}{2})^-}(\alpha_\varepsilon) = \alpha^{POLY}(s_i-\frac{\varepsilon}{2}) \tag{2.151}$$

$$\lim_{s\to(s_i-\frac{\varepsilon}{2})^-}(\alpha_\varepsilon) = -\varepsilon\cos(\frac{\vartheta_2-\vartheta_1}{2})\cos(\frac{\vartheta_2+\vartheta_1}{2})+\frac{\varepsilon}{2}\cos(\vartheta_2)+\alpha^{POLY}(s_i)$$

$$=-\varepsilon\cos(\frac{\vartheta_2-\vartheta_1}{2})\cos(\frac{\vartheta_2+\vartheta_1}{2})+\frac{\varepsilon}{2}\left\{\cos(\frac{\vartheta_2-\vartheta_1}{2})\cos(\frac{\vartheta_2+\vartheta_1}{2})-\sin(\frac{\vartheta_2-\vartheta_1}{2})\sin(\frac{\vartheta_2+\vartheta_1}{2})\right\}$$

$$+\alpha^{POLY}(s_i)$$

$$=\frac{\varepsilon}{2}\left\{-\cos(\frac{\vartheta_2-\vartheta_1}{2})\cos(\frac{\vartheta_2+\vartheta_1}{2})-\sin(\frac{\vartheta_2-\vartheta_1}{2})\sin(\frac{\vartheta_2+\vartheta_1}{2})\right\}+\alpha^{POLY}(s_i)$$

$$=-\frac{\varepsilon}{2}\cos(\vartheta_1)+\alpha^{POLY}(s_i) = \alpha^{POLY}(s_i-\frac{\varepsilon}{2})$$

For α_ε', we have

$$\lim_{s\to(s_i-\frac{\varepsilon}{2})^-}(\alpha_\varepsilon') = \cos(\vartheta_1) \tag{2.152}$$

$$\lim_{s\to(s_i-\frac{\varepsilon}{2})^+}(\alpha_\varepsilon') = \lim_{s\to(s_i-\frac{\varepsilon}{2})^+}\cos(\frac{\vartheta_2-\vartheta_1}{2})\cos(\frac{\vartheta_2+\vartheta_1}{2})$$

$$+\left\{\frac{-(s-(s_i-\varepsilon/2))^3}{\frac{\varepsilon}{2}^3}+1\right\}\sin(\frac{\vartheta_2-\vartheta_1}{2})\sin(\frac{\vartheta_2+\vartheta_1}{2})$$

$$=\cos(\frac{\vartheta_2-\vartheta_1}{2})\cos(\frac{\vartheta_2+\vartheta_1}{2})+\sin(\frac{\vartheta_2-\vartheta_1}{2})\sin(\frac{\vartheta_2+\vartheta_1}{2})=\cos(\vartheta_1)$$

For α_ε'', we have

$$\lim_{s\to(s_i-\frac{\varepsilon}{2})^-}(\alpha_\varepsilon'') = 0 \tag{2.153}$$

$$\lim_{s\to(s_i-\frac{\varepsilon}{2})^+}(\alpha_\varepsilon'') = \lim_{s\to(s_i-\frac{\varepsilon}{2})^+}\frac{-3(s-(s_i-\varepsilon/2))^2}{\frac{\varepsilon}{2}^3}\sin(\frac{\vartheta_2-\vartheta_1}{2})\sin(\frac{\vartheta_2+\vartheta_1}{2})=0$$

Finally, we check β_ε.

$$\lim_{s\to(s_i-\frac{\varepsilon}{2})^-}(\beta_\varepsilon) = \beta^{POLY}(s_i-\frac{\varepsilon}{2}) \tag{2.154}$$

$$\lim_{s\to(s_i-\frac{\varepsilon}{2})^+}(\beta_\varepsilon) = -\varepsilon\cos(\frac{\vartheta_2-\vartheta_1}{2})\sin(\frac{\vartheta_2+\vartheta_1}{2})+\frac{\varepsilon}{2}\sin(\vartheta_2)+\beta^{POLY}(s_i)$$

$$=-\varepsilon\cos(\frac{\vartheta_2-\vartheta_1}{2})\sin(\frac{\vartheta_2+\vartheta_1}{2})+\frac{\varepsilon}{2}\left\{\cos(\frac{\vartheta_2-\vartheta_1}{2})\sin(\frac{\vartheta_2+\vartheta_1}{2})+\cos(\frac{\vartheta_2+\vartheta_1}{2})\sin(\frac{\vartheta_2-\vartheta_1}{2})\right\}$$

$$=+\beta^{POLY}(s_i)$$

$$=-\frac{\varepsilon}{2}\left\{\cos(\frac{\vartheta_2-\vartheta_1}{2})\sin(\frac{\vartheta_2+\vartheta_1}{2})-\cos(\frac{\vartheta_2+\vartheta_1}{2})\sin(\frac{\vartheta_2-\vartheta_1}{2})\right\}+\beta^{POLY}(s_i)$$

$$=-\frac{\varepsilon}{2}\sin(\vartheta_1)+\beta^{POLY}(s_i)=\beta^{POLY}(s_i-\frac{\varepsilon}{2})$$

For β_ε', we have

$$\lim_{s\to(s_i-\frac{\varepsilon}{2})^-}(\beta_\varepsilon') = \sin(\vartheta_1) \tag{2.155}$$

$$\lim_{s\to(s_i-\frac{\varepsilon}{2})^+}(\beta_\varepsilon') = \lim_{s\to(s_i-\frac{\varepsilon}{2})^+}\cos(\frac{\vartheta_2-\vartheta_1}{2})\sin(\frac{\vartheta_2+\vartheta_1}{2})-\sin(\frac{\vartheta_2-\vartheta_1}{2})\cos(\frac{\vartheta_2+\vartheta_1}{2})$$

$$=\sin(\vartheta_1)$$

For β_ε'', we have

$$\lim_{s\to(s_i-\frac{\varepsilon}{2})^-}(\beta_\varepsilon'') = 0 \tag{2.156}$$

$$\lim_{s\to(s_i-\frac{\varepsilon}{2})^+}(\beta_\varepsilon'') = \lim_{s\to(s_i-\frac{\varepsilon}{2})^+}\frac{3(s-(s_i-\varepsilon/2))^2}{\frac{\varepsilon}{2}^2}\sin(\frac{\vartheta_2-\vartheta_1}{2})\cos(\frac{\vartheta_2+\vartheta_1}{2}) = 0$$

Thus, α_ε and β_ε and their first two derivatives are all continuous for $s_i-\frac{\varepsilon}{2}\le s\le s_i+\frac{\varepsilon}{2}$. We smooth the other corners in the same way to achieve the desired result: a convex curve $\gamma_1(s)$ of class C^2 lying inside the original curve γ a distance less than ε. This completes the proof.

2.4. Evolution of a Non-Convex Flame Front

We have anaylzed the motion of a closed, convex, piecewise C^2 and piecewise regular flame front. In this section, we wish to analyze the propagation of a non-convex initial front. By "non-convex", we mean that there exists a chord connecting two points $\gamma(s_1,0)$ and $\gamma(s_2,0)$, $s_1,s_2\in[0,S]$ on the initial curve that passes through some part of the unburnt fluid. We begin with a suggestive example.

Example 2.4 Let $\gamma(s)=(\alpha(s),\beta(s))=(-s,s^2)$, $s\in(-\infty,\infty)$. The trace of this curve is the parabola $y=x^2$. Suppose that the particles below the parabola are burnt, and the particles above are unburnt. (This agrees with our earlier formulations in which the burnt region is on the left as we travel along the curve in the direction of increasing s.) Suppose that at $t=0$ we ignite all the particles located along $\gamma(s)$. We assume that the flame propagates with unit speed.

As in Example 2.1, we may use equations (2.18) and (2.19) to determine the position of the front. Thus,

$$x(s,t) = \frac{2s}{(1+4s^2)^{1/2}}t - s \tag{2.157}$$

$$y(s,t) = \frac{1}{(1+4s^2)^{1/2}}t + s^2. \tag{2.158}$$

(See Figure (2.21))

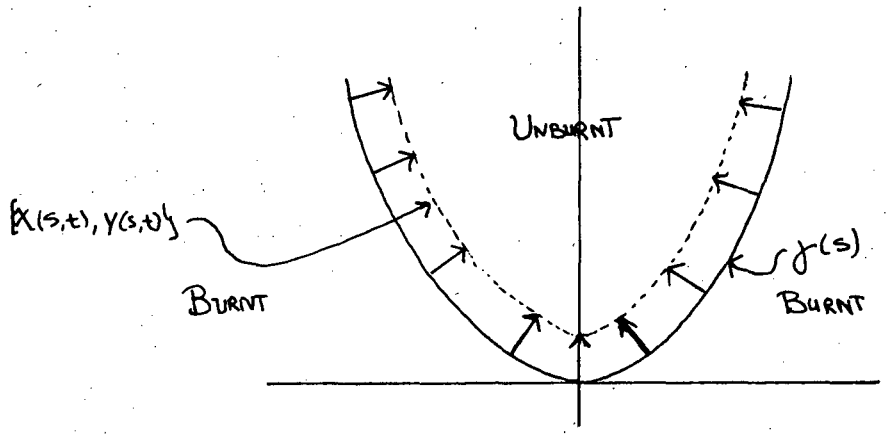

Figure 2.21

We make the following observations:

1) For $0 \le t \le \frac{1}{2}$, (2.157) and (2.158) are reversible. That is, the mapping $s,t \to (x(s,t),y(s,t))$ is invertible for all $t \in [0,\frac{1}{2})$. We prove this by checking that the Jacobian is non-zero for $0 \le t < \frac{1}{2}$. From (2.69) we have

$$\begin{bmatrix} x_s & x_t \\ y_s & y_t \end{bmatrix} = -\left\{ \frac{\beta_{ss}\alpha_s - \alpha_{ss}\beta_s}{\alpha_s^2+\beta_s^2} t + (\alpha_s^2+\beta_s^2)^{1/2} \right\} \qquad (2.159)$$

$$= -\left\{ \frac{-2}{4s^2+1} t + (4s^2+1)^{1/2} \right\}$$

$$= (4s^2+1)^{-1/2}(2t - (4s^2+1)) .$$

Since $2t < (4s^2+1)$ for $0 \le t < \frac{1}{2}$, the Jacobian is non-zero. Given any $s_1 \in (-\infty,\infty)$, the ignition curve leaving the point $(x(s_1,0),y(s_1,0))$ on the initial parabola does not intersect any other ignition curve for $0 \le t < \frac{1}{2}$.

2) For $t>\frac{1}{2}$, the situation is different; the mapping $s,t\to(x(s,t),y(s,t))$ is no longer invertible. To see that this is so, consider the point $(0,a)$, where $a>\frac{1}{2}$. (Note that this is a point in the unburnt fluid.) We claim that there are two distinct ignition curves passing through $(0,a)$. Let $s_1=(a-1/2)^{1/2}$ and $s_2=-(a-1/2)^{1/2}$. The ignition curve starting at the point $(x(s_1,0),y(s_1,0))$ is

$$x(s_1,t) = \frac{2(a-1/2)^{1/2}}{(1+4((a-1/2)^{1/2})^2)^{1/2}}t - (a-1/2)^{1/2} \tag{2.160}$$

$$= (a-1/2)^{1/2}\left\{\frac{2t}{(4a-1)^{1/2}} - 1\right\}$$

$$y(s_1,t) = \frac{1}{(1+4((a-1/2)^{1/2})^2)^{1/2}}t + ((a-1/2)^{1/2})^2 \tag{2.161}$$

$$= \frac{t}{(4a-1)^{1/2}} + (a-1/2).$$

Similarly, the ignition curve starting at the point $(x(s_2,0),y(s_2,0))$ is

$$x(s_2,t) = \frac{-2(a-1/2)^{1/2}}{(1+4(-(a-1/2)^{1/2})^2)^{1/2}}t + (-(a-1/2)^{1/2}) \tag{2.162}$$

$$= -(a-1/2)^{1/2}\left\{\frac{2t}{(4a-1)^{1/2}} - 1\right\}$$

$$y(s_2,t) = \frac{1}{(1+4(-(a-1/2)^{1/2})^2)^{1/2}}t\ (-(a-1/2)^{1/2})^2 \tag{2.163}$$

$$= \frac{t}{(4a-1)^{1/2}} + (a-1/2).$$

At $t=\bar{t}\equiv(1/2)(4a-1)^{1/2}$, these two curves intersect, since

$$x(s_1,\bar{t}) = 0 = x(s_2,\bar{t}) \tag{2.164}$$

$$y(s_1,\bar{t}) = a = y(s_2,\bar{t}). \tag{2.165}$$

Unlike the situation in Lemma 2 in which the convexity of the initial data implied that the ignition curves could not collide, in this example of a

non-convex initial curve, the ignition curves intersect.

In Figure (2.22), we graph (2.157) and (2.158) for various values of t.

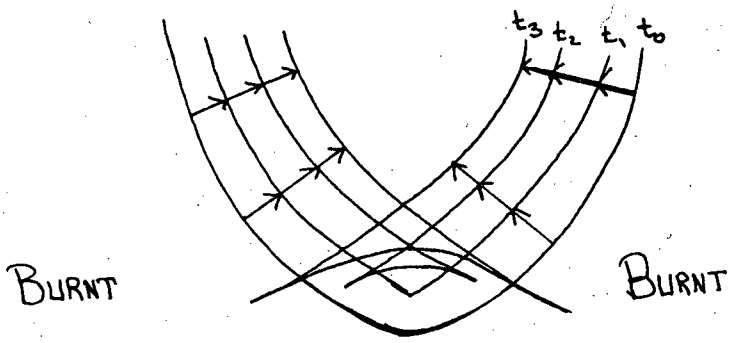

Figure 2.22

As the curve moves, it crosses itself at the point where the two ignition curves collide. The previous calculation shows that this collision occurs at the point $(0,a)$, $a>\frac{1}{2}$, when $t=(\frac{1}{2})(4a-1)^{1/2}$.

Figure (2.22) illustrates the situation. At any time $t>\frac{1}{2}$, the moving curve can be divided into two parts: the part above and including the crossover point, and the part below. The part above and including the crossover point is given by $(x(s,t),y(s,t))$, for all s such that $-\infty<s\leq(-1/2)(4t^2-1)^{1/2}$ or $(1/2)(4t^2-1)^{1/2}\leq s<\infty$. The part below corresponds to all s such that $(-1/2)(4t^2-1)^{1/2}<s<(1/2)(4t^2-1)^{1/2}$. The particles located along the part above and including the crossover point are the ones "on fire" at time t; they form the boundary between the burnt and unburnt particles. The part of the curve below the crossover point passes through fluid that is already burnt.

Thus, as any time $t>\frac{1}{2}$, the actual flame front is a subset of the moving curve. Hence, the position of the flame front at time t is given by $(x(s,t),y(s,t))$, $s\in(-\infty,\infty)$ for $t<\frac{1}{2}$, and $(x(s,t),y(s,t))$ $s\in(-\infty,(-1/2)(4t^2-1)^{1/2}]\cup[(1/2)(4t^2-1)^{1/2},\infty)$ for $t\geq\frac{1}{2}$, where $x(s,t)$ and $y(s,t)$ are given by (2.157) and (2.158). In Figure (2.23), the position of the flame front is shown for various values of t.

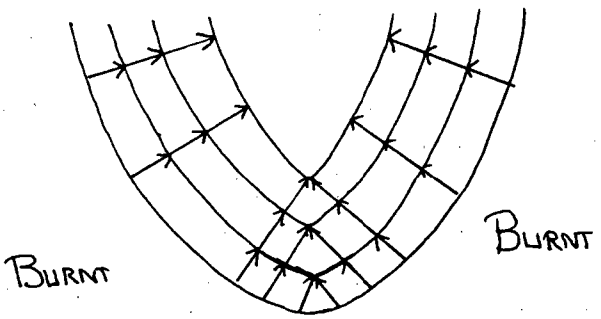

Figure 2.23

In addition, we can show that for $t>\frac{1}{2}$, the front develops a cusp, that is, a point where the curve is continuous but not differentiable. To verify this, we check the one-sided derivatives. Using (2.28), we see that

$$\lim_{s\to[(-1/2)(4t^2-1)^{1/2}]^-}(y_s/x_s)=\lim_{s\to[(-1/2)(4t^2-1)^{1/2}]^-}(\beta_s/\alpha_s) \qquad (2.166)$$

$$=\lim_{s\to[(-1/2)(4t^2-1)^{1/2}]^-}(2s)=-(4t^2-1)^{1/2}$$

while

$$\lim_{s\to[(-1/2)(4t^2-1)^{1/2}]^+}(y_s/x_s)=\lim_{s\to[(-1/2)(4t^2-1)^{1/2}]^+}(\beta_s/\alpha_s) \qquad (2.167)$$

$$=\lim_{s\to[(-1/2)(4t^2-1)^{1/2}]^+}(2s)=(4t^2-1)^{1/2}.$$

For $t>1/2$, these two limits are not equal, hence the tangent is discontinuous. Thus we have shown that an infinitely differentiable initial front can develop cusps as it burns and cease to be differentiable. Drawings to this effect were first made in [18]. This completes the example.

We now consider an arbitrary, non-convex initial curve and ask the following questions: How shall we continue the motion of the flame front beyond the point when ignition curves first collide? Which sections of our moving curve do we eliminate so that the remaining portions form the actual boundary between burnt and unburnt regions? (N.B. It is important to stress that for a convex initial curve, ignition curves cannot collide.)

We now develop an "entropy condition" for our propagating flame front. With the help of this condition, we will be able to continue our solution beyond the time when ignition curves first collide. Let $\gamma(s)=(\alpha(s),\beta(s))$, $s\in[0,S]$ be a simple, closed, regular curve of class C^2. Suppose that the particles inside γ are burnt and those outside are unburnt. At $t=0$, we ignite all the particles along γ and allow the front to propagate normal to itself with speed k. Let $\varphi(x,y,t)$ be the indicator function of the burnt region; $\varphi(x,y,t)=1$ if the particle located at (x,y) is burnt at time t and zero otherwise. Since the ignition curve connecting the initial curve and the point (x,y) is a straight line normal to the initial curve, its length equals the distance from (x,y) to the initial curve, and we have

$$\varphi(x,y,t) = \begin{cases} 1 & \text{if } (x,y) \text{ is burnt at } t=0 \\ 1 & (kt)^2 \geq \min\limits_{s\in[0,S]} (x-\alpha(s))^2+(y-\beta(s))^2 \\ 0 & (kt)^2 < \min\limits_{s\in[0,S]} (x-\alpha(s))^2+(y-\beta(s))^2 \end{cases} \tag{2.168}$$

$\varphi(x,y,t)$ measures when the "news" of the burning front reaches a particular particle. From the definition of φ, we see that if $\varphi(x_0,y_0,t_0)=1$, then $\varphi(x_0,y_0,t)=1$ for all $t>t_0$; once a particle changes from unburnt to burnt, it remains burnt for all t.

Definition. We say that a propagating flame front satisfies the entropy condition if once a particle burns, it remains burnt.

Our reasons for the name "entropy condition" will be made clear later. In this work, we assume that the flame front satisfies the entropy condition. Then if two ignition curves cross at a particular point, whichever one arrives first will ignite the particle located there.

Let $(x(s_1,t),y(s_1,t))$, $(x(s_2,t),y(s_2,t))$, $s_1,s_2\in[0,S]$, $t\in[0,\infty)$ be two ignition curves that collide at some point P, and suppose that the ignition curve leaving $(x(s_1,0),y(s_1,0))$ arrives at P before (or at the same time as) as the ignition curve leaving $(x(s_2,0),y(s_2,0))$. Then there exists t_1 and t_2 such that

$$(x(s_1,t_1),y(s_1,t_1))=P=(x(s_2,t_2),y(s_2,t_2)) \qquad t_1\leq t_2 \tag{2.169}$$

By the entropy condition, the ignition curve arriving first (of shortest length) will be the one that ignites the particle at P. In our next lemma, we prove that, for $t>t_2$, the later arriving ignition curve can only pass through fluid that has been previously burnt. That is, every particle on the ignition curve

$(x(s_2,t),y(s_2,t))$ beyond the intersection point is burnt before the "fuse" from $(x(s_2,0),y(s_2,0))$ reaches it. Thus, we can ignore its effects for $t \geq t_2$.

Lemma 3. Let $\gamma(s)=(\alpha(s),\beta(s))$, $s \in [0,S]$ be a simple, closed, regular curve of class C^2. Let $(x(s,t),y(s,t))$, $s \in [0,S]$, $t \in [0,\infty)$ be the ignition curves of γ as defined in (2.67) and (2.68). Suppose there exists $s_1,s_2 \in [0,S]$, $s_1 \neq s_2$, and t_1,t_2 such that $(x(s_1,t_1),y(s_1,t_1))=(x(s_2,t_2),y(s_2,t_2))$, with $t_1 \leq t_2$. Then, given any $t_3 > t_2$,

$$\min_{s \in [0,S]} \left\{ (x(s_2,t_3)-x(s,0))^2+(y(s_2,t_3)-y(s,0))^2 \right\} \tag{2.170}$$

$$< \left\{ (x(s_2,t_3)-x(s_2,0))^2+(y(s_2,t_3)-y(s_2,0))^2 \right\}$$

Furthermore, there exists a $\bar{t} < t_3$ such that $\varphi(x(s_2,t_3),y(s_2,t_3),\bar{t})=1$, where φ is defined in (2.168).

Note that if $t_1=t_2$, both curves can be eliminated beyond the intersection point.

Proof. Let l_1 be the distance from $(x(s_1,0),y(s_1,0))$ to $(x(s_1,t_1),y(s_1,t_1))$. Then $l_1=kt_1$. Let l_2 be the distance from $(x(s_2,0),y(s_2,0))$ to $(x(s_2,t_2),y(s_2,t_2))$. Then $l_2=kt_2$, and $l_1 \leq l_2$. Let P be the point where the ignition curves intersect; $P=(x(s_1,t_1),y(s_1,t_1))=(x(s_2,t_2),y(s_2,t_2))$. Choose $t_3 > t_2$ and let $Q=(x(s_2,t_3),y(s_2,t_3))$. Let A be the point $(x(s_1,0),y(s_1,0))$ and B be the point $(x(s_2,0),y(s_2,0))$. (See Figure (2.24))

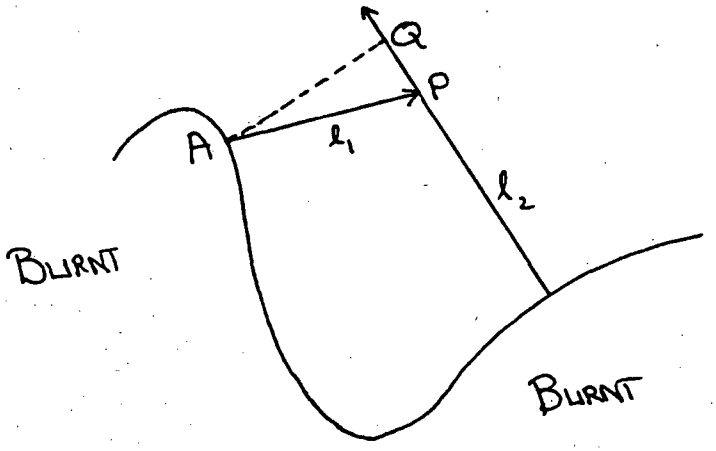

Figure 2.24

Then $\overline{AQ}<\overline{AP}+\overline{PQ}=l_1+\overline{PQ}\le l_2+\overline{PQ}=\overline{BQ}$. Thus, Q is closer to A than it is to B, hence, B cannot be the point that ignites Q. Define $\bar{t}$ such that $k\bar{t}=\overline{AQ}$. Then $k\bar{t}<\overline{BQ}=kt_3$. Thus $\varphi(x(s_2,t_3),y(s_2,t_3),\bar{t})=1$. This completes the proof.

Thus, we can eliminate the late-arriving ignition curve beyond the intersection point. In the next lemma, we prove that if an ignition curve is eliminated, it must be eliminated by an ignition curve of equal length, and hence, by Lemma 3, both can have no effect beyond the intersection point.

Lemma 4 Let $\gamma(s)=(\alpha(s),\beta(s))$, $s\in[0,S]$ be a simple closed, regular curve of class C^2. Let $(x(s,t),y(s,t))$, $s\in[0,S]$, $t\in[0,\infty)$ be the ignition curves of γ as defined in (2.67)-(2.68). Suppose, in accordance with Lemma 3, we eliminate those parts of ignition curves that reach previously burnt fuel. Then, if an ignition curve is eliminated for $t\ge t_1$, it is eliminated by an ignition curve of equal length. Hence, both pass through previously burnt fuel for $t\ge t_1$.

Proof. Suppose the curve leaving $\gamma(s_1)$, $s_1\in[0,S]$ is eliminated. Thus, there exists t_1 such that for $0\le t<t_1$, $(x(s_1,t),y(s_1,t))$ passes though unburnt fuel, and for $t\ge t_1$, $(x(s_1,t),y(s_1,t))$ passes through previously burnt fuel. Let the

curve leaving $\gamma(s_2)$, $s_2 \in [0,S]$ be the one that eliminates $x(s_1,t), y(s_1,t)$. That is, there exists t_2 such that $(x(s_2,t_2), y(s_2,t_2)) = (x(s_1,t_1), y(s_1,t_1))$ with $t_2 \leq t_1$. We prove that $t_2 = t_1$. Suppose not. Then $t_2 < t_1$, and all points $(x(s_1,\bar{t}), y(s_1,\bar{t}))$, $t_2 < \bar{t} < t_1$ on the first ignition curve are closer to $\gamma(s_2)$ then they are to $\gamma(s_1)$, and are thus burnt before the ignition curve leaving $\gamma(s_1)$ reaches them. This means that the curve leaving $\gamma(s_1)$ must have been eliminated before t_1, which contradicts the hypothesis. Hence, $t_2 = t_1$, and both ignition curves are eliminated at the same time. This completes the proof.

We can now describe the motion of a propagating flame front. We extend ignition curves from the front according to our formulae

$$x(s,t) = k \frac{\beta_s}{(\alpha_s^2+\beta_s^2)^{-1/2}} + \alpha \tag{2.171}$$

$$y(s,t) = -k \frac{\alpha_s}{(\alpha_s^2+\beta_s^2)^{1/2}} + \beta \tag{2.172}$$

and move the flame front along these ignition curves until there is a collision. Eliminate those ignition curves that carry the initial front into the intersection point, since they are of the same length. Continue moving the front along the remaining ignition curves, all the while eliminating curves that collide. This will give the position of the front at any time. At any time, each point of the front can be traced back along an ignition curve to the initial curve, since the motion of the front is solely determined by the ignition curves. However, there may be points on the initial curve whose ignition curves are eliminated before they reach the propagating front.

We return briefly to Example 2.4 and point out that we have already used this elimination procedure to follow the propagation of the parabolic flame front. For $0 \leq t < \frac{1}{2}$, the ignition curves do not intersect. For each value of

$t>\frac{1}{2}$, a pair of ignition curves of equal length intersect, one from $s=(-1/2)(4t^2-1)^{1/2}$ and one from $s=(1/2)(4t^2-1)^{1/2}$. To continue our solution beyond that time, we eliminate both of the curves. This is the solution we previously found.

We are now able to explain our choice of the phrase "entropy condition". If the initial curve is convex and of class C^2, the solution $(x(s,t),y(s,t))$ is reversible; given the position of the flame front at any time $\bar{t}$, we may reconstruct the initial data. This is because the ignition curves cannot intersect, and thus it suffices to follow the front backwards in time along the ignition curves for a time $\bar{t}$:

$$x(s,0) = k\,\frac{y_s(s,\bar{t})}{((x_s(s,\bar{t}))^2+(y_s(s,\bar{t}))^2)^{1/2}}(-\bar{t}) + x(s,\bar{t}) \qquad (2.173)$$

$$y(s,0) = -k\,\frac{x_s(s,\bar{t})}{((x_s(s,\bar{t}))^2+(y_s(s,\bar{t}))^2)^{1/2}}(-\bar{t}) + y(s,\bar{t})\,. \qquad (2.174)$$

However, if the initial curve is not convex, the ignition curves collide. Once they collide, the results of Lemmas 3 and 4 show that we can eliminate them, with no effect on the solution. Thus, the position of the flame front, after the time when the ignition curves first collide, has no "knowledge" of those discarded ignition curves. Information is "swallowed up" at the collision point and the solution ceases to be reversible; hence the name "entropy". Each time we use the entropy condition to discard ignition curves, more information about the initial data is lost.

Example 2.5. As another example of the elimination of ignition curves for non-convex initial data, suppose the initial front is in the shape of the cardioid $\gamma(s)=(\alpha(s),\beta(s))=(\cos(s),\sin(s)(1-\cos(s)))$, $s\in[0,2\pi]$. Assume that the parti-

cles inside γ are burnt and the particles outside are unburnt. We ignite the particles located along γ and allow the curve to propagate normally to itself with unit speed. (See Figure (2.25))

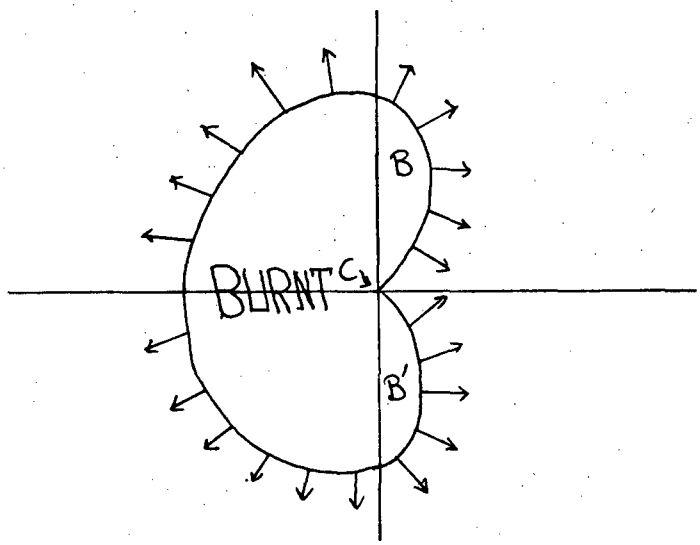

Figure 2.25

Let $B=\gamma(\pi/3)$ and $B'=\gamma(2\pi-\pi/3)$. These are the points whose ignition curves are in the positive x direction. Given s, $0<s<\pi/3$, the ignition curve leaving $\gamma(s)$ collides with the one leaving $\gamma(2\pi-s)$. When they collide, they are eliminated and the effect is that the cusp C "travels" along the x axis, "swallowing up" sections of the parameterization. We wish to establish the relationship between the distance the cusp has traveled and the set of ignition curves that have been eliminated. Let $P=\gamma(s_1)$, with $0<s_1<\pi/3$, and let l be the length of the ignition curve between P and the point $(\Delta,0)$ where it hits the x axis. (See Figure (2.26))

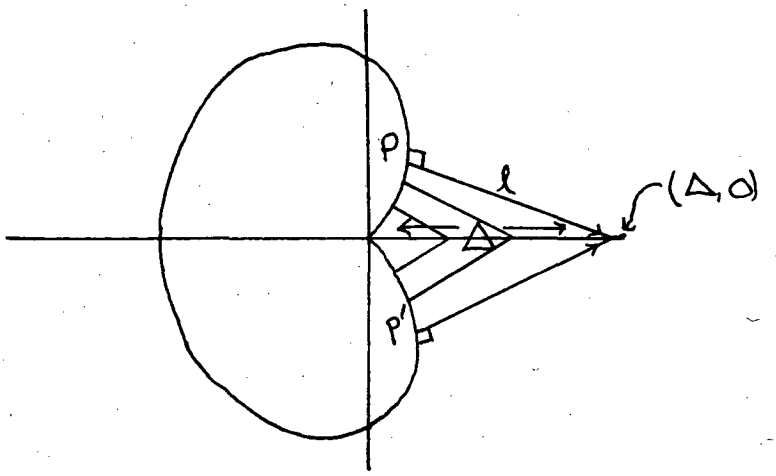

Figure 2.26

A calculation shows that

$$l = \frac{(1-\cos(s_1))\sin(s_1)}{\cos(3s_1/2)}. \tag{2.175}$$

Since the flame travels with unit speed, the time it takes the front to reach the point $(\Delta,0)$ is

$$t = \frac{(1-\cos(s_1))\sin(s_1)}{\cos(3s_1/2)}. \tag{2.176}$$

Let $g(s_1) = \frac{(1-\cos(s_1))\sin(s_1)}{\cos(3s_1/2)}$. Another calculation shows that

$$\Delta = \frac{(1-\cos(s_1))\cos(s_1/2)}{\cos(3s_1/2)}. \tag{2.177}$$

Let $h(s) = \frac{(1-\cos(s_1))\cos(s_1/2)}{\cos(3s_1/2)}$. At time t, ignition curves of equal length leaving $\gamma(s_1)$ and $\gamma(2\pi-s_1)$ reach $(\Delta,0)$, and all the curves leaving γ between $\gamma(2\pi-s_1)$ and $\gamma(s_1)$ have been eliminated. Thus, we know which ignition curves to eliminate at time t. Using (2.169) and (2.170), we have

$$x(s,t) = \begin{Bmatrix} h(g^{-1}(t)) & s \le g^{-1}(t) \\ \frac{\beta_s}{(\alpha_s^2+\beta_s^2)^{1/2}} t + \alpha & g^{-1}(t) < s < 2\pi - g^{-1}(t) \\ h(g^{-1}(t)) & 2\pi - g^{-1}(t) \le s \end{Bmatrix} \tag{2.178}$$

$$y(s,t) = \begin{Bmatrix} 0 & s \le g^{-1}(t) \\ \frac{-\alpha_s}{(\alpha_s^2+\beta_s^2)^{1/2}} t + \beta & g^{-1}(t) < s < 2\pi - g^{-1}(t) \\ 0 & 2\pi - g^{-1}(t) \le s \end{Bmatrix} \tag{2.179}$$

To uniquely define $g^{-1}(t)$, we use the smallest value of s_1 between 0 and 2π such that $g(s_1)=t$. Since $(\alpha_s^2+\beta_s^2)=2(1-\cos(s))$, calculating α_s and β_s we find

$$x(s,t) = \begin{Bmatrix} \frac{(1-\cos(g^{-1}(t)/2))\cos(g^{-1}(t)/2)}{\cos(3g^{-1}(t)/2)} & s \le g^{-1}(t) \\ \frac{\cos(s)-\cos(2s)}{(2(1-\cos(s)))^{1/2}} t + \cos(s) - \cos^2(s) & g^{-1}(t) < s < 2\pi - g^{-1}(t) \\ \frac{(1-\cos(g^{-1}(t)/2))\cos(g^{-1}(t)/2)}{\cos(3g^{-1}(t)/2)} & 2\pi - g^{-1}(t) \le s \end{Bmatrix} \tag{2.180}$$

$$y(s,t) = \begin{Bmatrix} 0 & s \le g^{-1}(t) \\ \frac{\sin(s)-\sin(2s)}{(2(1-\cos(s)))^{1/2}} t + \sin(s) - \cos(s)\sin(s) & g^{-1}(t) < s < 2\pi - g^{-1}(t) \\ 0 & 2\pi - g^{-}(t) \le s \end{Bmatrix} \tag{2.181}$$

A drawing of $(x(s,t),y(s,t))$ for various values of t is given in Figure (2.27).

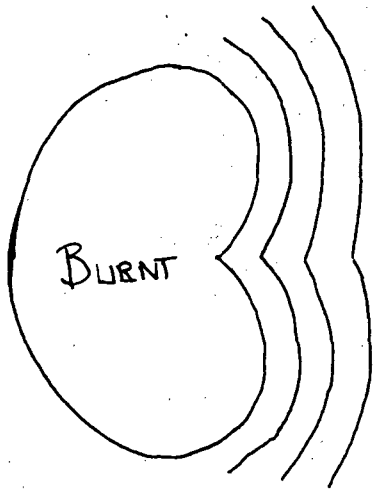

Figure 2.27

We now show that as $t \to \infty$, the cusp disappears and the propagating flame front becomes differentiable at the point where it intersects the positive x axis. Define $\varphi^+(t)$ by

$$\varphi^+(t) = \lim_{s \to (g^{-1}(t))^+} (\tan^{-1}(\frac{y_s}{x_s})) . \tag{2.182}$$

(See Figure (2.28))

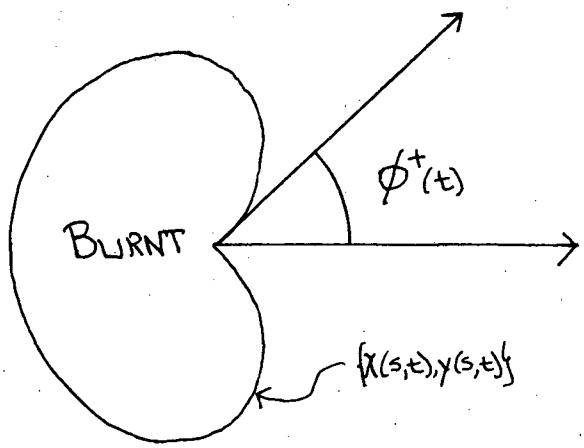

Figure 2.28

Using (2.28), we then have

$$\varphi^+(t) = \lim_{s \to (g^{-1}(t))^+} (\tan^{-1}(\frac{\beta_s}{\alpha_s})). \tag{2.183}$$

From the definition of $g(s_1)$, we have $\lim_{t \to \infty} g^{-1}(t) = \pi/3$. Therefore,

$$\lim_{t \to \infty} \varphi^+(t) = \lim_{s \to \pi/3} (\tan^{-1}(\frac{\beta_s}{\alpha_s})) \tag{2.184}$$

$$= \lim_{s \to \pi/3} \tan^{-1}\left\{ \frac{\cos(s) - \cos(2s)}{\sin(2s) - \sin(s)} \right\}$$

$$= \pi/2 .$$

Thus, the cusp opens to an angle of $\pi/2$. By symmetry, the angle $\varphi(s-(\pi/2))$ opens up to $\pi/2$ also. Thus the tangent to the curve becomes vertical and changes direction continuously at the point where the front intersects the positive x axis. This completes the example.

This example shows that the traveling cusp engulfs sections of the initial curve until it itself disappears. In Example 2.4, we showed that the collision of ignition curves can cause a cusp to form in the solution. The creation and disappearance of cusps is a consequence of the entropy condition. In the next theorem, we show that any simple, closed, regular curve of class C^2 (convex or not) burns into a circle as $t \to \infty$.

Remark. We shall need the following inequality: If $0<l<a<b$, then $a-(a^2-l^2)^{1/2}>b-(b^2-l^2)^{1/2}$. To show this, we let $f(t)=t-(t^2-l^2)^{1/2}$. Then $f'(t)=1-(1/2)(t^2-l^2)^{-1/2}(2t)=1-\frac{t}{(t^2-l^2)^{1/2}}$. For $t>l$, $\frac{t}{(t^2-l^2)^{1/2}}>1$, which implies that $f'(t)<0$.

Theorem 5. Let $\gamma(s)=(\alpha(s),\beta(s))$, $s\in[0,S]$ be a simple, closed, regular, positively oriented curve of class C^2. Assume that the convex hull $\gamma_H(s)$, $s\in[0,S^H]$ of γ is piecewise C^2 and piecewise regular. Assume that the front propagates in a direction normal to itself with speed k. Then, as $t \to \infty$, the shape of the burnt region approaches a circular region.

Remark. The convex hull of γ is the boundary of the smallest convex set that contains all points of γ; physically it corresponds to a membrane stretched as tightly as possible around γ. It consists of pieces of the original curve connected by straight lines, and is tangent to the original curve at every point where they touch.

Proof. The proof will consist of showing that γ and γ_H approach the same shape as $t \to \infty$. Since, by Theorem 4, γ_H must become circular as $t \to \infty$, so then must γ. Without loss of generality, we assume the front propagates at unit speed.

We first note that if γ is convex, then γ and γ_H are the same curve and we are done. In the non-convex case, along those sections of γ where γ_H and γ touch, the two curves are tangent and their ignition curves are the same. Thus, we focus our attention on those sections where γ_H and γ do not touch.

Let A and B be two points common to γ and γ_H, $A=\gamma(s_1)$ and $B=\gamma(s_2)$, such that the section of γ_H between A and B does not touch γ. Thus, between A and B, γ_H is a straight line segment connecting A to B. (See Figure (2.29))

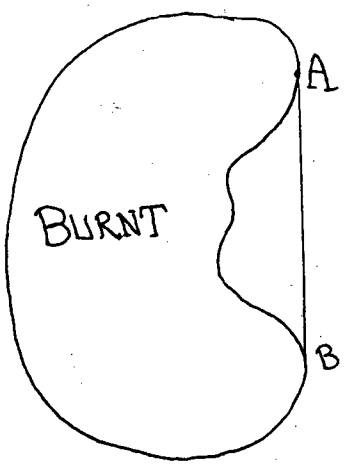

Figure 2.29

We want to show that the section of the curve γ between A and B burns into the same shape as does the line segment $\overline{AB}$ as $t \to \infty$. Draw the ignition curves of γ_H at A and B; since γ_H is tangent to γ at A and B, they must be the same

as the ignition curves of γ at A and B. Define I_A to be the ignition curve leaving A and I_B to be the ignition curve leaving B. (See Figure (2.30).)

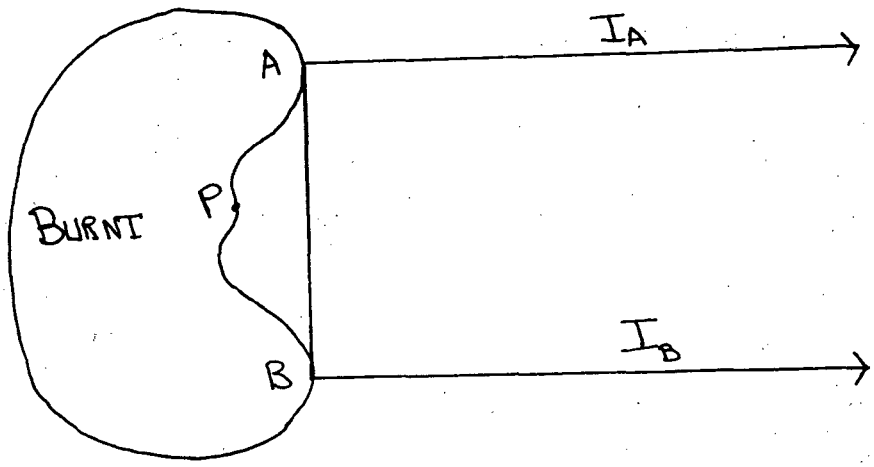

Figure 2.30

The ignition curves at A and B must be parallel, since they are both normal to the line segment $\overline{AB}$. We note that the ignition curve leaving any point P on γ between A and B can only influence the region between I_A and I_B, since any point outside that region must be nearer to A or to B (and hence will be ignited by the closer of the two) than it is to P.

Choose $\varepsilon>0$. We will show that there exists a t_0 such that for $t>t_0$, each point of the flame front that evolved from the section of the original curve γ between A and B lies less than a distance ε from the flame front that evolved from the section of the convex hull between A and B. In other words, as $t\to\infty$, the two propagating flame fronts get within ε of each other.

Let $2l$ be the distance between A and B, and consider the set of points that lie between I_A and I_B a distance greater than $\frac{\varepsilon^2+l^2}{2\varepsilon}$ from both A and B,

and a distance less than $\frac{\varepsilon^2+l^2}{2\varepsilon}$ from the line segment $\overline{AB}$;

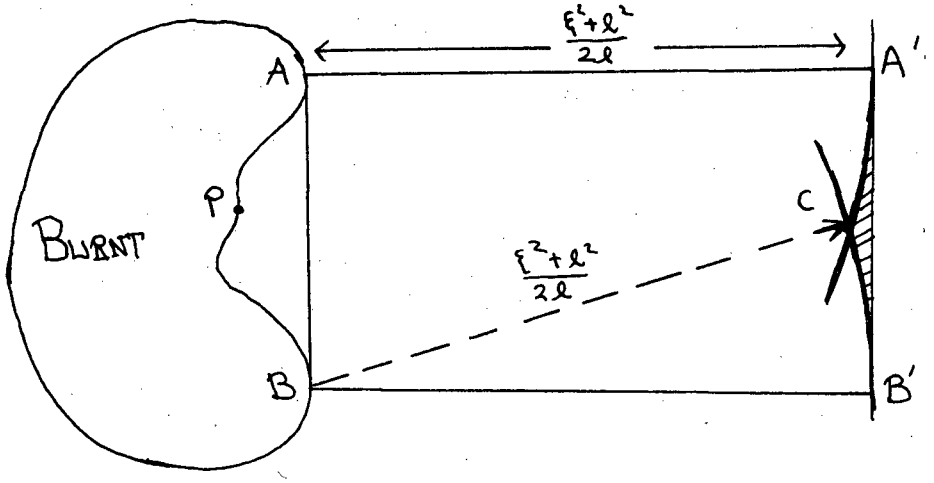

Figure 2.31

this corresponds to the shaded region in Figure (2.31). We claim that every point in that shaded region is a distance less than ε from the line segment $\overline{A'B'}$. To prove this, we note that the distance from C to $\overline{AB}$ is $((\frac{\varepsilon^2+l^2}{2\varepsilon})^2-l^2)^{1/2}$. Thus the distance from C to $\overline{A'B'}$ is

$$\frac{\varepsilon^2+l^2}{2\varepsilon} - ((\frac{\varepsilon^2+l^2}{2\varepsilon})^2-l^2)^{1/2} = \frac{\varepsilon^2+l^2}{2\varepsilon} - (\frac{\varepsilon^4+2\varepsilon^2l^2+l^4-4\varepsilon^2l^2}{4\varepsilon^2})^{1/2} \quad (2.185)$$

$$= \frac{\varepsilon^2+l^2}{2\varepsilon} - (\frac{\varepsilon^4-2\varepsilon^2l^2+l^4}{4\varepsilon^2})^{1/2}$$

$$= \frac{\varepsilon^2+l^2}{2\varepsilon} - (\frac{l^2-\varepsilon^2}{2\varepsilon})$$

$$= \varepsilon .$$

Since every point in the shaded region is closer than the point C to the segment $\overline{A'B'}$, every point of the shaded region is less than ε from $\overline{A'B'}$.

We can now complete the proof. Choose $t_0 = \frac{\varepsilon^2+l^2}{2\varepsilon}$. Allow the section of the convex hull between A and B to propagate at unit speed for a time $t>t_0$; this corresponds to a line segment $\overline{A'B'}$ displaced a distance t to the right. Similarly, allow the section of the original curve γ between A and B to propagate at unit speed for the same length of time. We claim that this flame front (labeled $\gamma(t)$) is within ε of the segment $\overline{A'B'}$. There are only two possibilities. No part of $\gamma(t)$ can be to the right of the segment $\overline{A'B'}$, since such a point would be located a distance greater than t from the original curve, which is impossible. Likewise, there can be no unburnt particle located to the left of the shaded region (see Figure (2.32)), since such a point is located a distance less than t from either A or B and thus must have been ignited by time t.

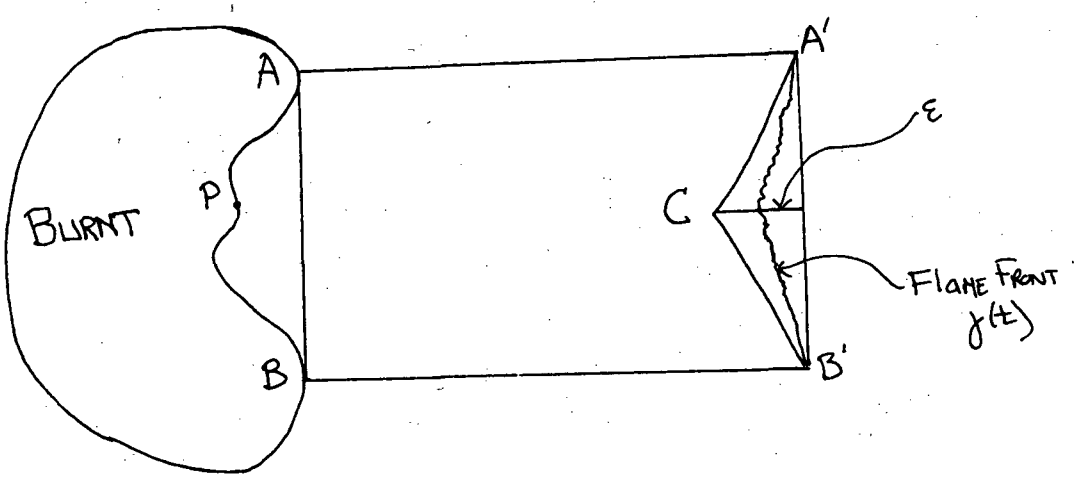

Figure 2.32

Thus, $\gamma(t)$ must lie in the shaded region. We repeat the earlier argument to see that every point in the shaded region lies a distance less than $t-(t^2-l^2)^{1/2}$

from $\overline{A'B'}$. Finally, using the inequality proved earlier, we have $t-(t^2-l^2)^{1/2}<t_0-(t_0^2-l^2)^{1/2}=\varepsilon$, since $t_0<t$. Thus, $\gamma(t)$ lies less than ε from $\overline{A'B'}$. This completes the proof.

2.5. Comparison of Flame Propagation with Gas Flow in One Dimension

The situation we have presented is analogous to gas flow in one dimension. In this section, we briefly explore the analogy. The comments that follow on the solution of a conservation law are taken from [3].

We consider the conservation law

$$u_t+(\frac{1}{2}u^2)_x = 0 . \tag{2.186}$$

The characteristics are straight lines along which the solution u of (2.186) is constant. Consider the initial data

$$u(x,0) = \begin{cases} 1 & x\geq 0 \\ 0 & x<0 \end{cases} \tag{2.187}$$

The characteristics do not fill out the (x,t) plane, as can be seen in Figure (2.33).

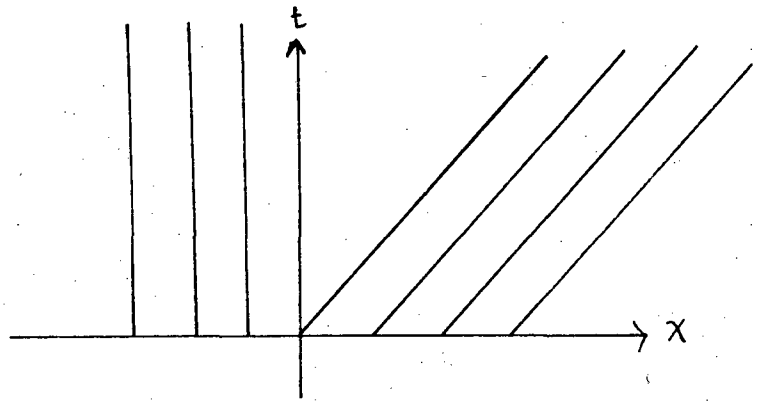

Figure 2.33

We fill out the (x,t) plane through the introduction of a rarefaction fan. This is a set of characteristics leaving the origin that fan out and provide the transition from the characteristic on the left leaving the origin to the characteristic on the right. (See Figure (2.34).)

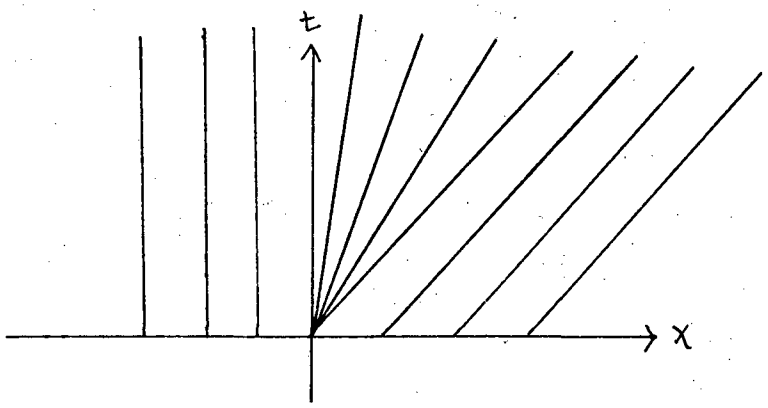

Figure 2.34

Conversely, consider the initial data

$$u(x,0) = \begin{cases} 0 & x \geq 0 \\ 1 & x < 0 \end{cases} \tag{2.188}$$

Here, the characteristics cross each other. We introduce a shock with propagation speed $s = 1/2$ to keep the characteristics from crossing. Thus, we get a globally defined weak solution, as shown in Figure (2.35).

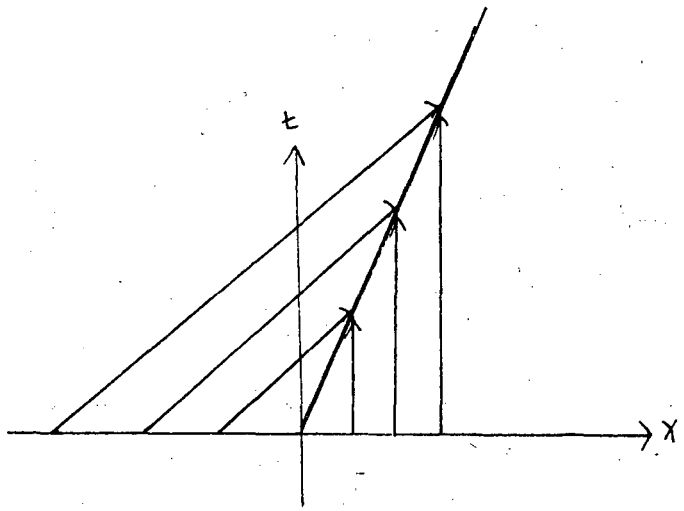

Figure 2.35

In the above, we have made use of an "entropy condition" which may be stated as follows: A shock satisfies the entropy condition if, when it separates the characteristics of one family, the characteristics can be traced back to the initial data.

The above discussion parallels our theory of flame propagation. We have introduced ignition curves along which the heat required for ignition is transported. These curves are analogous to the characteristics of (2.186): curves along which the solution u is carried. When the flame propagates with uniform

speed, the ignition curves are straight lines, just as the characteristics of the simple conservation law (2.186) are straight lines.

In Section 2.3, we gave an example of initial data for which the ignition curves separated, leaving an open area. In Theorem 4, we showed that ignition curves could be constructed to fill in the open area, with the requirement that each ignition curve reach back to the initial data. These ignition curves provided a transition from the ignition curves on the right to the ignition curves on the left. In Section 2.4, we gave an example of initial data for which the ignition curves collided. We introduced an entropy condition that stipulated that each particle burns only once. This enabled us to continue the solution beyond the first collision. Our constructed solution maintained the property that every point of the moving front reach back along an ignition curve to the initial data.

Thus, the two entropy conditions have a similar result: they ensure that we can always trace back along characteristics/ignition curves to the initial data. This promises that the solution depends only on the initial data.

In the following chapters, we return to our full set of combustion equations (1.15)-(1.20).

Chapter Three

Flame Propagation with Volume Expansion

In this chapter, we use the results of our theory of flame propagation to analyze the full set of combustion equations (1.15-1.20).

3.1. Effects of Volume Expansion

In Chapter Two, we studied the motion of a flame propagating in a premixed, combustible fluid with no boundaries. Since we assumed that the density of a particle remained constant as it changed from unburnt to burnt, there was no motion imparted to the fluid by the flame. If the fluid is initially at rest, it remains at rest. Each fluid particle is "glued down", and changes from unburnt to burnt when the flame reaches it.

We now consider the effects of volume expansion. Assume that the density of the unburnt fluid is ρ_u, the density of the burnt fluid is ρ_b, and the flame propagates in a direction normal to itself with speed k. Let $\rho_b < \rho_u$ (the case $\rho_b > \rho_u$ is physically unreasonable). Each particle along the flame front expands as it burns, pushing the surrounding particles. Since the flow of mass across the flame front is conserved, this sudden change in volume along the flame front must be accompanied by a jump in the normal component of the fluid velocity across the front of strength $2\left\{\frac{\rho_u - \rho_b}{\rho_u + \rho_b}\right\}k$. (See Chapter One). We rewrite this as $\left\{\frac{1-(\rho_b/\rho_u)}{1+(\rho_b/\rho_u)}\right\}k$. The smaller the density ratio (ρ_b/ρ_u) between the burnt and the unburnt fluids, the more the particles expand and the greater the velocity jump. Likewise, the larger the flame speed, the greater the velocity jump. The location of the boundary between the burnt and

unburnt regions, as seen from a fixed reference frame, is a product of two factors: first, the change in individual fluid particles from unburnt to burnt and second, the velocity field produced by their resulting expansion.

We appeal to the theory of single layer distributions. Let $\gamma(s)=(\alpha(s),\beta(s))$, $s\in[0,S]$ be a simple, closed, regular curve. We assume that γ is infinitely differentiable with respect to s. Suppose we spread a charge $\mu(s)$ along γ, where μ is a C^∞ function such that $\mu(0)=\mu(S)$, $\mu'(0)=\mu'(S)$, etc. If we define the single layer potential $\varphi(x,y)$ as

$$\varphi(x,y) = \frac{1}{2\pi}\int_0^S \frac{\mu(s)}{(\alpha_s^2+\beta_s^2)^{1/2}}\log((x-\alpha(s))^2+(y-\beta(s))^2)^{1/2}ds \qquad (3.1)$$

then it can be shown [5] that

1) At any point (x,y) not on γ, φ is twice differentiable and $\nabla^2\varphi(x,y) = 0$.

2) $\varphi(x,y)$ is continuous across γ.

3) The tangential derivative of φ is continuous across γ.

4) The normal derivative of φ undergoes a jump of strength μ across γ.

We use this to find the velocity field produced by volume expansion along the flame front. We uniformly spread a charge $\mu=2\left\{\frac{\rho_u-\rho_b}{\rho_u+\rho_b}\right\}k$ along a flame front $\gamma(s)=(\alpha(s),\beta(s)),s\in[0,S]$. Then the associated single layer potential is

$$\varphi(x,y) = \frac{1}{2\pi}\int_0^S 2\left\{\frac{\rho_u-\rho_b}{\rho_u+\rho_b}\right\}k\,(\alpha_s^2+\beta_s^2)^{-1/2}\log((x-\alpha(s))^2+(y-\beta(s))^2)^{1/2}ds \quad (3.2)$$

{N.B. The term $(\alpha_s^2+\beta_s^2)^{-1/2}$ in the integrand of (3.4) is the reciprocal of arc length. We need to divide μ by the arc length to insure that the charge μ corresponds to a charge per unit length of the flame }. Thus, if we let $\vec{u} = \nabla\varphi$, we have that

$$\nabla\cdot\vec{u} = \nabla\cdot\nabla\varphi = 0 \quad (3.3)$$

and the jump in the normal component of $\vec{u}$ across the flame front is of strength

$$2\left\{\frac{\rho_u-\rho_b}{\rho_u+\rho_b}\right\}k \quad (3.4)$$

We combine this velocity field with the burning motion of the front in a direction normal to itself. Equations (1.13) and (1.14) become

$$\frac{\partial X_F}{\partial t} = k\frac{\dfrac{\partial Y_F}{\partial s}}{((\dfrac{\partial X_F}{\partial s})^2+(\dfrac{\partial Y_F}{\partial s})^2)^{1/2}} + u(X_F,Y_F) \quad (3.5)$$

$$\frac{\partial Y_F}{\partial t} = -k\frac{\dfrac{\partial X_F}{\partial s}}{((\dfrac{\partial X_F}{\partial s})^2+(\dfrac{\partial Y_F}{\partial s})^2)^{1/2}} + v(X_F,Y_F) \quad (3.6)$$

where

$$\left\{u(X_F,Y_F),v(X_F,Y_F)\right\} = \frac{1}{2}\left\{\lim_{-}\nabla\varphi + \lim_{+}\nabla\varphi\right\}$$

and

$$\varphi(x,y) = \frac{1}{2\pi}\int_0^S 2\left\{\frac{\rho_u-\rho_b}{\rho_u+\rho_b}\right\}k\,((X_F)_s^2+(Y_F)_s^2)^{-1/2}\log((X-X_F(s))^2+(Y-Y_F(s))^2)^{1/2}ds$$

Here, $\lim_{-}$ means the limit as we approach the point (X_F, Y_F) on the front from the burnt region in a direction normal to the front, and $\lim_{+}$ means that limit as we approach the point (X_F, Y_F) on the front from the unburnt region in a direction normal to the front.

Example 3.1 Let $\gamma(s)=(\cos(s),\sin(s))$, $s\in[0,2\pi]$. Suppose the particles inside γ are burnt and those outside are unburnt. The ignition curves to this front are the set of radial lines $(x,y) = (t+1)(\cos(s),\sin(s))$, $0\le t<\infty$, $s\in[0,2\pi]$. At $t=0$ we ignite the particles located along γ. We wish to follow the motion of the flame front.

For a charge of strength $2\left\{\frac{\rho_u-\rho_b}{\rho_u+\rho_b}\right\}k$ per unit length placed along a circle of radius a, the resulting single layer potential φ, from (3.4), is

$$\varphi(x,y) = \frac{1}{2\pi}\int_C^S 2\left\{\frac{\rho_u-\rho_b}{\rho_u+\rho_b}\right\}k\ \log\left\{(x-a\cos\frac{s}{a})^2+(y-a\sin\frac{s}{a})^2\right\}^{1/2} ds \qquad (3.7)$$

where $\gamma(s)=(a\cos\frac{s}{a},a\sin\frac{s}{a})$, $s\in[0,2\pi a]$. {N.B. Since this is a parameterization by arc length, $(\alpha_s^2+\beta_s^2)^{-1/2}=1$}.

By symmetry, we must have

$$\varphi(x,y) = \varphi((x^2+y^2)^{1/2},0). \qquad (3.8)$$

Hence,

$$\varphi(x,y) = \frac{1}{2\pi}\int_C^{2\pi a} 2\left\{\frac{\rho_u-\rho_b}{\rho_u+\rho_b}\right\}k\log\left\{((x^2+y^2)^{1/2}-a\cos\frac{s}{a})^2+(a\sin\frac{s}{a})^2\right\}^{1/2} ds \qquad (3.9)$$

The substitution $z = \frac{s}{a}$ yields

$$\varphi(x,y) = \left(\frac{a}{2\pi}\right)2\left\{\frac{\rho_u-\rho_b}{\rho_u+\rho_b}\right\}k\int_0^{2\pi}\log\left\{(((x^2+y^2)^{1/2}-a\cos(z))^2+(a\sin(z))^2)\right\}^{1/2}dz$$

$$= \left(\frac{a}{2\pi}\right)\left\{\frac{\rho_u-\rho_b}{\rho_u+\rho_b}\right\}k\int_0^{2\pi}\log\left\{x^2+y^2-2a(x^2+y^2)^{1/2}\cos(z)+a^2\right\}dz \qquad (3.10)$$

$$= \left(\frac{a}{2\pi}\right)\left\{\frac{\rho_u-\rho_b}{\rho_u+\rho_b}\right\}k\int_0^{2\pi}\log\left\{a^2\left\{\frac{x^2+y^2}{a^2}-2\left\{\frac{x^2+y^2}{a^2}\right\}^{1/2}\cos(z)+1\right\}\right\}dz$$

$$= \left(\frac{a}{2\pi}\right)\left\{\frac{\rho_u-\rho_b}{\rho_u+\rho_b}\right\}k\int_0^{2\pi}\left\{\log a^2+\log\left\{\frac{x^2+y^2}{a^2}-2\left\{\frac{x^2+y^2}{a^2}\right\}^{1/2}\cos(z)+1\right\}\right\}dz$$

$$= \left(\frac{a}{2\pi}\right)\left\{\frac{\rho_u-\rho_b}{\rho_u+\rho_b}\right\}k\left[2\pi\log a^2 + \int_0^{2\pi}\log\left\{\frac{x^2+y^2}{a^2}-2\left\{\frac{x^2+y^2}{a^2}\right\}^{1/2}\cos(z)+1\right\}\right]dz$$

Using the formula [7]

$$\int_0^{2\pi}\log(w^2-2w\log(z)+1)dz = \begin{Bmatrix} 0 & w^2<1 \\ 2\pi\log w^2 & w^2>1 \end{Bmatrix} \qquad (3.11)$$

we have

$$\varphi(x,y) = \begin{Bmatrix} a\left\{\frac{\rho_u-\rho_b}{\rho_u+\rho_b}\right\}k\log(a)^2 & x^2+y^2<a^2 \\ a\left\{\frac{\rho_u-\rho_b}{\rho_u+\rho_b}\right\}k\log(x^2+y^2) & x^2+y^2>a^2 \end{Bmatrix} \qquad (3.12)$$

Thus φ is constant inside the circle. We rewrite φ in polar coordinates

$$\varphi(r) = \begin{Bmatrix} a\left\{\frac{\rho_u-\rho_b}{\rho_u+\rho_b}\right\}k\log a^2 & r^2<a^2 \\ a\left\{\frac{\rho_u-\rho_b}{\rho_u+\rho_b}\right\}k\log r^2 & r^2>a^2 \end{Bmatrix} \qquad (3.13)$$

where

$$r^2 = x^2+y^2$$

Let $\vec{u} = \nabla\varphi$. Then $\nabla\cdot\vec{u} = \nabla\cdot\nabla\varphi = 0$ inside and outside the circle. φ is continuous

across the boundary, since

$$\lim_{r\to a^-}\varphi(r) = a\left\{\frac{\rho_u-\rho_b}{\rho_u+\rho_b}\right\}k\,\log a^2 = \lim_{r\to a^+}\varphi(r) \tag{3.14}$$

The radial symmetry of φ implies that the component of $\vec{u}$ in the direction tangent to the circle is zero and thus continuous across the flame front. Evaluation of the normal derivative across the front yields

$$\frac{\partial\varphi^-}{\partial r} = \lim_{r\to a^-}\frac{\partial\varphi}{\partial r} = 0 \tag{3.15}$$

$$\frac{\partial\varphi^+}{\partial r} = \lim_{r\to a^+}\frac{\partial\varphi}{\partial r} = \lim_{r\to a^+} 2a\left\{\frac{\rho_u-\rho_b}{\rho_u+\rho_b}\right\}k\frac{1}{r} \tag{3.16}$$

$$= 2\left\{\frac{\rho_u-\rho_b}{\rho_u+\rho_b}\right\}k$$

where $\frac{\partial\varphi^-}{\partial r}$ is the normal derivative from the inside and $\frac{\partial\varphi^+}{\partial r}$ is the normal derivative from the outside. Thus, $\frac{\partial\varphi}{\partial r}$ undergoes a jump of magnitude $2\left\{\frac{\rho_u-\rho_b}{\rho_u+\rho_b}\right\}k$. Note that the normal velocities on either side of the circle are independent of the circle's radius.

The propagation of the flame and the advection velocity field yield the position of the front. Since $\gamma(s)$ is originally a circle, each point both propagates radially outwards and is carried in a radial direction by the velocity field.

We rewrite (3.5) and (3.6) in polar coordinates. Let $(R(s,t),\Theta(s,t))$, $s\in[0,2\pi]$, $t\in[0,\infty)$ be the position of the front at time t; then $(R(s,0),\Theta(s,0))=(\cos(s),\sin(s))$. Then,

$$\frac{\partial R}{\partial t} = k + \varphi_r(R,\Theta) \tag{3.17}$$

$$\frac{\partial \Theta}{\partial t} = 0 \tag{3.18}$$

$$R(s,0) = 1 \qquad \Theta(s,0) = s$$

In (1.13)-(1.14), we chose the fluid velocity at the front to be the average of the fluid velocity from the burnt side and the fluid velocity from the unburnt side. Thus,

$$\varphi_r(R,\Theta) = \frac{1}{2}\left[\frac{\partial \varphi^+}{\partial r} + \frac{\partial \varphi^-}{\partial r}\right] = \left\{\frac{\rho_u - \rho_b}{\rho_u + \rho_b}\right\}k \tag{3.19}$$

Substitution into (3.17)-(3.19) yields

$$\frac{\partial R}{\partial t} = k\left[1 + \frac{\rho_u - \rho_b}{\rho_u + \rho_b}\right] \tag{3.20}$$

$$\frac{\partial \Theta}{\partial t} = 0 \tag{3.21}$$

$$R(0,s) = 1 \qquad \Theta(0,s) = s$$

Integration yields

$$R(s,t) = 2k\left[\frac{1}{1+\rho_b/\rho_u}\right]t + 1 \tag{3.22}$$

$$\Theta(s,t) = s \tag{3.23}$$

Thus,

$$(x(s,t),y(s,t)) = \left\{2k\left[\frac{1}{1+\rho_b/\rho_u}\right]t + 1\right\}(\cos(s),\sin(s)) \tag{3.24}$$

$$s \in [0,2\pi]$$

The larger the expansion ratio $\frac{\rho_u}{\rho_b}$, the faster the flame moves. This completes the example.

The potential φ (3.12) is constant along the circular flame front. Thus, the streamlines of this velocity field there are everywhere tangent to the family of ignition curves associated with such a front burning without volume expansion. The fluid merely "pushes" the front at a uniform speed along the original set of ignition curves. Each point on the front travels along its ignition curve with speed equal to the propagation speed k plus the advection speed $\left\{\frac{\rho_u-\rho_b}{\rho_u+\rho_b}\right\}k$. (See Figure (3.1))

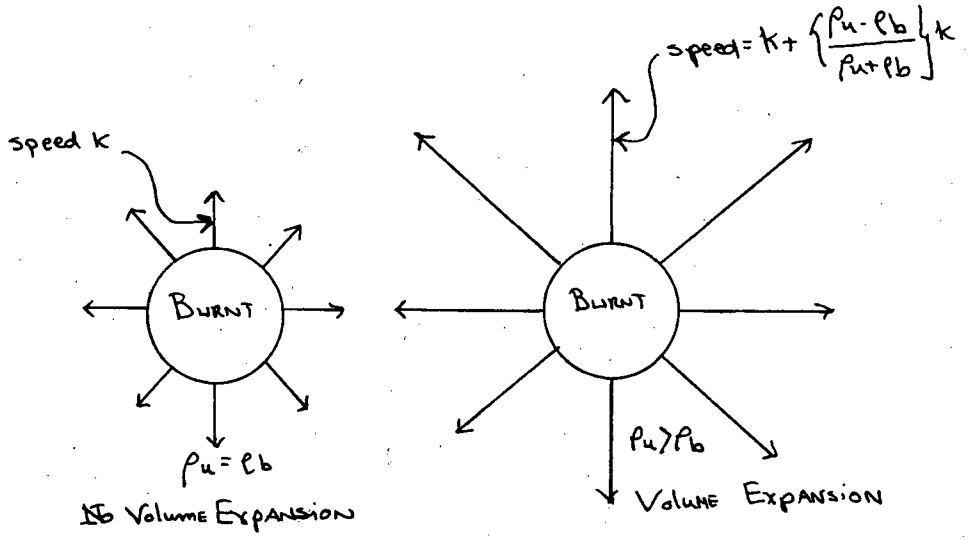

Figure 3.1

Thus, we are able to recast our equations of motion (3.8)-(3.9) as equations along the ignition curves associated with a front burning with no volume expansion.

Given a more general curve, however, the potential associated with a single layer distribution of constant charge density will not be constant along the front. There will be a component of the velocity field tangential to the front. The motion of the front, as seen from a fixed reference frame, will result from

its propagation in a direction normal to itself and the effects of the fluid velocity, which carry it in a different direction. If the curve is non-convex, the situation is even more complex. Since both the flame and the fluid are advected by the flow, one can no longer tell when a particle will be ignited by simply measuring its distance to the initial front. The motion of the front depends on the ignition curves, the velocity field induced by volume expansion and our entropy condition. We have not attempted in this paper to present a general theory to account for such situations.

3.2. Boundary Conditions

We now consider the effect of boundary conditions on flame propagation. Suppose the flame is burning inside a partially closed vessel. That is, let D be a domain and let γ be a simple, closed curve lying in D. Let ∂D be the boundary of D, and assume that $\partial D^* \subset \partial D$ is the part of the boundary of D that does not correspond to solid wall. We assume that the particles inside γ are burnt and those outside are unburnt. At $t=0$, we ignite the particles along γ.

Let $\vec{u}$ be the velocity field created by volume expansion along the flame front. Our boundary conditions (1.17) force $\vec{u}$ to be zero on solid walls. Since the flow is incompressible in the burnt region, by the divergence theorem we have that

$$\int_{\gamma} (\vec{u} \cdot \vec{n}_b) ds = \int_{Burnt} \nabla \cdot \vec{u} = 0 \tag{3.25}$$

where at any point P on the flame front, $\vec{n}_b$ is the inner unit normal and $(\vec{u} \cdot \vec{n}_b) = \lim_{R \to P} (\vec{u} \cdot \vec{n}_b)$ with R approaching P from the burnt region along the nor-

mal. (See Figure (3.2))

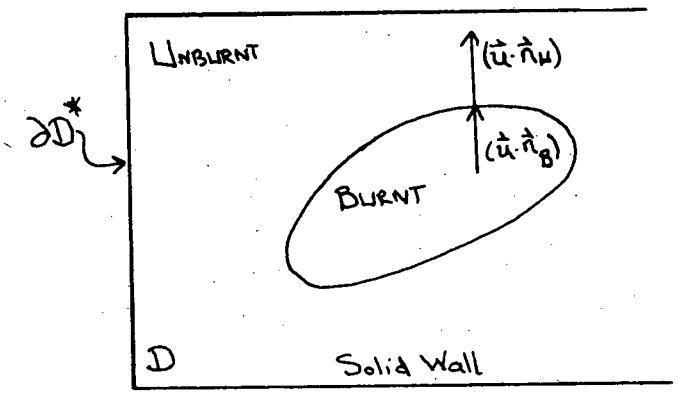

Figure 3.2

Equation (3.25) states that if no volume is created or destroyed inside the burnt region, then the net flow through its boundary is zero. Since the normal velocity must undergo a jump of $2\left\{\frac{\rho_u-\rho_b}{\rho_u+\rho_b}\right\}k$ across the flame front, then

$$0 = \int_\gamma (\vec{u}\cdot\vec{n}_b)ds = \int_\gamma \left\{(\vec{u}\cdot\vec{n}_u) - 2\left\{\frac{\rho_u-\rho_b}{\rho_u+\rho_b}\right\}k\right\}ds \tag{3.26}$$

where, at any point P on the flame front, $\vec{n}_u$ is the outer unit normal and $(\vec{u}\cdot\vec{n}_u)=\lim_{Q\to P}(\vec{u}\cdot\vec{n}_u)$ with Q approaching P from the unburnt region along the normal. Hence,

$$2\left\{\frac{\rho_u-\rho_b}{\rho_u+\rho_b}\right\}k \;\; l(\gamma) = \int_\gamma (\vec{u}\cdot\vec{n}_u)ds \tag{3.27}$$

where $l(\gamma)$ is the length of the flame front. The flow is also incompressible out-

side the burnt region, thus

$$\int_{\gamma}(\vec{u}\cdot\vec{n}_u)ds - \int_{\partial D}(\vec{u}\cdot\vec{n})ds = \int_{Unburnt}\nabla\cdot\vec{u} = 0 \tag{3.28}$$

where $\vec{n}$ is the outward pointing normal. Substitution of (3.27) into (3.28) yields

$$\int_{\partial D}(\vec{u}\cdot\vec{n})ds = 2\left\{\frac{\rho_u-\rho_b}{\rho_u+\rho_b}\right\}k\ l(\gamma) \tag{3.29}$$

Since $\vec{u}$ is zero on the complement of ∂D^*,

$$\int_{\partial D^*}(\vec{u}\cdot\vec{n})ds = 2\left\{\frac{\rho_u-\rho_b}{\rho_u+\rho_b}\right\}k\ l(\gamma) \tag{3.30}$$

Equation (3.30) states that the volume produced along the flame front must be allowed to flow out through ∂D^*. The longer the flame, the more volume produced. The more volume produced, the faster the exit velocity of the fluid through ∂D^*. This flow of fluid out the exit is reflected in the velocity field at the flame front. Furthermore, we cannot close off the vessel completely and still require that the densities of the unburnt and burnt fluids remain constant.

3.3. Numerical Modeling by Finite Differences

In this section, we use our theory of flame propagation to show that finite difference methods that attempt to model the flame's motion face serious obstacles. We assume the motion satisfies Equations (1.15)-(1.20) and the entropy condition.

Let $\gamma(s), s \in [0,S]$, $\gamma(0)=\gamma(S)$ be a simple, closed curve. The particles inside γ are burnt and those outside are unburnt. At $t=0$, we ignite the particles along γ. In this discussion, we neglect pre-existing vorticity. {N.B. Our objective is to show the inapplicability of finite difference techniques to this problem. The addition of another advection field to the flame's motion can only make matters worse.}

Consider an attempt to represent the flame by a set of marker particles. Choose n points $0=s_1<s_2<\ldots\ldots<s_n=S$. We interpolate the initial position of the flame front at the points s_i.

We wish to move each marker in the direction given by our equations of motion for flame propagation. With (x_i,y_i) as the position of the i^{th} marker at time t, we hope to interpolate and obtain a good approximation to the position of the flame front.

To move the marker (x_i,y_i), we must know the fluid velocity and the normal direction at that point. At time t_1, one way to determine this direction is to make use of the neighboring marker points. For example, one could approximate the front at (x_i,y_i) by the parabola through (x_{i-1},y_{i-1}), (x_i,y_i), and (x_{i+1},y_{i+1}), and use this to determine the normal direction. Let

$$NX_i((x_{i-j},y_{i-j}),\ldots\ldots,(x_i,y_i),\ldots\ldots,(x_{i+k},y_{i+k})) \quad j,k\geq 0 \qquad (3.31)$$

be the x component of the approximated unit normal at (x_i,y_i). Similarly, let

$$NY_i((x_{i-j},y_{i-j}),\ldots\ldots,(x_i,y_i),\ldots\ldots,(x_{i+k},y_{i+k})) \quad j,k\geq 0 \qquad (3.32)$$

be the y component of the approximated unit vector. For brevity, we write NX_i and NY_i. Thus, NX_i and NY_i represent finite difference approximations to the spatial derivatives in the equations of motion (1.19) and (1.20). The motion of each marker point is described by

$$\frac{\partial x_i}{\partial t} = k \cdot NX_i + u(x_i, y_i) \tag{3.33}$$

$$\frac{\partial y_i}{\partial t} = -k \cdot NY_i + v(x_i, y_i) \tag{3.34}$$

$$i = 1, n-1$$

The velocities u and v represent the velocity field induced by volume expansion and depend on the position of the flame front (and thus all the marker points). We have written them as functions of only (x_i, y_i) for the sake of brevity. For an example of a numerical scheme for the propagation of a flame written in this form, see [9]. One then solves Equations (3.33)-(3.34). The simplest technique is to use Euler's method to advance the position of the marker points in time. Of course, the functions u and v may be complicated, having arisen from the solution of an elliptic partial differential equation.

We now use our theory of flame propagation to see the problems involved in such a formulation. We can ignore the effects of the advection field for our analysis.

Let γ_H be the convex hull of γ. We have seen in Chapter Two that, along those sections of γ touching γ_H, the length of any given piece of the initial front cannot decrease as it moves. Moreover, if the section is not straight, its length must increase (Equation 2.44). The greater the curvature of the initial front between two neighboring marker points, the more that section

lengthens. As the marker points get further apart, the approximating curve becomes more suspect. Unfortunately, those sections that change the least are the ones that keep their marker particles closest together.

The situation is even worse for those sections of the initial front that lie inside the convex hull. We have shown in Chapter Two that, as such a section propagates, cusps form and the flame front ceases to be differentiable. These cusps "swallow up" sections of the front. Consider a collection of marker points placed along such a section of the initial front. The first problem to confront is our entropy condition. Example 2.4 shows that one doesn't want to follow that part of the front which moves into previously burnt areas. It is hard to imagine a technique that could reconstruct the flame front at each time step from those points that are actually on the boundary between burnt and unburnt fluid, and know how to avoid the rest of them. The second problem is that the marker points tend to cluster together in a small area around the cusp. As the markers cluster, small errors in their positions can cause huge errors in the determination of the normal direction to the front. For example, for a parabola through three points, two of which are close together, small changes in their position cause radical changes in the shape of the parabola. Thus the tendency of the marker points to cluster can cause a large error in the determination of the direction in which the front is to move. Typically, the front becomes highly unstable and develops wild oscillations.

In summary, since one needs to know the orientation of the front at a point to determine where next to move it, too fine a discretization leads to great numerical error in this determination as marker points cluster together, and too coarse a discretization leads to an overly simplified and unsatisfying resolution of the front. As if almost by design, the effect of the

motion of a flame in a direction normal to itself is to bunch up marker points where they do the most harm and spread them out where they would have done the most good.

In the next chapter, we present a numerical method for following flame fronts that does not depend on a discrete parameterization of the front.

Chapter Four

Numerical Simulations

In the last chapter, we showed that numerical methods that attempt to follow a flame front by finite difference techniques face serious and possibly insurmountable obstacles. In this chapter, we present a numerical method, developed by Chorin [2], which does not rely on a discrete parameterization of the moving front. This method has been used with great success in the numerical simulation of turbulent combustion ([6] and [14]). We show that the reason for the success of Chorin's method is clear when viewed from within the framework of our theory of flame propagation, and that the method arises naturally from our theory of ignition curves. The central idea of this method is an expression of our entropy condition that once a particle burns it remains burnt. We use this method to demonstrate the results of our theorems, illustrating spreading and colliding ignition curves, cusp formation and flame reversibility.

4.1. The Method

We first use our theory of flame propagation to set the stage for the numerical method.

Let $\gamma(s)=(\alpha(s),\beta(s))$ be a simple, closed curve. Assume that the particles inside γ are burnt and the particles outside are unburnt. At $t=0$, we ignite the particles along γ, and assume that the front propagates in a direction normal to itself with speed k. For the moment, we assume that $\rho_u=\rho_b$, thus the fluid remains at rest.

In (2.168), we defined the indicator function $\varphi(x,y,t)$ of the burning front; $\varphi(x,y,t)=1$ if the particle located at (x,y) is burnt at time t, and zero

otherwise.

We found that

$$\varphi(x,y,t) = \begin{cases} 1 & \text{if } (x,y) \textit{ is burnt at } t=0 \\ 1 & (kt)^2 \geq \min_{s\in[0,S]} ((x-\alpha(s))^2+(y-\beta(s))^2) \\ 0 & (kt)^2 < \min_{s\in[0,S]} ((x-\alpha(s))^2+(y-\beta(s))^2) \end{cases} \tag{4.1}$$

At time t_1, the boundary of the set of (x,y) such that $\varphi(x,y,t_1)=1$ corresponds to the position of the flame front at time t_1.

We now formulate $\varphi(x,y,t,)$ in a different way. For each $s\in[0,S]$, let $D_s(t)$ be the closed disk of radius kt centered at $\gamma(s)$. (See Figure (4.1))

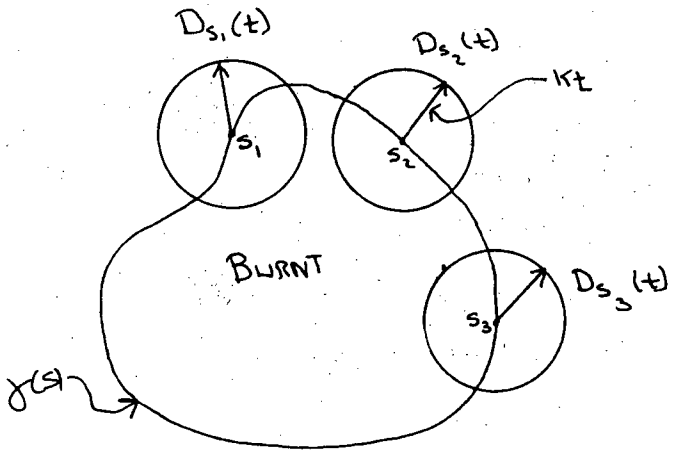

Figure 4.1

Choose any point $s_1\in[0,S]$ on the initial curve. Clearly, every point $(x,y)\in D_{s_1}(t)$ must be burnt by time t, since any such point is located a distance less than kt from $\gamma(s_1)$. Consider the set $D(t)$, defined as the union of the interior of γ with $D_s(t)$ as we range over all possible values of $s\in[0,S]$.

That is,

$$D(t) = \left[D_\gamma \right] \cup \left[\bigcup_{s \in [0,S]} D_s(t) \right] \tag{4.2}$$

where D_γ is the interior of γ.

We claim that, given a point (x,y) and a time t_1, $\varphi(x,y,t_1)=1$ if and only if $(x,y) \in D(t_1)$. First, suppose $\varphi(x,y,t_1)=1$. Then, by the definition of φ, there exists an $\bar{s}$ such that $|(x,y)-\gamma(\bar{s})| \leq kt_1$. Therefore, $(x,y) \in D_{\bar{s}}(t_1) \subset D(t_1)$. Conversely, suppose $(x,y) \in D(t_1)$. Then either i) for some $\bar{s}$, $(x,y) \in D_{\bar{s}}(t_1)$ and so $\varphi(x,y,t_1)=1$ or ii) $(x,y) \in D_\gamma$ and $\varphi(x,y,t_1)=1$ for all t.

Thus, at any time t, the position of the flame front is given by the boundary of $D(t)$. Note that our construction of $D(t)$ obeys our entropy condition. This is because $D(t)$ is formed from the union of all disks of radius kt with centers on the initial front. Any particle within that union is "counted" ,i.e., ignited, only once, regardless of how many disks $D_s(t)$ contain it. The position of the front at any time t is the envelope of the region formed by the expanding disks $D_s(t)$, $s \in [0,S]$ and the original area D_γ.

We now describe an alternate way of constructing $D(t)$. Let $D_\gamma^\Theta(t)$ be the translation of the original region D_γ a distance kt in the direction $(\cos\Theta, \sin\Theta)$. That is, $(x,y) \in D_\gamma^\Theta(t)$ if and only if $(x-(kt)\cos\Theta, y-(kt)\sin\Theta) \in D_\gamma$. By taking the union of all such possible translations as Θ ranges from 0 to 2π, we see that

$$D(t) = D_\gamma \cup \left[\bigcup_{\Theta \in [0,2\pi]} D_\gamma^\Theta(t) \right] \tag{4.3}$$

We now present a numerical method, developed by Chorin, that moves the front by approximating the above construction.

Assume for the moment that we possess an algorithm that will translate the region D_γ in a given direction at a given speed (we shall describe such an algorithm shortly). Consider the eight angles $\Theta_l = (l-1)\pi/4$, $l=1,2,.....8$. If we form the eight regions $D_\gamma^{\Theta_l}(\Delta t)$, each one being the translation of the original region D_γ a distance $k\Delta t$ in the direction $(\cos\Theta_l, \sin\Theta_l)$, then the union of these regions together with D_γ will approximate the burnt region at time Δt.

The algorithm Chorin used to translate D_γ in the eight directions is the Simple Line Interface Calculation (SLIC) method, developed by Noh and Woodward [13]. We impose a square grid i,j of uniform mesh length on the combustion domain, and assign a number f_{ij}, $0 \le f_{ij} \le 1$ to each square. The number f_{ij} corresponds to the fraction of fluid within the square i,j that is burnt. Thus, if $\gamma(s)$ separates the fluid at $t=0$ into the two regions, burnt and unburnt, the squares outside γ have $f_{ij}=0$, squares inside have $f_{ij}=1$, and those that straddle γ have f_{ij} between 0 and 1. The field of numbers f_{ij} allow one to recreate the approximate position of the front.

The algorithm moves the burnt region by drawing in each cell an interface which represents the boundary between the burnt and unburnt fluid. The orientation of the interface depends on the value of f_{ij} and the f_{ij}'s in the cell's neighbors. The burnt fluid is then transported in the given direction, and a new set of f_{ij}'s are created, which approximate the burnt region translated a distance $k\Delta t$ in the given direction.

Using this algorithm, we may approximate the position of the flame front at any time t. At time $t=n\Delta t$, n an integer, Δt a time step, we have an array of cell fractions $f_{ij}(n)$, which can be used to describe the burnt region at time t. We move the burnt region in each of our eight directions Θ_l a distance $k\Delta t$. Let $f_{ij}^{\Theta_l}(n)$ be the array of cell fractions obtained from moving the burnt

region at time t in the direction Θ_l. Let $f_{ij}^{\Theta_0}(n)=f_{ij}(n)$. Then the burnt region at time $(n+1)\Delta t$ will be approximated by

$$f_{ij}(n+1) = \max_{0\le l\le 8} f_{ij}^{\Theta_l}(n) \tag{4.4}$$

This advances the front in a direction normal to itself a distance $k\Delta t$.

We have been content to merely sketch the outlines of the numerical method and of SLIC. For a complete presentation, see [2] and [13], respectively.

4.2. Examples of Numerical Simulations

In this section, we use the numerical method presented above to illustrate some of the results of our theory of flame propagation.

Let γ be the boundary of the square centered at the origin with sides of unit length, and assume that the particles inside γ are burnt and those outside are unburnt. At $t=0$, we ignite the particles along γ. We assume that the front travels in a direction normal to itself with speed $k=\frac{1}{2}$.

From our theory of flame propagation, we know that the ignition curves extend from each corner in a radial manner, filling in the space between the ignition curve on the left at a corner and the ignition curve on the right. (See Figure (4.2)).

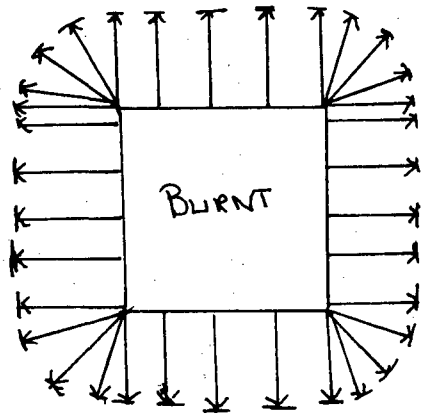

Figure 4.2

At any time t, the position of the flame front may be described as follows: Each of the four sides has moved in a direction normal to itself a distance kt, and these segments are connected together by four circular arcs.

In Figure (4.3), we show the results of a numerical simulation. We chose a mesh width $h=.05$, a flame speed $k=.5$ and a time step of $\Delta t=.1$. For display purposes, we shaded those squares with $f_{ij} \geq .25$. We display the results at $t=0$, $t=2.0$ and $t=4.0$. The results show the propagation of each side of the square, and the circular arcs connecting these sides. This illustrates our construction of radial ignition curves at the corners.

We now show the idea of flame reversibility. Since the initial curve γ is convex, our theory of flame propagation maintains that we should be able to take the position of the front at any time t and "burn it backwards" until we reach the initial shape. Numerically, we let $f_{ij}^{new} = 1 - f_{ij}^{old}$; this will interchange the places of the burnt and unburnt regions. At $t=4.0$, we switch the burnt and unburnt regions. In Figure (4.4), we show the results of this front

propagating inwards at t=4.0, t=6.0 and t=8.0. At t=8.0, the position of the front is about the same as it was at t=0. Thus, the numerical method preserves our notion of flame reversibility.

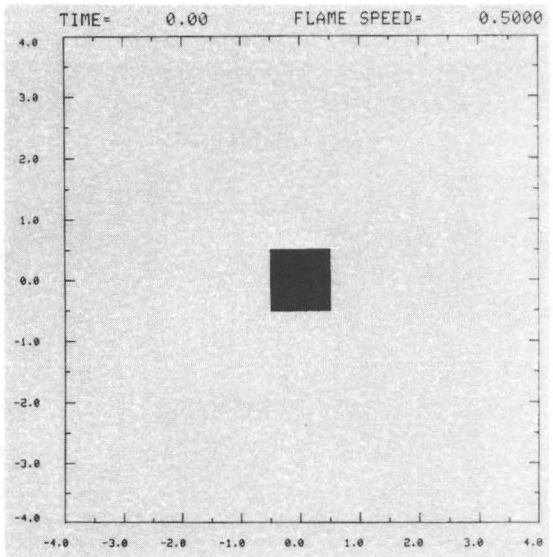

Figure 4.3a

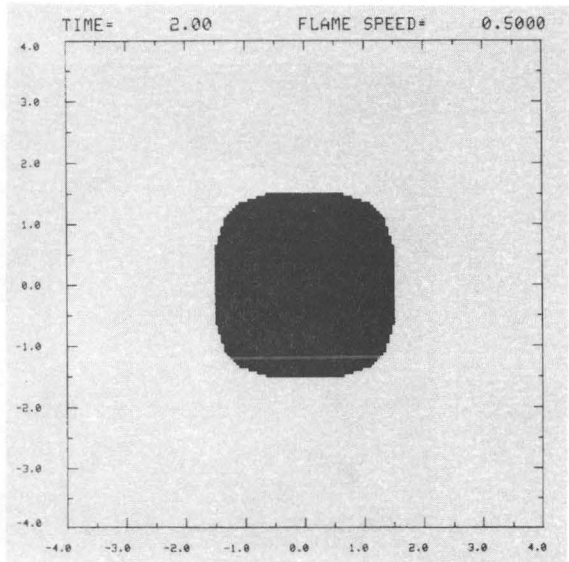

Figure 4.3b

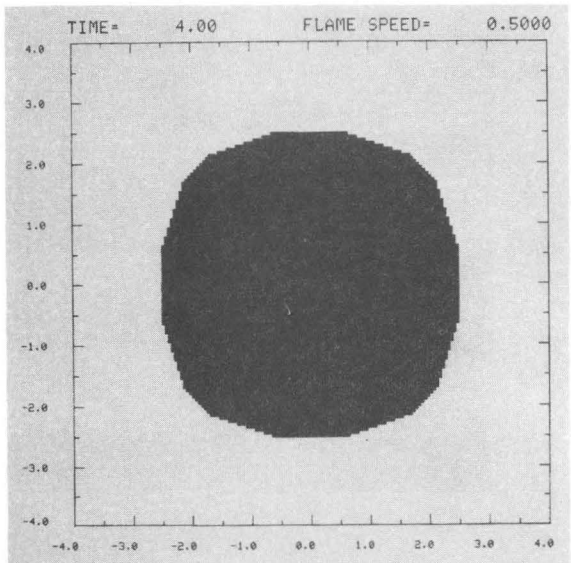

Figure 4.3c

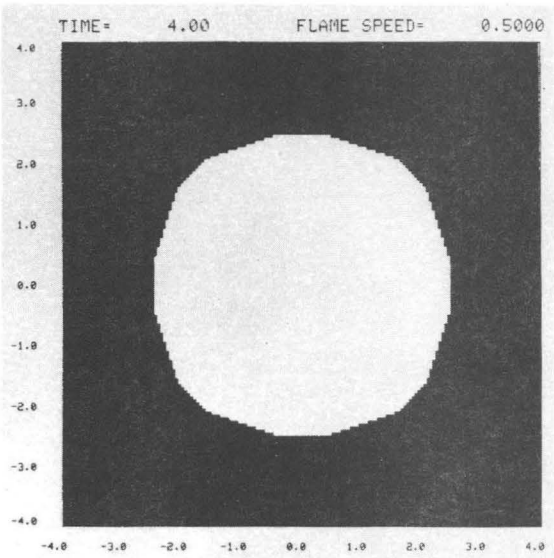

Figure 4.4a

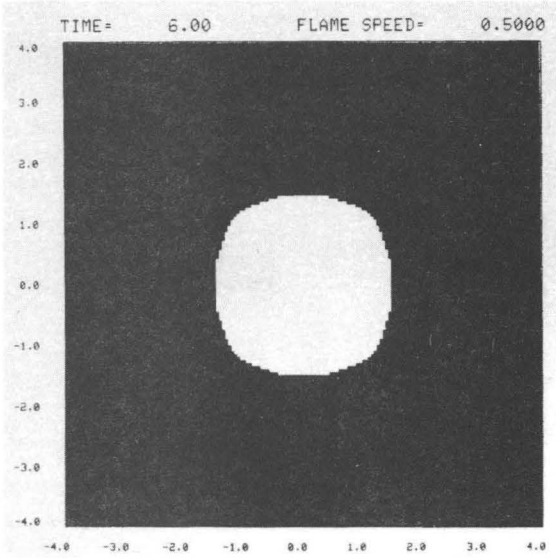

Figure 4.4b

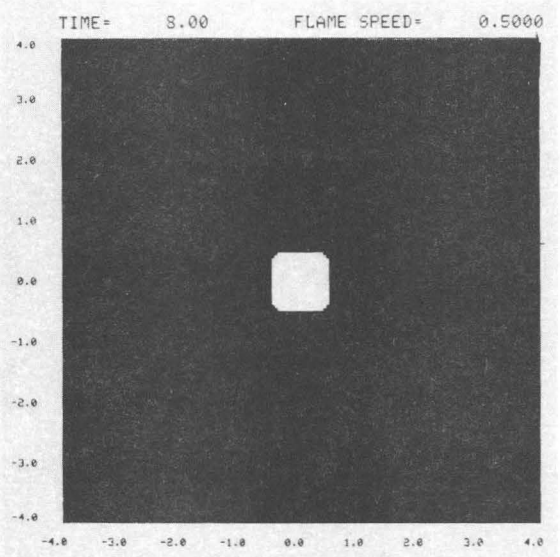

Figure 4.4c

Furthermore, the numerical method does an equally good job of illustrating the irreversibility of non-convex initial flame shapes. Let γ be the boundary of the square centered at the origin with sides of length 5. Assume that the particles outside γ are burnt and those inside are unburnt. Thus, the initial curve is not convex (that is, the burnt region is not a convex set) and the ignition curves intersect for any $t>0$. (See Figure (4.5))

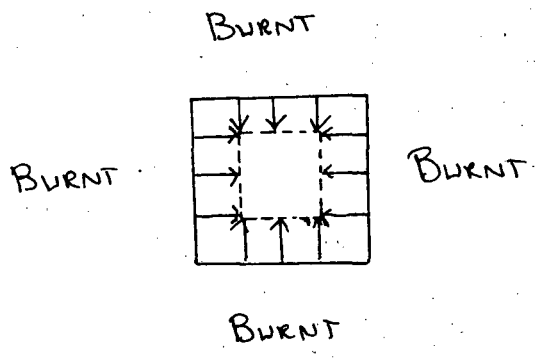

Figure 4.5

If we allow this front to propagate, our theory of flame propagation dictates that information about the initial shape of the flame will be lost. In Figure (4.6), we show the results at $t=0$, $t=2$ and $t=4$. At $t=4$, we interchange the burnt and unburnt fluids, and allow the front to burn "in the other direction". In Figure (4.7), we show the results at $t=4$, t=6 and $t=8$. Clearly, the front at $t=8$ does not look like the front at $t=0$. This illustrates the irreversibility of a non-convex initial shape.

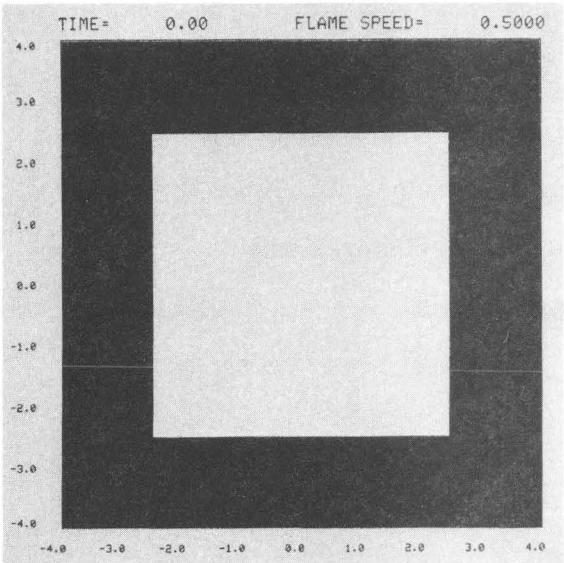

Figure 4.6a

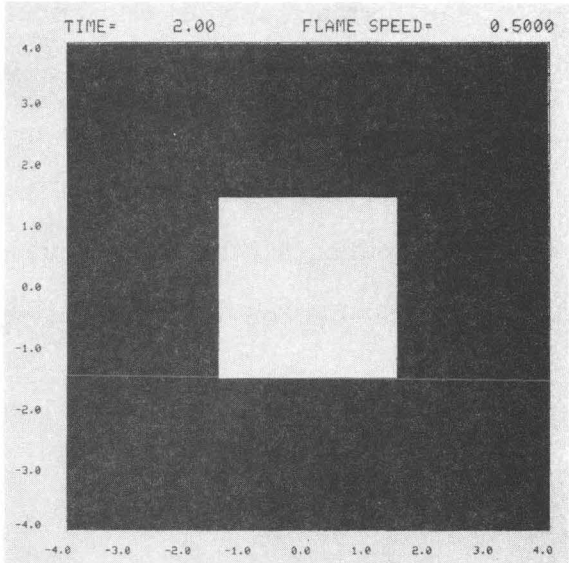

Figure 4.6b

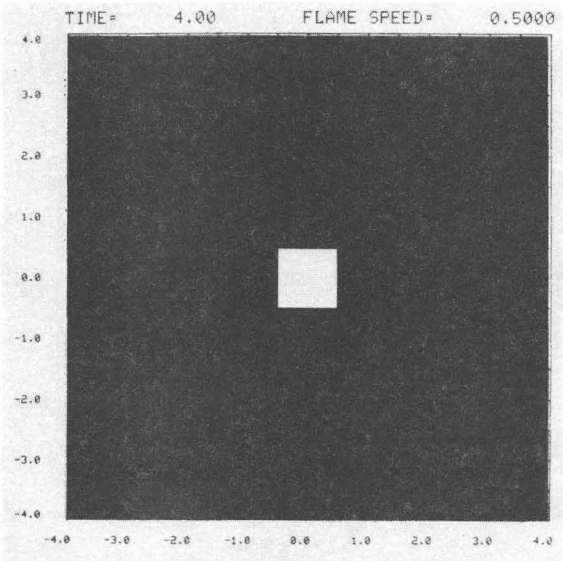

Figure 4.6c

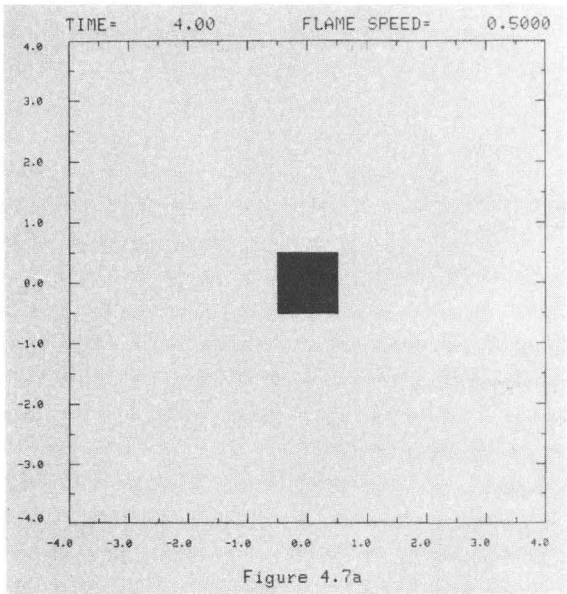

Figure 4.7a

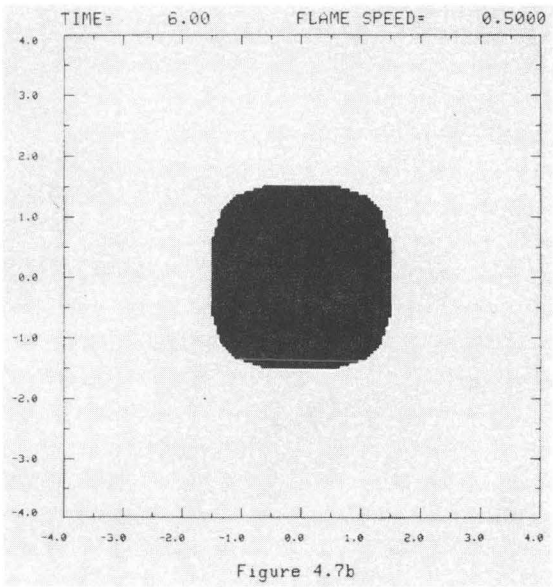

Figure 4.7b

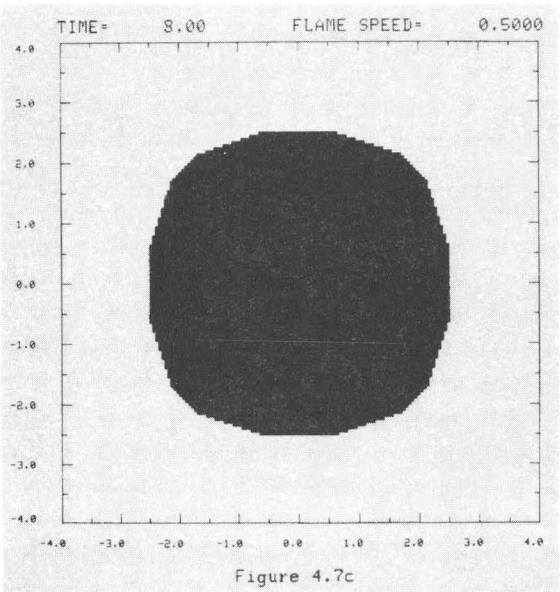

Figure 4.7c

Finally, we consider a smooth, non-convex curve that develops a cusp as it moves. Let $\gamma(s)=(\alpha(s),\beta(s))$, $s\in[0,6\pi]$, where α and β are defined as follows:

$$\alpha(s) = \begin{cases} -\cos(s) & 0\le s<\pi/2 \\ -\cos(s) & \pi/2\le s<3\pi/2 \\ 3\cos(s/3) & 3\pi/2\le s<9\pi/2 \\ -\cos(s) & 9\pi/2\le s<11\pi/2 \\ -\cos(s) & 11\pi/2\le s\le 6\pi \end{cases} \tag{4.5}$$

$$\beta(s) = \begin{cases} \sin(s) & 0\le s<\pi/2 \\ -\sin(s)+2 & \pi/2\le s<3\pi/2 \\ 3\sin(s/3) & 3\pi/2\le s<9\pi/2 \\ -\sin(s)-2 & 9\pi/2\le s<11\pi/2 \\ \sin(s) & 11\pi/2\le s\le 6\pi \end{cases} \tag{4.6}$$

Note that γ is parameterized by arc length, and possesses a smoothly turning normal vector. We assume that the particles inside γ are burnt and those outside are unburnt. At $t=0$, we ignite the particles along γ. We let the front propagate with speed $=\frac{1}{2}$. Using our formula for ignition curves, a lengthy but straightforward calculation shows that the position of the front $(x(s,t),y(s,t))$ is given by

For $t\le 1$

$$x(s,t) = \tfrac{1}{2}\beta_s t + \alpha \tag{4.7}$$

$$y(s,t) = -\tfrac{1}{2}\alpha_s t + \beta$$

$$0\le s\le 6\pi$$

For $t>1$

$$x(s,t) = \frac{1}{2}\beta_s t + \alpha \tag{4.8}$$

$$y(s,t) = -\frac{1}{2}\alpha_s t + \beta$$

$$\left[\cos^{-1}\left(\frac{2}{(1+t)}\right)+\frac{\pi}{2}\right] \leq s \leq 6\pi - \left[\cos^{-1}\left(\frac{2}{(1+t)}\right)+\frac{\pi}{2}\right]$$

The position of the front for various values of t is shown in Figure (4.8). We note that as the front moves, a cusp forms at $t=1$, and travels along the positive x axis, "swallowing up" sections of the front. In Figure (4.9), we show the results of the application of Chorin's flame propagation algorithm to this problem for various values of t. The method does an excellent job of showing the formation and absorption of the cusp.

The above computations were performed on a VAX computer at the Lawrence Berkeley Laboratory, Berkeley, California.

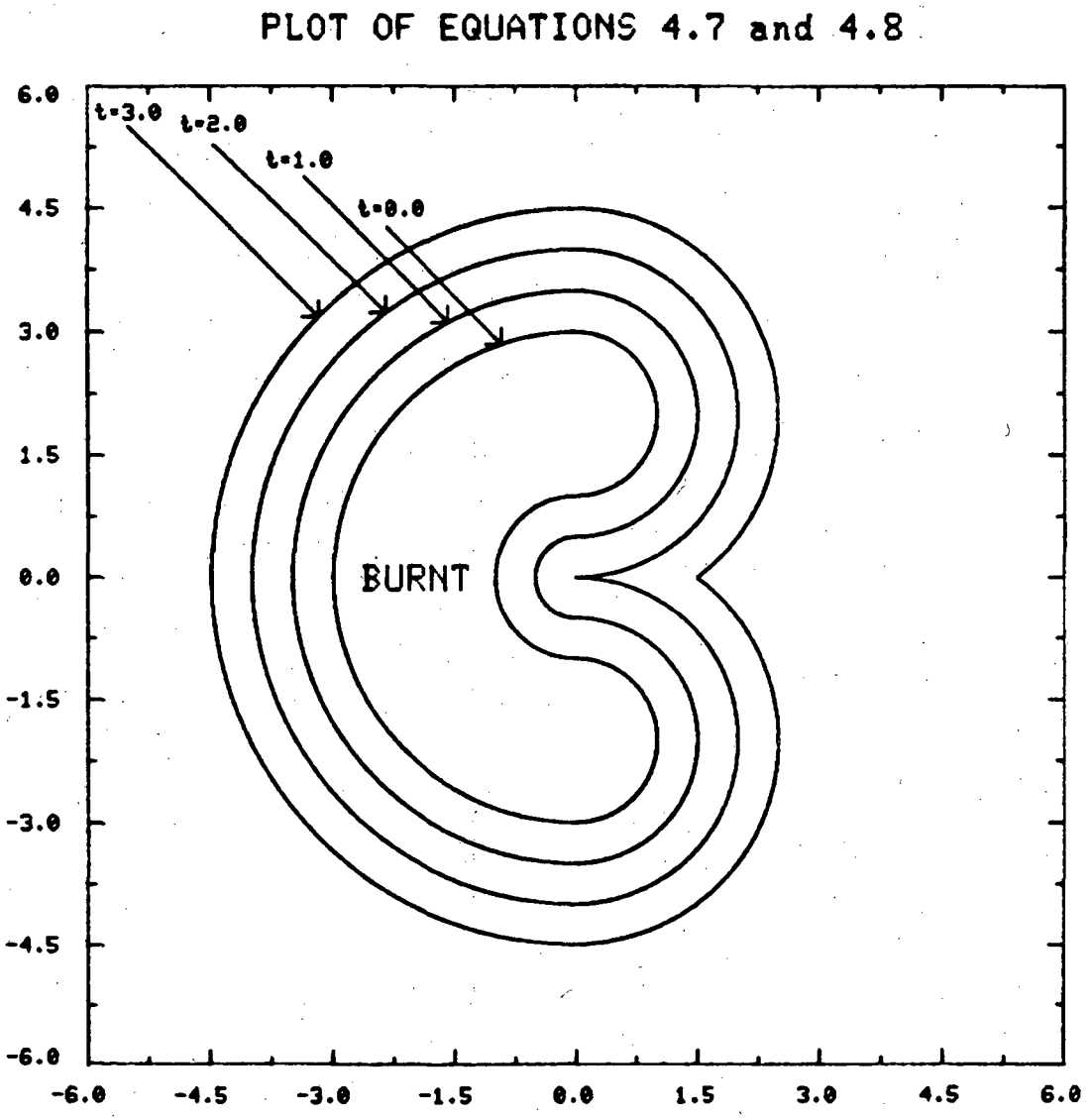
PLOT OF EQUATIONS 4.7 and 4.8
t=3.0
t=2.0
t=1.0
t=0.0
BURNT
6.0
4.5
3.0
1.5
0.0
-1.5
-3.0
-4.5
-6.0
-6.0
-4.5
-3.0
-1.5
0.0
1.5
3.0
4.5
6.0

Figure 8

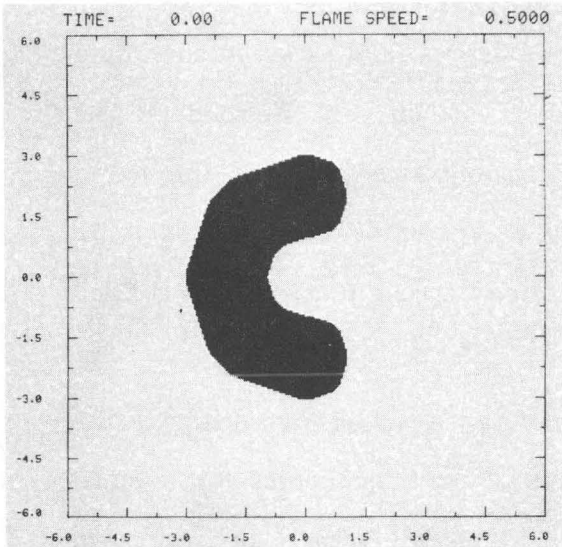

Figure 4.9a

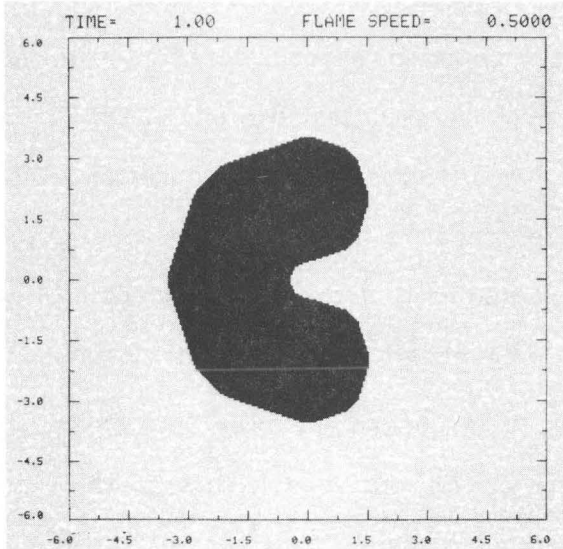

Figure 4.9b

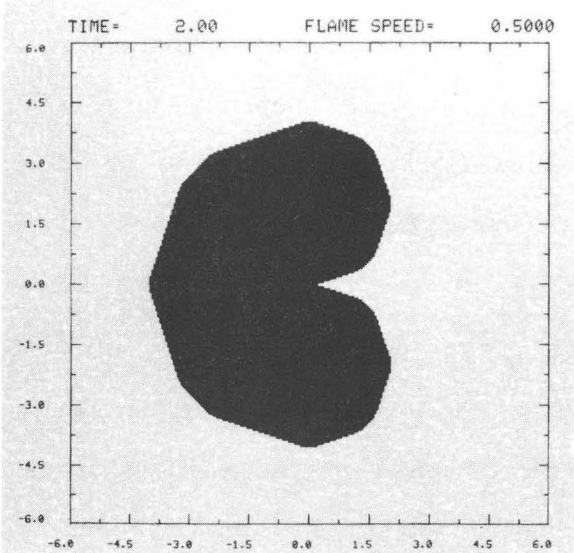

Figure 4.9c

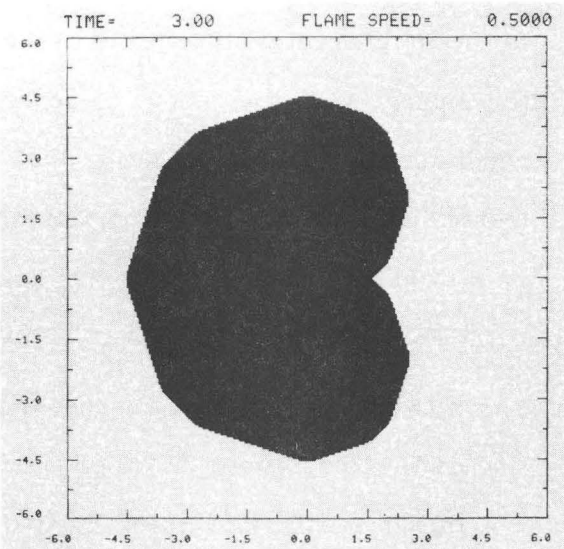

Figure 4.9d

Conclusion

We have developed a theory of flame propagation for a simplified model of combustion. We considered a premixed, combustible fluid in which each fluid particle could exist in one of two states, burnt and unburnt. We modeled the flame front between the burnt and unburnt regions as an infinitely thin curve propagating in a direction normal to itself at a constant, prescribed speed. We assumed that the specific volume of each fluid particle increased by a fixed amount as it changed from unburnt to burnt.

We began (Chapter One) by presenting the full set of combustion equations for our model, that is, the equations of fluid mechanics for viscous, incompressible flow together with our equations of flame propagation. In Chapter Two, we suppressed the effects of the velocity field produced by volume expansion. Through the introduction of ignition curves, we were able to solve our equations of flame propagation. These ignition curves carry the temperature required for ignition, and play a role in our equations analogous to that of characteristics in the solutions of hyperbolic equations. Continuing the analogy with the theory of conservation laws, we developed an entropy condition for flame propagation that stipulated that no particle could burn more than once. With this theory of ignition curves and our entropy condition, we proved the following:

1) If two initial fronts start close together, then they remain close together as they propagate. In other words, flame fronts are stable. As the front moves, oscillations in its initial shape are smoothed, with the result that the burning front asymptotically approaches a circular shape.
2) As the front moves and deforms, it develops cusps. At such points, the curve ceases to be differentiable. These cusps are a result of colliding

ignition curves and our entropy condition. They form in a manner similar to the way in which shocks form when characteristics collide. These cusps "swallow up" sections of the flame front as they move and destroy information about the initial shape of the flame front. Once a cusp forms, it is impossible to retrieve the original flame shape by solving the equations of motion backwards in time. Each ignition curve carries information about the initial shape of the front, and that information is lost in a collision.

In Chapter Three, we returned to our full set of combustion equations and showed that the streamlines of the velocity field produced by volume expansion are not, in general, normal to the flame front. Thus, when viewed from a fixed frame of reference, the motion of the flame is no longer solely in a direction normal to the front.

We then used our theory of flame propagation to show that a numerical approximation to the equations of motion based on finite difference techniques contains numerous drawbacks. As the front burns, the parameterization changes dramatically as certain sections expand while others are wholly eliminated through the formation of cusps. Those numerical methods that discretely parameterize the curve will have great difficulty following the flame front, since the formation and absorption of these cusps takes place on a variety of scales. In particular, since one needs to determine the orientation of the front at a point to establish where next to move it, too fine a discretization can lead to great numerical error in the determination of this direction as marker points cluster together, and too coarse a discretization can lead to an overly simplified resolution of the front.

In Chapter Four, we presented a numerical method, developed by Chorin, for following flame fronts which did not rely on a discrete parameterization of the front. We showed that the reason for the great success of Chorin's method is clear when viewed from within the framework of our theory of flame propagation, and that the method arises naturally from our theory of ignition curves. The central idea of this method, the application of Huygen's principle to move the front in a direction normal to itself, is an expression of our entropy condition that once a particle burns it remains burnt. Finally, we used this numerical technique to illustrate the results of our theorems, demonstrating the idea of spreading and colliding ignition curves, flame reversibility and cusp formation.

There are several directions suggested for further work. One possibility is to investigate the model proposed by Markstein in which the flame speed is taken as function of the curvature at any point. In this case, although the ignition curves are always normal to the front, they are no longer straight lines. Thus, a simple solution to the appropriate equations of motion is not readily apparent. With or without a solution, can one still show that any flame front asymptotically approaches a circle? Although our entropy condition is still appropriate, do cusps form in the same manner, if at all?

Another possibility is to analyze the interaction of ignition curves with the velocity field produced by volume expansion along the flame front. As mentioned earlier, the motion of the flame is a combination of the transformation of particles from unburnt to burnt and the advection field produced by their

resulting expansion. How does one rigorously deal with the effects of volume expansion at places where the curve is not differentiable? A third possibility is to remove the constant pressure approximation in the equations of motion. Finally, how does one show that the solutions to these sorts of problems are unique?

Bibliography

1) K.A. Brakke. *The Motion of a Surface by Its Mean Curvature*. Princeton University Press, Princeton University, New Jersey, 1978.

2) A.J. Chorin. *Flame Advection and Propagation Algorithms*. Journal of Computational Physics,35(1980). pp.1-11.

3) A.J. Chorin, J.E. Marsden. *A Mathematical Introduction to Fluid Mechanics*. Springer-Verlag, New York, 1979.

4) M.P. Do Carmo. *Differential Geometry of Curves and Surfaces*. Prentice-Hall, Inc.; Englewood Cliffs, New Jersey, 1976.

5) P.R. Garabedian. *Partial Differential Equations*. John Wiley and Sons, New York. 1961.

6) A.F. Ghoniem, A.J .Chorin, A.K. Oppenheim. *Numerical Modeling of Turbulent Combustion*. To appear.

7) I.S. Gradshteyn and I.M. Ryzhik. *Table of Integrals, Series and Products*. Academic Press, New York, 1965.

8) A.G. Istratov and V.B. Librovich. *On the Stability of Propagation of Spherical Flames*. Zhurnal Prikladnoi Mekhaniki i Tekhnicheskoi Fiziki. 1(1966). pp. 67-68.

9) I. Karasalo, A.J. Chorin, I. Namer, F. Robben, L. Talbot. *Numerical Simulation of the Interaction of a Flame with a Karman Vortex Street*. LBL Report-10679, Lawrence Berkeley Laboratory, 1980.

10) L. Landau. *On the Theory of Slow Combustion*. Acta Physicochimica URSS, 19(1944). pp. 77-85.

11) G.H. Markstein. *Experimental and Theoretical Studies of Flame Front Stability*. Journal of the Aeronautical Sciences, 18(1951). pp. 199-209.

12) G.H. Markstein. *Nonsteady Flame Propagation*. Pergammon Press, MacMillan Company, New York, 1964.

13) W. Noh and P. Woodward. *A Simple Line Interface Calculation*. Proceedings, Fifth International Conference on Fluid Dynamics, A.I. van de Vooran and P.J. Zandberger, Eds., Springer-Verlag, 1976.

14) J.A. Sethian. *Numerical Study of Turbulent Combustion*. To appear.

15) G.I. Sivashinsky. *Instabilities, Pattern Formation, and Turbulence in Flames*. To appear.

16) Y.B. Zeldovich. *An Effect Which Stabilizes the Curved Front of a Laminar Flame*. Zhurnal Prikladnoi Mekhaniki i Tekhnicheskoi Fiziki, 1(1966). pp. 102-104.

17) Y.B. Zeldovich. *Flame Propagation in Tubes: Hydrodynamics and Stability*. Combustion, Science and Technology, 24(1980). pp. 1-13.

18) Y.B. Zeldovich. *Structure and Stability of Steady Laminar Flame at Moderately Large Reynolds Number*. Combustion and Flame, 40(1981).

TECHNICAL INFORMATION DEPARTMENT
LAWRENCE BERKELEY LABORATORY
UNIVERSITY OF CALIFORNIA
BERKELEY, CALIFORNIA 94720